Comparison of Effects of Bromination and Iodination on the Spectroscopic Properties of Natural Organic Matter

by

Sixuan He

A thesis submitted in partial fulfillment of the

requirements for the degree of

Master of Science

University of Washington

2013

Program Authorized to offer degree: Civil and Environmental Engineering

University of Washington

Graduate School

University of Washington

Abstract

Comparison of Effects of Bromination and Iodination on the Spectroscopic Properties of Natural Organic Matter

by Sixuan He

Chairperson of the Supervisory Committee:

Dr. Gregory Korshin

Department of Civil and Environmental Engineering

Toxicological studies of disinfection by-products (DBPs) suggest that brominated and iodinated DBPs may be more carcinogenic than their chlorinated analogues. This makes it important to examine the pathways of formation of brominated and iodinated DBPs on a microscopic level. Examination the engagement of natural organic matter (NOM) that interacts with dissimilar halogen species can be done by the *in situ* methods of differential absorbance and fluorescence. spectroscopy. These measurements were carried out using three different NOM sources. In selected experiments, gas chromatography was used to determine concentrations of trihalomethanes and haloacetic acids formed in the studied systems at varying bromide concentration and reaction times. The data showed that chlorine and bromine species engage similar reactive sits in NOM but bromine incorporation takes place much faster than that of chlorine. The incorporation of bromine in NOM was observed to be

associated with largely similar changes of the absorbance spectra of NOM but changes of NOM fluorescence were more specific and exhibited an increasingly prominent decrease of emission intensity. This was hypothesized to be caused by the heavy atom effect on NOM fluorophores. Several phenomena specific to NOM iodination were observed as well. NOM reactions with iodine species formed via the oxidation of iodide by chloramine were accompanied by the emergence of a prominent peak at around 225 nm; this peak reflected the consumption of iodine species. Changes of differential absorbance of NOM in wavelengths above 300 nm also indicated the presence of weak but indicative bands that were absent in the cases of chlorination or bromination. Fluorescence measurements indicated that, similarly to the observations made for NOM bromination, the incorporation of iodine caused the intensity of NOM fluorescence to decrease, most likely due to the heavy atom quenching effect. The decrease of NOM fluorescence immediately after the beginning of NOM halogenation in the presence of bromide or iodide appears to be correlated with increases of the fraction of bromine or iodine incorporated into the reactive sits of NOM. This observation was confirmed by the attendant changes of DBP speciation and concentration. The observed effects can have high importance for further exploration of NOM halogenation pathways and kinetics but more research is necessary to examine these effects in more detail.

Table of Contents

List of figures iii

CHAPTER 1 INTRODUCTION 1

1.1 Basic Aspects of the Chemistry of Aqueous Chlorine and chloramine 1

1.2 Natural Organic Matter Characterization 3

1.3 NOM Chlorination and chloramination Reactions 5

1.4 Disinfection by-products 8

1.5 Effects of Disinfection on Absorbance and Fluorescence of NOM 15

1.6 Objectives of the Study 18

CHAPTER 2 MATERIALS AND METHODS 20

2.1 Water sources 20

2.2 Glassware preparation 20

2.3 Materials 21

2.4 Experimental methods 22

2.5 Analytical procedures 24

CHAPTER 3 EFFECTS OF BROMIDE ON ABSORBANCE AND FLUORESCENCE OF NOM AND FORMATION OF BROMINATED DISINFECTION BY-PRODUCTS 31

3.1 Changes of Absorbance of NOM Caused by Chlorination in the Presence of Bromide 31

3.2 Changes of Fluorescence Caused by Chlorination in the presence of Varying Concentrations of Bromide 45

3.3 Disinfection by products 58

CHAPTER 4 EFFECT OF IODINATION ON THE ABSORBANCE AND FLUORESCENCE OF NOM 75

4.1 Changes of absorbance of NOM caused by chloramination in the presence of iodide 76
4.2 Changes of fluorescence of NOM caused by chloramination in the presence of iodide 87
Conclusions 94
References 98

List of figures

Figure 1 Hypothetic structural formulas of Natural Organic Matter. Adopted from Leenheer, 2007. 4

Figure 2 (a) Base-catalyzed reaction pattern for the chlorine reaction with aldehydes and ketones; (b) Reaction scheme for the chlorination of phenoxide ion. Adopted from Deborde and Von Gunten, 2008. 7

Figure 3 Simplified view of major different between chlorine and chloramine reaction pathway. Adopted from Hua and Reckhow,2008. 8

Figure 4 Distribution of individual of HAA species in chlorinated Palm Beach, pH 8. Adopted from Cowman and Singer, 1995. 12

Figure 5 Relationship between total trihalomethanes(TTHMs) and total haloacetic acids (THAAs) as a percentage of total organic halogen (TOX). Adopted from Pourmoghaddas and Stevens, 1995. 13

Figure 6 Experimental sampling procedure diagram 24

Figure 7 UV absorbance spectra of chlorinated SRFA chlorinated in the presence of varying bromide concentration, DOC 5 mg/L, chlorine to DOC ratios of 1.1 mg/mg, pH 7.0, reaction time from 5min to 4h, bromide concentrations: (a) 0 mg/L, (b) 0.5 mg/L, (c) 1 mg/L, (d) 2 mg/L, (e) 4 mg/L, (f) 8 mg/L, (g) 16 mg/L, (h) 25.2 mg/L, (i) 40 mg/L. 33

Figure 8 Differential absorbance spectra of chlorinated SRFA in the presence of varying bromide concentrations, DOC 5 mg/L, chlorine to DOC ratios of 1.1 mg/mg, pH 7.0, reaction time from 5min to 4h, bromide concentrations (a) 0 mg/L, (b) 0.5 mg/L, (c) 1 mg/L, (d) 2 mg/L, (e) 4 mg/L, (f) 8 mg/L, (g) 16 mg/L, (h) 25.2 mg/L, (i) 40 mg/L. 35

Figure 9 Differential Ln (A/A_0) of chlorinated SRFA in the presence of varying bromide concentrations, DOC 5mg/L, chlorine to DOC ratios of 1.1 mg/mg, pH 7.0, reaction time from 5min to 4h, bromide concentrations (a) 0 mg/L, (b) 0.5 mg/L, (c) 1 mg/L, (d) 2 mg/L, (e) 4 mg/L, (f) 8 mg/L, (g) 16 mg/L, (h) 25.2 mg/L, (i) 40 mg/L. 38

Figure 10 UV absorbance spectra of chlorinated Lake Washington (winter sampling) in the presence of varying bromide concentration, DOC 2.3mg/L, chlorine to DOC ratios of 1 mg/mg, pH 7.0, reaction time from 5min to 4h, bromide dose (a) 0 mg/L, (b) 0.1 mg/L, (c) 0.2 mg/L, (d) 0.5 mg/L, (e) 1 mg/L, (f) 2 mg/L, (g) 4 mg/L. 39

Figure 11 Differential absorbance spectra of chlorinated Lake Washington (winter sampling) in the presence of varying bromide concentrations. DOC 2.3mg/L, chlorine to DOC ratios of 1 mg/mg, pH 7.0, reaction time from 5min to 4h, bromide concentration (a) 0 mg/L, (b) 0.1 mg/L, (c) 0.2 mg/L, (d) 0.5 mg/L, (e) 1 mg/L, (f) 2 mg/L, (g) 4 mg/L. 41

Figure 12 Differential Ln (A/A_0) of chlorinated Lake Washington (winter sampling) in the presence of varying bromide concentrations. DOC 2.3mg/L, chlorine to DOC ratios of 1 mg/mg, pH 7.0, reaction time from 5min to 4h, bromide dose (a) 0 mg/L, (b) 0.1 mg/L, (c) 0.2 mg/L, (d) 0.5 mg/L, (e) 1 mg/L, (f) 2 mg/L, (g) 4 mg/L. 43

Figure 13 UV absorbance spectra of chlorinated Lake Washington (summer sampling) in the presence of varying bromide concentrations. DOC 3.65 mg/L, chlorine to DOC ratios of 2 mg/mg, pH 7.0, reaction time from 5min to 8h, bromide dose (a) 0 mg/L, (b) 0.1 mg/L, (c) 0.2 mg/L, (d) 0.5 mg/L. 43

Figure 14 Differential absorbance spectra of chlorinated Lake Washington (winter sampling) in the presence of varying bromide concentration, DOC 3.65 mg/L, chlorine to DOC ratios of 1 mg/mg, pH 7.0, reaction time from 5min to 8h, bromide dose (a) 0 mg/L, (b) 0.1 mg/L, (c) 0.2 mg/L, (d) 0.5 mg/L.....44

Figure 15 Differential Ln(A/A_0) spectra of chlorinated Lake Washington (winter sampling) in the presence of arying bromide concentrations. DOC 3.65 mg/L, chlorine to DOC ratios of 1 mg/mg, pH 7.0, reaction time from 5min to 8h, bromide dose (a) 0 mg/L, (b) 0.1 mg/L, (c) 0.2 mg/L, (d) 0.5 mg/L.....45

Figure 16 Fluorescence spectra of chlorinated SRFA in the presence of varying bromide concentrations. DOC 5mg/L, chlorine to DOC ratios of 1.1 mg/mg, pH 7.0, reaction time from 5min to 4h, bromide concentration (a) 0 mg/L, (b) 0.5 mg/L, (c) 1 mg/L, (d) 2 mg/L, (e) 4 mg/L, (f) 8 mg/L, (g) 16 mg/L, (h) 25.2 mg/L, (i) 40 mg/L. 49

Figure 17 Differential relative changes of fluorescence spectra of SRFA chlorinated in the presence of varying bromide concentration. DOC 5mg/L, chlorine to DOC ratios of 1.1 mg/mg, pH 7.0, reaction time from 5min to 4h, bromide concentration (a) 0 mg/L, (b) 0.5 mg/L, (c) 1 mg/L, (d) 2 mg/L, (e) 4 mg/L, (f) 8 mg/L, (g) 16 mg/L, (h) 25.2 mg/L, (i) 40 mg/L.....52

Figure 18 Fluorescence spectra of Lake Washington (winter sampling) chlorinated in the presence of varying bromide concentrations. DOC 2.3mg/L, chlorine to DOC ratios of 1 mg/mg, pH 7.0, reaction time from 5min to 4h, bromide concentrations (a) 0 mg/L, (b) 0.1 mg/L, (c) 0.2 mg/L, (d) 0.5 mg/L, (e) 1 mg/L, (f) 2 mg/L, (g) 4 mg/L. 54

Figure 19 Relative changes of fluorescence of Lake Washington chlorinated in the presence of varying bromide concentrations. DOC 2.3mg/L, chlorine to DOC ratios of 1 mg/mg, pH 7.0, reaction time from 5min to 4h, bromide concentrations (a) 0 mg/L, (b) 0.1 mg/L, (c) 0.2 mg/L, (d) 0.5 mg/L, (e) 1 mg/L, (f) 2 mg/L, (g) 4 mg/L. 56

Figure 20 Fluorescence spectra of Lake Washington (summer sampling) chlorinated in the presence of varying bromide concentrations. DOC 3.65 mg/L, chlorine to DOC ratios of 1 mg/mg, pH 7.0, reaction time from 5min to 8h, bromide concentrations (a) 0 mg/L, (b) 0.1 mg/L, (c) 0.2 mg/L, (d) 0.5 mg/L. 57

Figure 21 Relative changes of the fluorescence spectra of chlorinated Lake Washington (summer sampling) in the presence of varying bromide concentration,.

DOC 3.65 mg/L, chlorine to DOC ratios of 1 mg/mg, pH 7.0, reaction time from 5min to 8h, bromide concentration (a) 0 mg/L, (b) 0.1 mg/L, (c) 0.2 mg/L, (d) 0.5 mg/L. .58

Figure 22 Molar concentrations of THM4 species formed at varying reaction time and initial bromide ion concentrations. pH=7, Lake Washington DOC=3.65mg/L, chlorine to DOC ratios of 1.0 mg/mg, (a) chloroform, (b) bromodichloromethane, (c) dibromochloromethane, (d) bromoform. 60

Figure 23 Mass concentrations of THM4 species formed at varying reaction times and initial bromide ion concentrations. pH=7, Lake Washington DOC=3.65mg/L, chlorine to DOC ratios of 1.0 mg/mg, (a) chloroform, (b) bromodichloromethane, (c) dibromochloromethane, (d) bromoform. 61

Figure 24 Molar concentrations of TTHM (a) and concentrations of bromine incorporated in TTHM (b) as function of chlorination reaction time and initial bromide ion concentration, pH=7, Lake Washington DOC=3.65mg/L, chlorine to DOC ratios of 1.0 mg/mg. 61

Figure 25 Mass concentrations of TTHM (a) and concentrations of bromine incorporated in TTHM (b) as function of chlorination reaction time and initial bromide ion concentration, pH=7, Lake Washington DOC=3.65mg/L, chlorine to DOC ratios of 1.0 mg/mg. 62

Figure 26 Molar fractions of THM species in TTHM concentrations as function of chlorination time and initial bromide ion concentration, pH=7, Lake Washington DOC=3.65mg/L, chlorine to DOC ratios of 1.0 mg/mg, (a) chloroform, (b) bromodichloromethane, (c) dibromochloromethane, (d) bromoform. 63

Figure 27 Mass fractions of THM species in TTHM concentration as function of chlorination time and initial bromide ion concentration, pH=7, Lake Washington DOC=3.65mg/L, chlorine to DOC ratios of 1.0 mg/mg, (a) chloroform, (b) bromodichloromethane, (c) dibromochloromethane, (d) bromoform. 64

Figure 28 Effect of bromide on the molar yields (a) and mass yields (b) of individual THM species in chlorinated Lake Washington sampling DOC=3.65 mg/L, chlorine to DOC ratios of 1.0 mg/mg, reaction time 8 h, pH 7. 65

Figure 29 Distribution of individual THM species on a mole fractional basis (a) and on a mass fractional basis (b) in chlorinated Lake Washington sampling DOC=3.65 mg/L, chlorine to DOC ratios of 1.0 mg/mg, reaction time 8 h, pH 7. 66

Figure 30 Molar concentration of HAAs species formed at varying chlorination times and initial bromide ion concentration, pH=7, Lake Washington DOC=3.65mg/L, chlorine to DOC ratios of 1.0 mg/mg, (a) DCAA, (b) TCAA, (c) BCAA, (d) DBAA, (e) BDCAA, (f) DBCAA,. 67

Figure 31 Mass concentrations of HAAs species formed as function of varying chlorination time and initial bromide ion concentration, pH=7, Lake Washington

DOC=3.65mg/L, chlorine to DOC ratios of 1.0 mg/mg, (a) DCAA, (b) TCAA, (c) BCAA, (d) DBAA, (e) BDCAA, (f) DBCAA,. 68

Figure 32 Molar concentrations of THAA (a) and overall bromine incorporated in the HAA species (b) as function of chlorinated reaction time and initial bromide ion concentration, pH=7, Lake Washington DOC=3.65mg/L, chlorine to DOC ratios of 1.0 mg/mg. 69

Figure 33 Mass concentrations of THAA (a) and overall bromine incorporated in the HAA species (b) as function of chlorinated reaction time and initial bromide ion concentration, pH=7, Lake Washington DOC=3.65mg/L, chlorine to DOC ratios of 1.0 mg/mg. 69

Figure 34 Molar fractions of individual HAAs species in THAA as a function of chlorination time and initial bromide ion concentration, pH=7, Lake Washington DOC=3.65mg/L, chlorine to DOC ratios of 1.0 mg/mg, (a) DCAA, (b) TCAA, (c) BCAA, (d) DBAA, (e) BDCAA, (f) DBCAA. 70

Figure 35 Weight fractions of individual HAAs species in THAA as a function of chlorination time and initial bromide ion concentration, pH=7, Lake Washington DOC=3.65mg/L, chlorine to DOC ratios of 1.0 mg/mg, (a) DCAA, (b) TCAA, (c) BCAA, (d) DBAA, (e) BDCAA, (f) DBCAA. 71

Figure 36 Effect of bromide on the molar (a) and mass yields (b) of individual HAA species in chlorinated Lake Washington water. DOC=3.65 mg/L, chlorine to DOC ratios of 1.0 mg/mg, reaction time 8 h, pH 7. 72

Figure 37 Fractional contributions of individual HAA species expressed using mole fractional basis (a) and on mass fractional basis (b) in chlorinated Lake Washington sampling DOC=3.65 mg/L, chlorine to DOC ratios of 1.0 mg/mg, reaction time 8 h, pH 7. 73

Figure 38 Effect of bromide on the molar yields of THMs and HAAs in chlorinated Lake Washington sampling DOC=3.65 mg/L, chlorine to DOC ratios of 1.0 mg/mg, reaction time 8 h, pH 7. 74

Figure 39 Absorbance spectra of Nordic NOM recorded at varying iodide concentrations in the presence of chloramine. DOC 5mg/L, chlorine to DOC ratios of 1.5 mg/mg, NH_4^+ to chlorine ratios of 1.5 mol/mol, pH 7.0, reaction time from 5min to 4 h, iodide concentration (a) 0 mg/L, (b) 0.1 mg/L, (c) 0.2 mg/L, (d) 0.5 mg/L, (e) 1 mg/L, (f) 2 mg/L, (g) 3 mg/L, (h) 4 mg/L. 78

Figure 40 Differential absorbance spectra of Nordic NOM obtained for varying iodide concentrations in the presence of chloramine. DOC 5mg/L, chlorine to DOC ratios of 1.5 mg/mg, NH_4^+ to chlorine ratios of 1.5 mol/mol, pH 7.0, reaction time from 5min to 4h, iodide dose (a) 0 mg/L, (b) 0.1 mg/L, (c) 0.2 mg/L, (d) 0.5 mg/L, (e) 1 mg/L, (f) 2 mg/L, (g) 3 mg/L, (h) 4 mg/L. 81

Figure 41 Differential absorbance spectra of Nordic NOM, in a region of 250 to 500 nm at varying iodide concentration in the presence of chloramine. DOC 5mg/L, chlorine to DOC ratios of 1.5 mg/mg, NH_4^+ to chlorine ratios of 1.5 mol/mol, pH 7.0, reaction time from 5min to 4h, iodide dose (a) 0 mg/L, (b) 0.1 mg/L, (c) 0.2 mg/L, (d) 0.5 mg/L, (e) 1 mg/L, (f) 2 mg/L, (g) 3 mg/L, (h) 4 mg/L. 82

Figure 42 Differential Ln(A/A_0) spectra of Nordic NOM obtained for varying iodide concentrations in the presence of chloramine. DOC 5mg/L, chlorine to DOC ratios of 1.5 mg/mg, NH_4^+ to chlorine ratios of 1.5 mol/mol, pH 7.0, reaction time from 5min to 4h, iodide dose (a) 0 mg/L, (b) 0.1 mg/L, (c) 0.2 mg/L, (d) 0.5 mg/L, (e) 1 mg/L, (f) 2 mg/L, (g) 3 mg/L, (h) 4 mg/L. 83

Figure 43 Effects of iodide on the differential absorbance spectra of Nordic NOM recorded for fixed chloramination times. DOC 5mg/L, chlorine to DOC ratios of 1.5 mg/mg, NH_4^+ to chlorine ratios of 1.5 mol/mol, pH 7.0, iodide concentration from 0 to 4mg/L, reaction time (a) 5 min, (b) 10min, (c) 30min, (d) 60min, (e) 90min, (f) 120min, (g) 240min. 85

Figure 44 Effects of iodide on the log-transformed differential absorbance spectra of Nordic NOM recorded for fixed chloramination times. DOC 5mg/L, chlorine to DOC ratios of 1.5 mg/mg, NH_4^+ to chlorine ratios of 1.5 mol/mol, pH 7.0, iodide concentration from 0 to 4mg/L, reaction time (a) 5 min, (b) 10min, (c) 30min, (d) 60min, (e) 90min, (f) 120min, (g) 240min. 86

Figure 45 Differential Ln (A/A_0) and differential absorbance of Nordic NOM at a fixed wavelength with varying iodide dose, DOC 5mg/L, chlorine to DOC ratios of 1.5 mg/mg, NH_4^+ to chlorine ratios of 1.5 mol/mol, pH 7.0, (a) differential absorbance at 225nm, (b) differential Ln (A/A_0) at 225nm, (c) differential Ln (A/A_0) at 425nm. 87

Figure 46 Fluorescence spectra of Nordic NOM obtained for varying iodide concentration in the presence of chloramine. DOC 5mg/L, chlorine to DOC ratios of 1.5 mg/mg, NH_4^+ to chlorine ratios of 1.5 mol/mol, pH 7.0, reaction time from 5 min to 4 h, iodide dose (a) 0 mg/L, (b) 0.1 mg/L, (c) 0.2 mg/L, (d) 0.5 mg/L, (e) 1 mg/L, (f) 2 mg/L, (g) 3 mg/L, (h) 4 mg/L. 89

Figure 47 Differential fluorescence spectra of Nordic NOM obtained for varying iodide concentration in the presence of chloramine. DOC 5mg/L, chlorine to DOC ratios of 1.5 mg/mg, NH_4^+ to chlorine ratios of 1.5 mol/mol, pH 7.0, reaction time from 5min to 4h, iodide dose (a) 0 mg/L, (b) 0.1 mg/L, (c) 0.2 mg/L, (d) 0.5 mg/L, (e) 1 mg/L, (f) 2 mg/L, (g) 3 mg/L, (h) 4 mg/L. 91

Figure 48 Effects of iodide on the differential fluorescence spectra of Nordic NOM recorded for fixed chloramination times. DOC 5mg/L, chlorine to DOC ratios of 1.5 mg/mg, NH_4^+ to chlorine ratios of 1.5 mol/mol, pH 7.0, iodide concentration from 0 to 4mg/L, reaction time (a) 5 min, (b) 10min, (c) 30min, (d) 60min, (e) 90min, (f) 120min, (g) 240min. 92

Figure 49 Relationships between differential absorbance of NNOM at 225 nm and changes of the fluorescence intensity at 460 nm at varying reaction times and initial iodide concentrations. (a) differential slop $(I_0-I_t)/I_0$ at 460nm with differential absorbance at 225nm, (b) differenial slop $(I_0-I_t)/I_0$ at 460nm with differential Ln(A/A0) at 225 nm.....93

CHAPTER 1 INTRODUCTION

1.1 Basic Aspects of the Chemistry of Aqueous Chlorine and chloramine

Chlorine is the most commonly employed and conveniently available disinfecting agent used in the world. When dissolved in water, chlorine deactivates or kills most of microorganisms present in the water being treated but it also interacts with natural organic matter (NOM) via complex chlorination reactions. When chlorine gas is dissolved into water, it undergoes a disproportionation reaction that yields both hypochlorous acid (HOCl) and hydrochloric acid (HCl):

$$Cl_2(g) + H_2O \leftrightarrow HOCl + H^+ + Cl^- \quad (1)$$

The published values of the equilibrium constant, K_{Cl2} of reaction (1) range from 1.3×10^{-4} to 5.1×10^{-4} M^2 for temperatures between 0 to 25 ℃ (Deborde and Von Gunten, 2008). Reaction (1) is very fast and the equilibrium is reached within seconds or less.

The chlorine atom in molecules of hypochlorous acid (HOCl) is able to accept two electrons thus changing its oxidation state from +1 to -1 state. This oxidizing power of this reaction and its kinetics depend greatly on pH. In conditions typical for drinking water treatment, the contribution of hydrated Cl_2 is very small and the system is dominated by the species hypochlorous acid. It is present in its protonated formed at pH 6, but this changes for pHs between 6.0 and 8.5 and almost all HOCl dissociates completely at pH > 8.5:

$$HOCl \leftrightarrow H^+ + OCl^- \quad (2)$$

The reaction equilibrium constant K_{HClO} of reaction (2) ranges from 1.5×10^{-8} to 2.9×10^{-8} M, temperatures between 0 to 25 ℃ (Deborde and Von Gunten, 2008).

Chlorine can be added to water as Cl_2 and also as sodium hypochlorite (NaOCl) or calcium hypochlorite ($Ca(ClO)_2$). In all cases, these reagents yield HOCl and/or OCl^- but their concentration are typically reported as equivalent Cl_2 concentrations. In the absence of chloramine species, these concentrations are referred to as free available chlorine or free chlorine (Davis, 2010). In addition to them, bromine species can also be present in many waters. This is because bromide naturally exists in surface and ground waters, especially those found in coastal areas and affected by seawater intrusion. When bromide (Br^-) is present, it can be rapidly oxidized by chlorine to hypobromous acid (HOBr) and its anion OBr^-:

$$Br^- + HOCl \rightarrow HOBr + Cl^- \quad (3)$$

The rate constant of reaction (3) is 1550 M^{-1} s^{-1} (Hua et al., 2006). Due to the high rate of reaction (3), the bromide present in water and concentrations of free chlorine exceeding those of Br-, the latter is typically completely converted to HOBr, OBr^- and other bromine-containing species whose concentrations tend to be much lower than those of HOBr and OBr^-.

Recently, many drinking water utilities have switched from chlorination to chloramination. This has been done to comply with THMs and HAAs regulatory limits. Chloramine is more stable than free chlorine in distribution systems and it is also an effective secondary disinfectant that can be used to reduce algal development in reservoirs and suppress bacterial regrowth in distribution system (Hua and Reckhow, 2007; Jones et al., 2011; Wolfe et al., 1984). Reactions of chlorine or hypochloric acid with ammomia proceed stepwise to form three species of inorganic chloramines:

$$HOCl + NH_3 \leftrightarrow NH_2Cl \text{ (monochloramine)} + H_2O \quad (4)$$

$$HOCl + NH_3 \leftrightarrow NHCl_2 \text{ (dichloramine)} + H_2O \quad (5)$$

$HOCl + NH_3 \leftrightarrow NCl_3$ (nitrogen trichloride) $+H_2O$ (6)

These reactions are strongly effected by pH and chlorine to nitrogen concentration ratios. Monochloramine (equation 4) tends to be produced in the range of pH 7-11 and weight ratio Cl_2:N ≤ 5:1. Dichloramine (equation 5) is dominant in the pH 4.4-7 and Cl_2:N (5:1-7.6:1) while nitrogen trichloride (equation 6) is formed primarily in pH <4.4 and Cl_2:N > 7.6:1 (Wolfe et al., 1984). Monochloramine is typically the desired species since it is an effective disinfectant and it does not produce high levels of THMs and HAAs.

Iodide (its concentrations are typically very low, below 50 μg/L) (Bichsel and Von Gunten, 1999, 2000) and bromide are present in many surface and ground waters. Iodide can be easily oxidized to hypoiodous acid by monochloramine while chlorine tends to oxidize most of iodide ca. 90%) to iodate thus removing iodine species from reactions with natural organic matter, NOM (Hua and Reckhow, 2007). However, monochloramine is not a strong enough oxidant to oxidize bromide to hypobromous acid, especially at pH above 7.5, However, when pH is adjusted to 6, acid-catalyzed hydrolysis of monochloramine forms HOCl, and this species can convert Br^- to HOBr that can also react with NH_3 to form bromamines (Bichsel and Von Gunten, 1999; Karanfil et al., 2007).

1.2 Natural Organic Matter Characterization

The major challenge associated with the use of chlorine for drinking water disinfection is the generation of disinfection by-products (DBPs) formed as a result of reactions of chlorine species with natural organic matter (NOM). NOM is ubiquitous in the environment and generated via many complex biogeochemical processes. The formation and properties of NOM can also be affected human activities, for instance via the introduction of wastewater in the environment. Concentrations of NOM are

commonly reported units of concentration of dissolved organic carbon (DOC). This is because NOM comprises thousands of different molecules and it is impossible to characterize the concentrations and properties such as molecular weight of each of them.

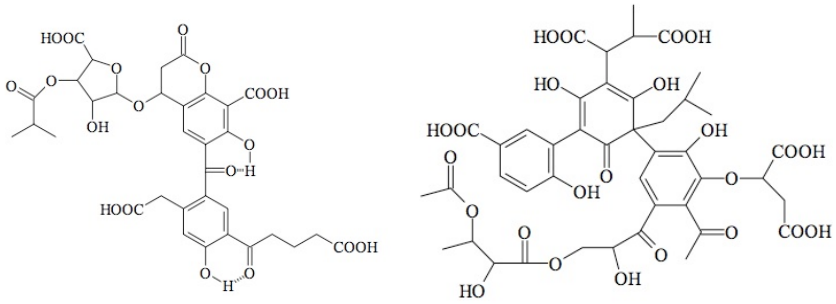

Figure 1 Hypothetic structural formulas of Natural Organic Matter. Adopted from Leenheer, 2007.

However, it is possible to provide some level of NOM characterization in terms of its predominant fractions (Figure 1), typical functional group and their reactivities. Operationally, NOM is typically separated into hydrophilic, transphilic and hydrophobic fractions. Hydrophilic fractions of NOM comprise many species, notably humic species with relatively low molecular weights and high abundances of carboxylic groups as well as carbohydrates, carboxylic acids, amino acids, amino sugars, and proteins. Hydrophobic NOM fractions (traditionally separated into humic and fulvic acids, the former fraction forming a precipitate at pH < 2) tend to be dominated by humic species (Croue et al., 1999). These compounds are characterized by the prominence of phenolic and carboxylic functional groups that readily participate in protonation and metal complexation reactions. While the properties of NOM vary from site to site and over time, the domination of humic species in most natural waters is widely observed. Humic species with varying apparent molecular

weights and hydrophobicities contributing 0% to 90% of the overall NOM mass balance. (Croue et al., 1999)

1.3 NOM Chlorination and chloramination Reactions

Chlorination

NOM reacts with chlorine via three major types of reactions 1) oxidation, 2) addition of halogen atoms to unsaturated bonds and 3) electrophilic substitution at nucleophilic sites in NOM. Due to the intrinsic complexity of NOM chemistry, the elucidation of separate contributions of these pathways as well as the determination of precise chemical nature of the reactive site in NOM is very difficult if not impossible.

However, some general facts pertinent to this discussion can be outlined. While humic substances are complex and their molecules have numerous chemical functionalities (Minear and Amy, 1996), hydroxy- and methoxy-substituted (lignin) aromatic groups that are primary constituents of plant tissues from which a large part of humic species is deemed to be generated constitute the moiety of phenolic species in NOM. This moiety is extremely important in DBP generation as these phenolic substructures can interact selectively with halogen species, be altered in reactions with them and ultimately undergo breakdown to form various individual DPBs (Norwood et al., 1987). Selected studies suggest that functional groups other than the phenolic moiety can be important precursors of DBPs as well. For instance, Dickenson et al., 2008 posited that aliphatic-type structures in humic species are responsible for as high over 80% of the yields of mono and trihaloacetic acids formed via the engagement of aliphatic β-dicarbonyl groups in NOM.

In general, electrophilic chlorine species tend to react with electron-rich sites in NOM, for instance with activated aromatic rings, aliphatic β-dicarbonyls

and amino nitrogen. For water-borne humic substances, rates of chlorination reactions increase with increasing percentage of activated aromatic carbon in NOM, or NOM aromaticity. The aromaticity of NOM can be determined via ex situ measurements using structure-sensitive methods of pyrolysis GC/MS and ^{13}C NMR, or in situ method of absorbance spectroscopy. All these measurements confirm the finding that the phenolic carbon content of NOM is the most important predictor of the reactivity of humic substances with chlorine and it determines the most important aspects of DBPs formation (Minear and Amy, 1996).

Mechanistically, the formation of DBP has been frequently explained based on the classical haloform reaction (Deborde and Von Gunten, 2008). In this reaction, a carbonyl functional group initially reacts with chlorine. Specifically, its ketone isomeric group is engaged in chlorination as shown in Figure 2 (a). In this step, a hydrogen atom is replaced with a chlorine atom and sequential halogenation steps occur successively producing via both chlorine incorporation and C-C bond cleavage, a molecule with a carboxylic group (e.g., acetate) and chloroform. This halogenation reaction can be acid-catalyzed or base-catalyzed. In dilute aqueous solution at pH > 5, the base-catalyzed haloform is predominant.

Reactions of chlorine with aromatic compounds occur mainly via electrophilic substitution in the ortho or para positions of the aromatic ring. The chlorination of phenols accordingly proceed via step-wise substitutions at 2, 4 and 6 positions that are activated by the ortho/para-positioned hydroxyl groups (Acero et al., 2005; Gallard and von Gunten, 2002) as shown in Figure 2 (b).

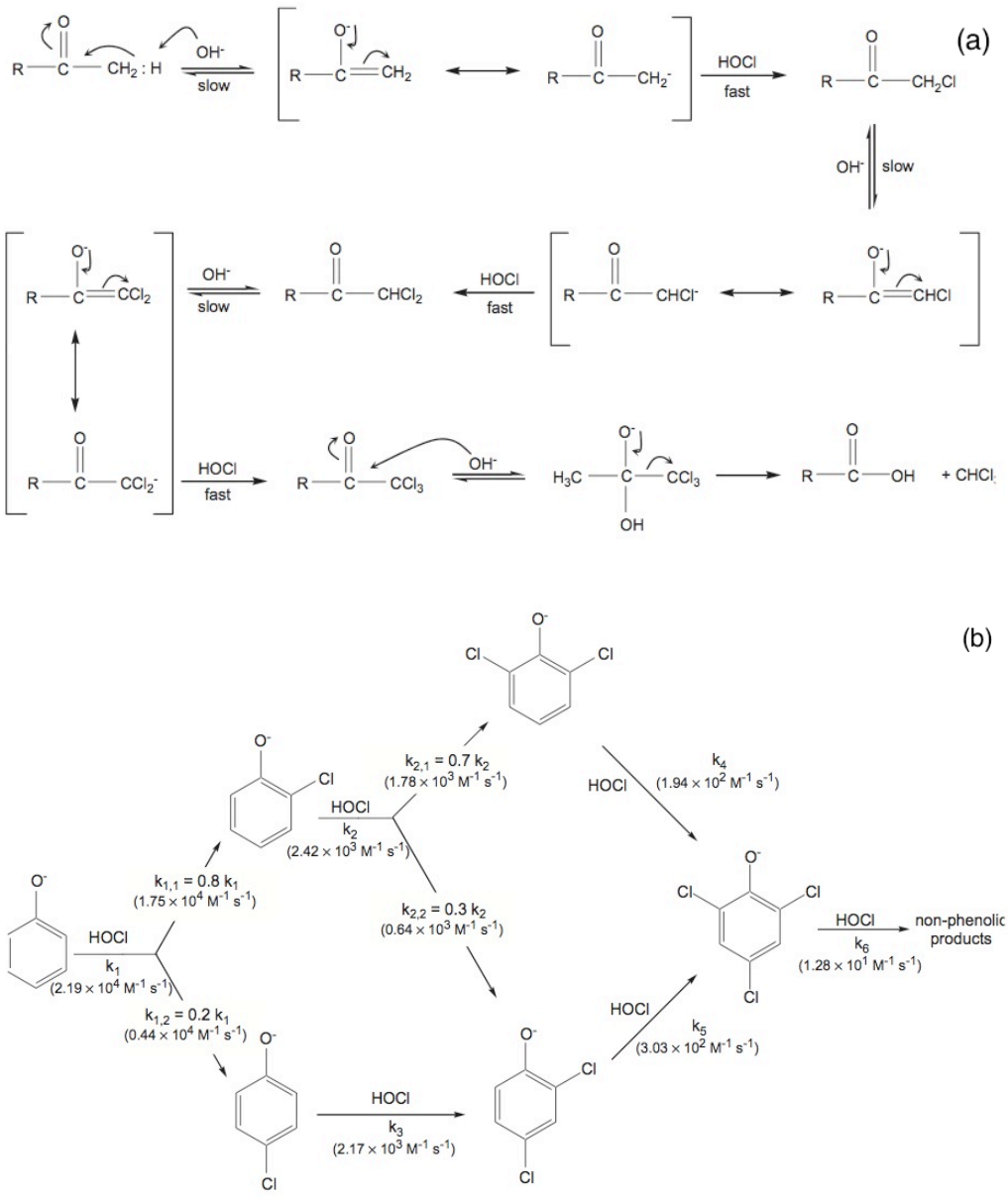

Figure 2 (a) Base-catalyzed reaction pattern for the chlorine reaction with aldehydes and ketones; (b) Reaction scheme for the chlorination of phenoxide ion. Adopted from Deborde and Von Gunten, 2008.

Chloramination

Chloramination of NOM appears to proceed through two types of reactions, oxidation and substitution. These reactions result in a relatively high formation of haloacetic acids such as dichloroacetic acid and also in multiple unidentified DBPs whose relative contribution in the case of chloramination is much higher than that in the case of chlorination. Several researchers have

postulated that formation of DBPs in the case of chloramination results from the presence of a small amount of free chlorine released from monochloramine while other researchers have hypothesized that chloramine is kinetically slow in incorporating a third halogen in a halogenation site in NOM; this prevents the formation of trihalogenated DBPs, a well-known fact for NOM chloramination (Figure 3)(Hua and Reckhow, 2008).

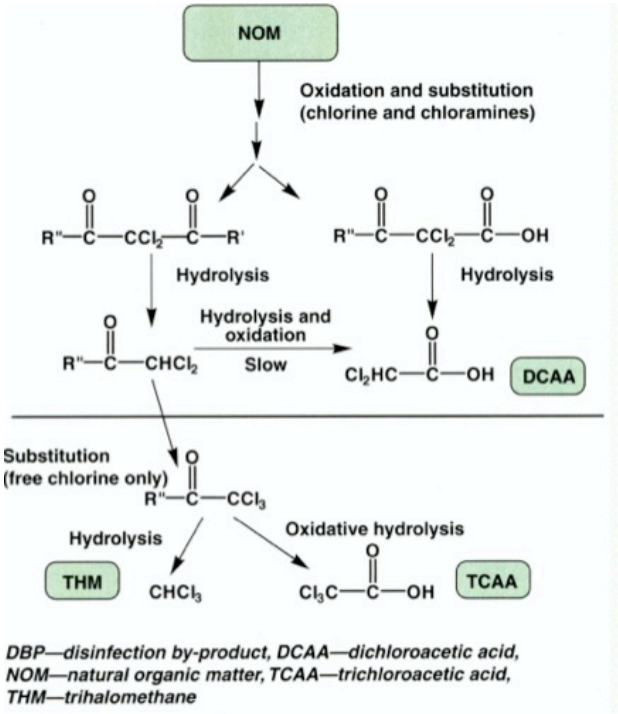

Figure 3 Simplified view of major different between chlorine and chloramine reaction pathway. Adopted from Hua and Reckhow,2008.

1.4 Disinfection by-products

The ultimate purpose of disinfection of water is to control pathogens and to prevent waterborne disease. During drinking water or wastewater chlorination, chlorine can be consumed in multiple reactions. For instance it rapidly reacts with inorganic such as bromide, iodide, nitrite, sulfide, ferrous ion, and also in reactions

with NOM that cause potentially DBPs to form. As outlined above, chlorine reacts with NOM by oxidizing its and substituting into the organic substrate (Johnson and Jensen, 1986).

Over 700 individual DBPs have been reported to occur in the presence of major disinfectants such as chlorine, ozone, chlorine dioxide and chloramines. Despite these efforts focused on the identification of individual DBPs' identities, numerous chlorinated organic species formed in drinking water remain to be identified and it is commonly believed that only a fraction of actually present DBP species has been identified. In addition, only a limited number of DBPs have been examined to elucidate their suspected adverse health effects which include mutagenicity and carcinogenicity.

The major classes of identified individual DBPs include trihalomethanes (THMs), haloacetic acids (HAAs), haloacetonitriles (HANs), haloketones (HKs), glyoxals and aldehydes (formed in the presence of ozone), chloral hydrate (CH), chloropicrin (CP), and chlorinated furanones (MX).

Of the groups mentioned above, THMs and HAAs are by far the major DBP classes existing in all chlorinated surface drinking waters. Many factors effect their formation as well as that of other DBP groups. These factors include the concentration and properties of NOM in the source water, pH, temperature, concentrations of the disinfectant, bromide and ammonia, and contact time. These effects are complex but it is widely reported that yields of THMs increase at higher pH while the formation of haloacetic acids (HAAs) tends to be more prevalent at low pHs.

Trihalomethanes (THMs)

Chloroform for the first identified DBPs which was discovered by Rook in the 1970-ties. Control of chloroform and other trihalomethanes (general formula CCl_xBr_{3-x}) in drinking water has been of great concern since then. In 1979, a maximum contaminant level (MCL) for the sum of four THMs typical for drinking water was established at a 100 μg/L level, and later this was decreased to 80 μg/L. The THM species considered in this regulation include chloroform, bromoform, bromodichloromethane, and chlorodibromomethane. The sum of their concentrations is referred to as TTHM. The contribution of TTHMs to total organic halogen associated with all DBP species accounts to from <5% (e.g., in the case of chloramination) to > 25% of detectable DBPs in most chlorinated waters (Bellar et al., 1974). In general, the formation of TTHMs is favored for high concentration of chlorine and NOM, and elevated pHs and temperatures.

Haloacetic Acids (HAAs)

Another major class of DBPs formed upon disinfection is haloacetic acids (HAAs) (general formula $CH_{3-x-y}Br_xCl_yCOOH$). HAAs that contain chlorine and/or bromine atoms include nine compounds. These are monochloroacetic acid (MCAA), monobromoacetic acid (MBAA), dichloroacetic acid (DCAA), trichloroacetic acid (TCAA), dibromoacetic acid (DBAA), bromochloroacetic acid (BCAA), tribromoacetic acid (TBAA), bromodichloroacetic acid (BDCAA), and dibromochloroacetic acid (DBCAA). In the Unites States, the sum of MBAA, MCAA, DBAA, DCAA, and TCAA is usually referred to HAA5 (Chen and Weisel, 1998). DCAA and TCAA have been identified extensively as the major HAA species both in chlorinated drinking water occurring in distribution networks and also upon laboratory-scale chlorination of humic substances and model compounds. In the case of water chlorination, the most prominent fraction of HAAs is contributed by

trihalogenated species (61-67%), while the dihalogenated HAAs contribute 30-36% of the total, and the monohalogenated species made up 3-5% (Cowman and Singer, 1995). The MCL established for the five HAA compounds (HAA5) is 60 µg/L.

Brominated Disinfection By-Products

Bromide concentrations in seawater are commonly in the range from 65 mg/L to 80 mg/L, but the concentration of bromide in fresh waters are typically below 0.5 mg/L, with a wide variability. Bromide levels in surface or ground waters ranges from 0 to 2 mg/L, and in desalinated sea water bromide concentrations may be around 1 mg/L or more. The bromide existing in source water can be oxidized rapidly by chlorine to hypobromous acid (HOBr) which is a much faster kinetically halogenating agent than HOCl. HOBr and potentially its anion OBr^- react with NOM to form brominated DBPs, and as a result the presence of bromide ions in water leads to notable increases of brominated THMs or HAAs to total THMs or HAA5 (Cooper et al., 1985; Krasner et al., 1994, Ates et al., 2007). Brominated DBPs compounds have been reported to be more toxic and mutagenic compared with chlorinated ones (BULL et al., 1995; Bull et al., 2001; Richardson, 2003).

Effects of varying bromide concentrations on the formation of THMs and/or HAAs have been studied in prior literature. Some studies have demonstrated that yields of THMs and HAAs increase rapidly with increasing bromide concentration in source water during chlorination. These studies also presented formal models to quantify such changes (Chang et al., 2001; Duong et al., 2003; Yang and Shang, 2004) (Figure 4).

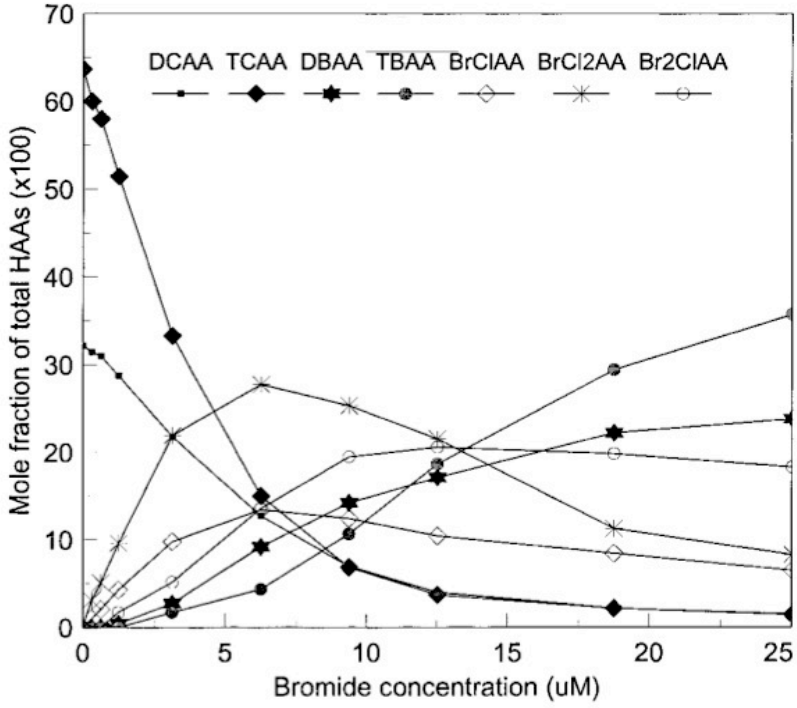

Figure 4 Distribution of individual of HAA species in chlorinated Palm Beach, pH 8. Adopted from Cowman and Singer, 1995.

For a constant DOC and increasing Br/DOC ratios, the total molar THM concentrations tend to increase thus indicating that bromine and chlorine incorporation into NOM and then to THM increase due to the more reactive nature of HOBr (Chellam and Krasner, 2001). Pourmoghaddas and Stevens 1995 have determined that the percentage of total THMs and HAAs in total organic halogen (TOX) also increases at higher bromide ion concentrations and pHs while the yields of HAAs decrease in these conditions (Hua et al., 2006; Pourmoghaddas and Stevens, 1995) (Figure 5).

The value of pH is a very important parameter that defines many aspects of DBP formation. Several studies have found that apparent rate constants for NOM reactions with bromine species increses in the pH range from 4 to 8. These studies also show that di- and trihalogenated DBP species containing bromine are more

noticeably affected by the pH compared with the formation of corresponding chlorinated species such as DCAA and TCAA (Acero et al., 2005; Cowman and Singer, 1995).

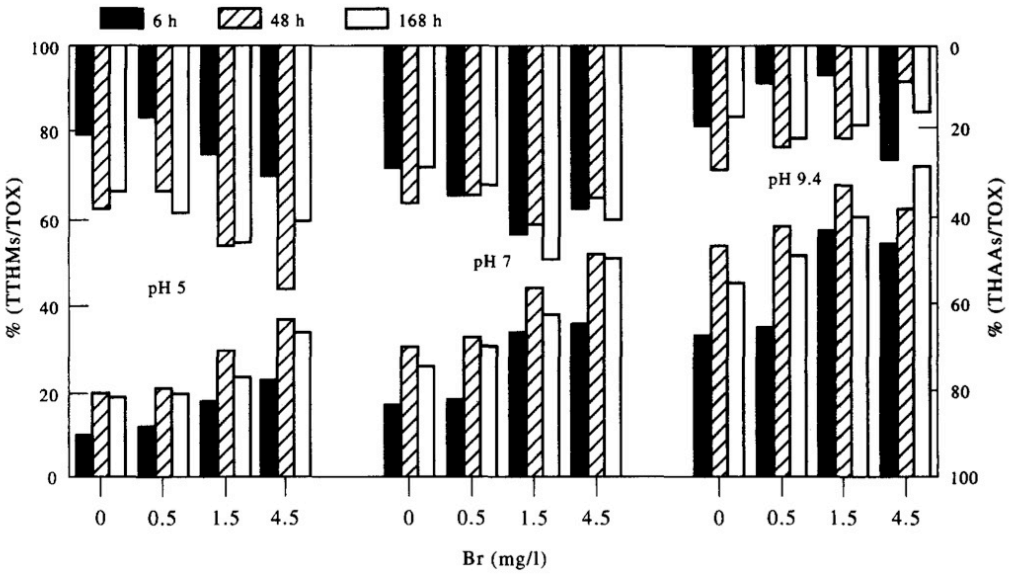

Figure 5 Relationship between total trihalomethanes(TTHMs) and total haloacetic acids (THAAs) as a percentage of total organic halogen (TOX). Adopted from Pourmoghaddas and Stevens, 1995.

Iodinated Disinfection By-products

Iodide and iodate ion are main inorganic species of iodine present in freshwater. The total of them concentration is range from 0.5 to 10 µg/L in water resources, when seawater intrusion of groundwater near the coast is result in elevated iodine concentration exceeding 50 µg/L (Bichsel and Von Gunten, 1999, 2000).

IO_3^- is not of toxicological concern because ingested iodate is rapidly reduced to I- in vivo by glutathione. On the other hand, iodide is oxidized to HOI by monochloramine, which can react with NOM.

Monochloramine have been widely used to reduce the production of regulated THMs and HAAs, but formation of iodinated DBPs in its presence may be more favorable because HOI has a long half-life that is affected by its disproportionation to I^- which may take up to 1 year. Iodinated DBPs have been reported to be represented by iodoacetic and similar iodinated acids (iodoacetic acid, bromoiodoacetic acid, (Z)-3-bromo-3-iodo-propenoic acid, (E)-3-bromo-3-iodo-propenoic acid and (E)-2-iodo-e-methylbutenedioic acid), iodo-trihalomethanes (iodoform, chlorodiiodomethane, bromodiiodomethane, dichloroiodomethane, dibromoiodomethane, and bromochloroiodomethane) and a wide range of unknown TOI (Bichsel and Von Gunten, 2000; Richardson et al., 2008). Iodinated DBPs are more cytotoxic and genotoxic than brominated or chlorinated DBPs due to the stronger releasing potential of the iodine atom. Several studies show that iodoform is 60 times and 146 times more toxic than bromoform and chloroform, respectively and iodoacetic acid is 3 times and 287 times more cytotoxic than bromoacetic acid and chloroacetic acid (Krasner et al., 1994; Plewa et al., 2004; Richardson et al., 2007). In addition to their toxicity, I-THM have very low odor and taste threshold. They impart a plastic or medicine-like taste when iodoform is at a concentration as low as 5 μg/L (Cancho et al., 2001).

Several researchers have analyzed factors that affect the formation of I-THM, primarily in the case of chloramination which favors the formation of HOI and results competing kinetics of iodine oxidation and NOM substitution (Hua

and Reckhow, 2007; Jones et al., 2012). The value of pH, NOM character, ratios of bromide/iodide, bromide/NOM, and iodide/NOM are important for I-THM formation and speciation (Jones, 2009). The yield of I-THM has been observed to increase with decreased pH, increasing I-/DOC ratios. Elevated formation of I-THM has been observed for pH≥7.5. $CHCl_2I$ and CHBrClI tend to be the most dominant species formed at pH 6 and iodoform CHI_3 appear to be always the most important species for pH≥7.5. The formation of I-THM has also been observed to increase at higher bromide and iodide concentration at a fixed ratio of Br-/I- (Jones et al., 2011, 2012).

1.5 Effects of Disinfection on Absorbance and Fluorescence of NOM

NOM present in natural waters always contains various chromophores, typically dominated by aromatic groups. These groups are especially notable in humic molecules and they absorb visible and ultraviolet light. In addition, a small part of the absorbed energy is emitted back. These phenomena are responsible for NOM absorbance and fluorescence, which as discussed below is very sensitive to NOM halogenation processes.

UV absorbance of NOM

In principle, absorbance and/or fluorescence of NOM can be used to infer information about the involved NOM functional groups. NOM chromophores are dominated by both activated and non-activated aromatic ring but contributions of the former group are deemed to be more prominent. The absorbance of NOM can be easily measured although inorganic species such as nitrate can interfere at $\lambda<210$ nm. At higher wavelengths, the absorbance of natural waters is mainly defined by NOM.

Prior research has shown that UV spectra of humic species and NOM in general can be used to predict its reactions with disinfecting agents and coagulants (Korshin et al., 1996, 1997a). Most studies have used the monitoring of absorbance at a fixed wavelength of 254 nm which is deemed to be a reasonably good indicator of NOM concentration. On the other hand, value of DOC-normalized absorbance or SUVA at 254 nm are indicative of the aromatic character of the NOM or contribution of the hydrophobic fractions of NOM to DOC (Novak et al., 1992; Traina et al., 1990).

The absorbance of NOM has been observed to change during reactions of chlorine with activated aromatic rings that are recognized to be DBP precursors that break down in NOM reactions with halogen species. Relationships between changes of UV absorbance of NOM and its reactions with chlorine with NOM have been assessed using absorbance at several wavelengths, for instance 254 and 272 nm. Several studies have attempted to correlate DBPs formation with the differential absorbance of NOM that is defined as shown in equation 7:

$$\Delta A_{\lambda} = A_{\lambda}^{chl} - A_{\lambda}^{initial} \qquad (7)$$

In this equation, ΔA_{λ} is the differential absorbance at wavelength λ, A_{λ}^{chl} is the absorbance after chlorination at wavelength λ, $A_{\lambda}^{initial}$ is the absorbance prior to chlorination at wavelength λ.

By definition, the differential absorbance of NOM becomes non-zero when the chlorine reacts with NOM destroying its chromophores and DBPs are formed as a result. Correlations between the formation of various DBPs and ΔA_{λ} have been reported in prior literature and they are frequently linear. For instance, (Korshin et al., 1997b) found the formation of chloroform and TOX correlate near-linearly with ΔA

$_{272}$, but this correlation is affected by pH in the case of chloroform but not in the case of the formation of TOX. A similar correlation was found for ΔA_{272} and other individual DBPs species. In all cases it was observed that individual DBP-ΔA_{272} relationships were more sensitive to site-specific characteristics of NOM and other water quality parameters as pH than the TOX-ΔA_{272} correlations.

For different water sources, the shape of differential absorbance spectra obtained for the chlorination of NOM has been reported to be highly reproducible (Korshin et al., 2002). In all, these data show that the differential absorbance of NOM can be an excellent indicator and a technique to monitor the chlorination of NOM and formation of DBPs due to its inherent sensitivity of NOM halogenation as well as simplicity of sample preparation and availability of the relevant equipment.

Fluorescence

Fluorescence methods can detect the emission of NOM even at its low concentrations, Fluorescence spectra of NOM can be affected by pH, ionic strength, temperature, and complexation between metal ions and NOM. Chlorination has also been shown to affect NOM fluorescence (Fabbricino and Korshin, 2004; Roccaro et al., 2009).

Like the chromophores which refer to the groups absorbing light, the functional groups contributing to emission of light are called fluorophores. In the case of NOM, the fluorophores are primarily a sub-group of phenolic groups in the humic part of NOM (Croue et al., 1999).

Several prior studies have examined correlations between DBP formation and NOM fluorescence (Hua et al., 2007; Marhaba and Kochar, 2000) but these

correlations may be complex. The intensity of NOM fluorescence is strongly associated with molecular weight of the molecules, their conformation, their complexation with metallic ions and with other organic molecules (Puchalski et al., 1992). Fractions of NOM with lower average molecular weights tend to have higher emission excitation and emission intensity (Chen et al., 2003; Hautala et al., 2000; Peuravuori et al., 2002).

The phenolic nature of NOM fluorophores means that NOM fluorescence can be used to monitor NOM changes during chlorination, and such changes can be expected to be related to chlorine demand and DBP formation (Beggs et al., 2009). Recent studies have confirmed this point and presented the relationships between DBPs formation and changes of NOM fluorescence that were measured using several parameters such as the position of the half maximum of the fluorescence intensity $\lambda_{0.5}$ and change of fluorescence intensity ratio of $\Delta(I_{500}/I_{400})$ (Fabbricino and Korshin, 2004; Roccaro et al., 2009). Other studies of NOM fluorescence showed that the oxidation of NOM with ClO_2 and O_3 also results strong changes of NOM fluorescence indicating that the occurrence of a break-up of organic molecules to smaller fractions and less aromatic structures (Świetlik and Sikorska, 2004).

1.6 Objectives of the Study

Reactions between activated aromatic units in NOM and disinfectants causes the absorbance of NOM to decrease. These changes quantified via the use of differential absorbance (ΔA_{254}, ΔA_{272}) have been shown to be well correlated with the concentrations of TOX , THMs and HAAs (Korshin et al., 1997a, 1997b, 2002). These correlations are reproducible and applicable to a wide variety of water sources and a wide range of halogenation conditions.

Changes of fluorescence of NOM are also affected by reaction of the phenolic chromophores with disinfectants, and several parameters of NOM fluorescence ($\lambda^{em}_{0.5}$, $\Delta(I_{500}/I_{400})$) are well correlated with the formation of individual DBPs (Fabbricino and Korshin, 2004; Roccaro et al., 2009).

One of the goals of this study is to evaluate in more detail changes of UV absorbance, fluorescence and, in some extent, concentrations of DBPs at varying concentration of bromide and chlorination reaction times. .

Another objective of this study is to assess the changes of NOM absorbance and fluorescence in the case of chloramination in the presence of different iodide concentrations. While the interest to the kinetics and outcomes of NOM iodination has been rapidly growing, information concerning effects of iodination on NOM fluorescence and absorbance is practically absent.

CHAPTER 2 MATERIALS AND METHODS

2.1 Water sources

Experiments carried out in this study used three water matrixes containing different types of natural organic matter (NOM). One of them was water collected from Lake Washington, which is a large freshwater lake in the bounds of the metropolitan city of Seattle. The sampling site was close to the University of Washington Waterfront Activity Center. Lake Washington water was sampled twice, in February and June 2012. Water from Lk. Washington was collected into pre-cleaned 5-gallon plastic carboys and transported immediately to the research laboratory of the Department of Civil and Environmental Engineering of the University of Washington. It was filtered through a sequence of 5 μm, 1μm and 0.45μm filters before use. This was done in the context of independent experiments designed to quantify effects of hardness cations on the spectroscopic properties of NOM.. DOC concentrations in these samples were 2.35 mg/L and 3.65 mg/L, respectively.

Another types of NOM was standard Suwannee River Fulvic acid (SRFA) and Nordic NOM (NNOM) purchased from the International Humic Substances Society (IHSS). Properties of SRFA and NNOM are described in considerable detail in the relevant Web pages of IHSS

(http://www.humicsubstances.org/acidity.html).

2.2 Glassware preparation

All glassware was cleaned with detergent (Alconox) and tap water and rinsed thoroughly with de-ionized water (DIW). Glassware which was used to analyze THMs and HAAs was soaked in 10% nitric acid (HNO_3) for 3 hrs, rinsed

with DIW and then with methanol following which it was allowed to dry in a fume hood before use.

2.3 Materials

Glassware for sampling and extraction was obtained from VWR (West Chester, PA). All deionized water (DIW) was produced by a Barnstead Easypure (Dubuke, IA). Sodium phosphate, (monobasic dehydrate salt $NaH_2PO_4 \bullet 2H_2O$) and sodium phosphate (dibasic anhydrous salt Na_2HPO_4) used to prepare phosphate buffer were purchased from JT Baker (Phillipsburg, NJ). Anhydrous sodium sulfite (Na_2SO_3, ACS) that was used as a quenching agent was purchased from Fisher Scientific (Fair Lawn, NJ). Sodium bromide (≥99.0% NaBr) and sodium chloride (≥99.0%NaCl) were obtained from Sigma-Aldrich. Sodium hypochlorite solution (5% available chlorine NaOCl) was obtained from JT Baker (Phillipsburg, NJ). Iodine (99.8% I_2, ACS reagent grade) was acquired from ACROS (NJ). 2,3-dibromopropionic acid solution (1000 µg/mL in methyl tert-butyl ether, analytical standard) that was used as an internal surrogate additive was obtained from Sigma-Aldrich. EPA 552.2 haloacetic acids mix (2000 µg/mL each component in methyl tert-butyl ether, analytical standard) that was diluted to levels needed to prepare HAAs calibration standard solutions was obtained from Sigma-Aldrich. Methanol (MeOH) and sodium sulfate (Na_2SO_4) were obtained from VWR (West Chester, PA). Methyl tertiary-butyl ether (MtBE) and pentane that were used as extraction solvents and to prepare standards were obtained from VWR (West Chester, PA). EPA 551A halogenated volatiles mix (2000 µg/mL each component in acetone, analytical standards) that was diluted to prepare THMs calibration standard solutions was obtained from Sigma-Aldrich. 1,2-Dibromopropane(97%) used as the internal standard in the EPA

551A determinations was purchased from Sigma-Aldrich. Sulfuric acid (95-98% H_2SO_4) used to acidify the extraction solution during analysis for HAAs and sodium bicarbonate ($NaHCO_3$) were purchased from JT Baker and Sigma-Aldrich, respectively. Anhydrous magnesium sulfate (≥99.5% $MgSO_4$) used as a drying agent was obtained from Sigma-Aldrich.

2.4 Experimental methods

General conditions

All experiments were carried out at pH 7 in the presence of phosphate buffer whose concentration was 7.5 mmol/L in all samples except those used to examine pH effects. All solutions also contained 0.001 mol/L sodium chloride to maintain a constant ionic strength and predictable speciation of chlorine and, when applicable, bromine species.

Free chlorine stock solution was prepared by dilution of reagent sodium hypochlorite solution (5% available chlorine) with Milli-Q water. The solution was standardized by the DPD Colorimetric Method (Standards Method 4500-CL G) after the instrument was calibrated with potassium permanganate solution.

All experiments were conducted at room temperature (15-20°C) in the closed system. NOM stock solutions were stored at 4°C. Lk. Washington water, SRFA, Nordic NOM solutions were allowed to react with added chlorine for up to 8 hours. Aliquots that were processed to determine their UV and fluorescence spectra as well as concentrations of HAAs and THMs were collected at contacts times of 0, 5, 10, 20, 30 and 60 minutes, and then at 2, 4 and 8 hours. All samples taken at these times were quenched with sodium sulfite (frequently preparing sodium sulfite to avoid oxidation by oxygen) which was added in a slight excess over the specified stoichiometric ratio. In most cases, measurements of the UV

absorbance and fluorescence were carried out immediately after sampling. THMs and HAAs analyses of the samples were conducted within 14 days after the samples collection, storage in the refrigerator.

Experimental procedures

The entire experimental process is illustrated in the figure below (Figure 6). In all cases, halogenation experiments were performed using a 4-liter amber bottle that was closed to the atmosphere.

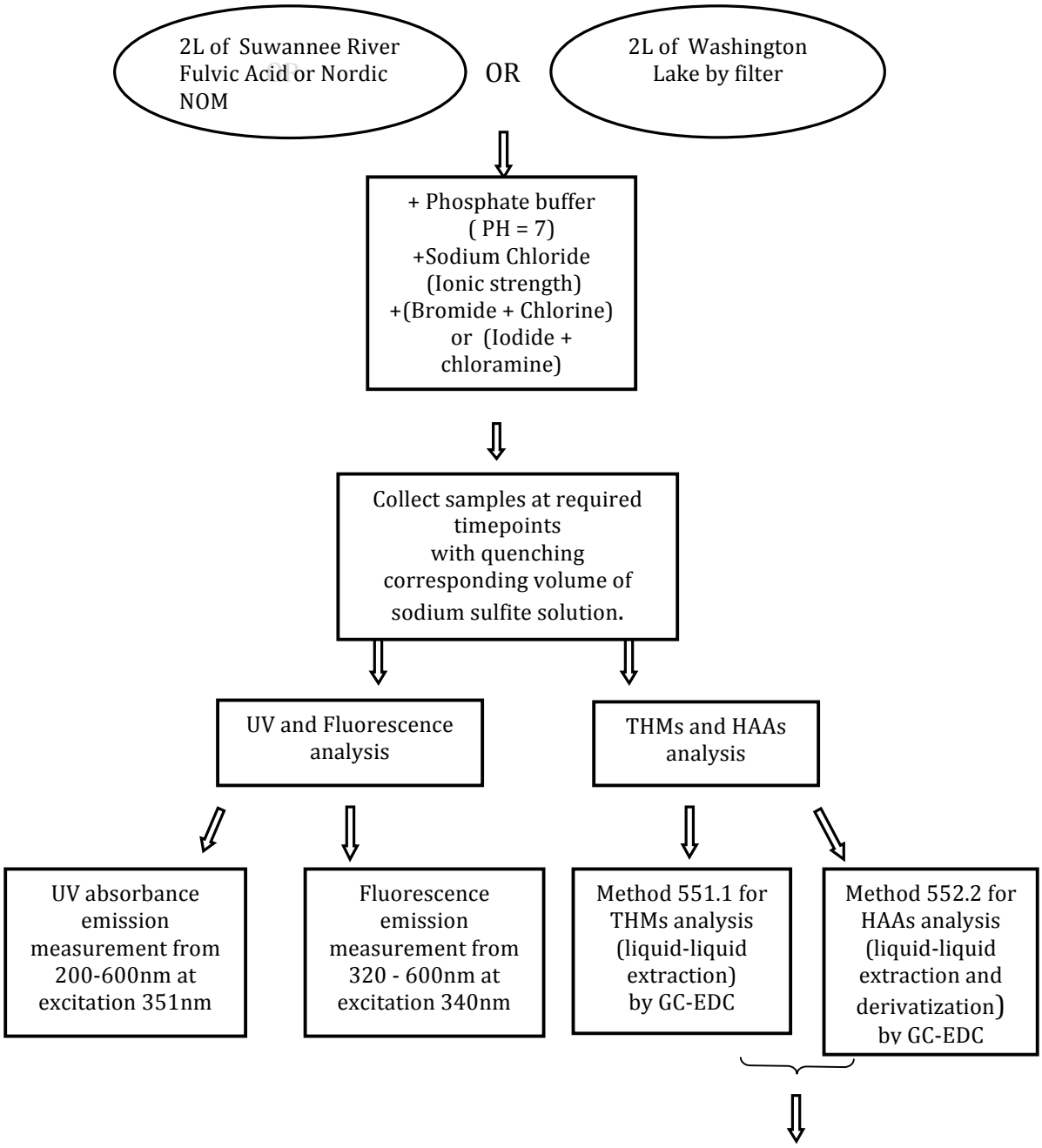

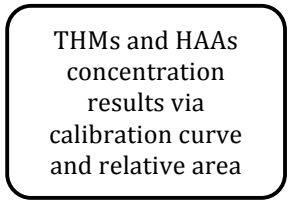

Figure 6 Experimental sampling procedure diagram.

Sampling

Halogenation experiments were performed as follows. 2 L Lake Washington water (or SRFA or NNOM solution) was placed in a 4L amber glass bottle to which appropriate volumes of stock solutions (0.3M phosphate buffer, 1M sodium chloride, 200 mg/L bromide, chlorine (or 100mg/L iodide and chloramine)) were added. The solution was completely mixed and capped with a 40mL dispenser. At time zero, a requisite amount of chlorine (or chloramine) was added. Following this, 160 mL of samples for various analyses were collected at reaction times described above and quenched with sodium sulfite. For each time point, samples to be analyzed for THMs and HAAs were collected into two headspace free 40mL glass vials fitted with a Teflon-sealed cap. Sample for absorbance and fluorescence measurements were collected into 40 mL glass vials and measured immediately.

2.5 Analytical procedures

Dissolved organic carbon (DOC), Ultraviolet Absorbance and Fluorescence

Dissolved organic carbon was measured with an Shimazu TOC Analyzer. Absorbance spectra were measured with a PerkinElmer Lambda 18 instruments

using a 5 cm quartz cell. Wavelengths were scanned from 600 nm to 200 nm. The instrument baseline was set up with DI water before each set of measurements.

Fluorescence

Fluorescence spectra were acquired using a Perkin Elmer LS-50B fluorimeter as a 1 cm rectangular quartz cell. Conventional (2D) emission spectra were acquired with a 320 or 340 excitation wavelength, with emission wavelength 340 to 600 nm. 3D excitation emission matrixes (EEM) were generated using a 240 to 275 nm range of wavelengths, (a 5 nm increment) while the range of emission wavelengths in these measurements was 270 to 600 nm. The spectra were routinely processes to correct for non-specific Raman scattering which was measured using DI water. In 3D EEM measurements, all data for emission wavelengths less or equal to that of the excitation were excluded. Likewise, the data for emission wavelengths exceeding or equal to the double of the excitation wavelengths were excluded. This was done to exclude results affected by the very intense light through the system at these conditions.

Modified Method 551.1 for Analysis of Trihalomethanes (THMs) and 552.2 for Analysis of Haloacetic Acids (HAAs)

Analyses for THMs and HAAs were performed with a Shimazu GC-2010 Plus gas chromatograph equipped with an electron capture detector (GC-EDC)

Supplies needed for these analyses included 10-100 µL micropipetters fitted with clean glass capillary tips, eight 100-mL glass volumetric flasks and glass stoppers, clean 40-mL glass vials with Teflon-lined silicone septa screw caps, 10 mL glass beaker, 10-mL pump pipetting dispenser fitted to a 500-mL

bottle, disposable glass Pasteur pipettes, amber glass chromatography autosampler vials with rubber/TFE aluminum seals, graduated round-bottom centrifuge tubes with Teflon-Lined Screw Caps15mL, a hand crimper for sealing gas chromatography autosampler vials and a vortexer.

Trihalomethanes (THMs) Analysis

Preparation of THM calibration solutions. Initially, 25mL of 0.3 mol/L phosphate buffer and 1mL sodium sulfite (1 mol/L) were added in a 1 L volumetric flask, which was then filled with DI water to the mark. This solution was used to fill to the mark eight 100 mL volumetric flasks, to which a measured amount of the calibration standard #1 20µg/mL and #2 100µg/mL was injected using a gas-tight syringe. The table below shows for calibration value and calibration standard volume.

Table 1 Calibrations conditions for THM measurements

		Calibration standard #2		Calibration standard #1		
Calibration concentration	0µg/L	2.5µg/L	10µg/L	30µg/L	70µg/L	100µg/L
Calibration standard volume	0µL	12.5 µL	50 µL	30µL	70µL	100µL

20 mL aliquots of all calibration solutions were transferred into 40 mL clean glass vials. Additional two vials, one for matrix spike analyses and a matrix spike duplicate, calibration point should have duplicate point. Matrix spike (MS) and matrix spike duplicate (MSD) were prepared as follows: 30 µL calibration standard # 2 was added into 20 mL samples that were labeled as matrix spike

and matrix spike duplicate, respectively, They were used to determine the THMs recovery. Theoretically, MS and MSD samples were expected to have 30 µg/L more THMs than the same sample without injected calibration standard.

Extraction

THM extraction included the following procedures. First, 250 mL internal standard extraction solution (50 µg/L internal standard in pentane) was added to a bottle fitted with a dispenser, which was flushed to ensure any bubble possibly present in the pump. Following this, 4 mL of the internal standard extraction solution was carefully pipetted into each 20 mL samples, calibration solutions, matrix spike and matrix spike duplicate. Two layers were formed as a result, the top layer was organic pentane layer and the bottom layer was the aqueous solution.

Approximately 6 g of pre-baked sodium sulfate (Na_2SO_4) was added into 20 mL vials containing the internal standard extraction solution and vortexed immediately for 1 minute to prevent the clumping of the added sodium sulfate. Sodium sulfate is dosed using a 10mL glass beaker marked to a 6 grams level.

The samples were allowed to stand for 5 minutes to form the two layers to separate and dissolved sodium sulfate to settle to the bottom of the vials. Using a disposable glass Pasteur pipette, approximately 1.5 ml from the middle of the pentane layer was transferred into a clean GC autosampler vial, tightly capped and crimped with a hand crimper. Care was taken to avoid transferring from water and sodium sulfate crystals from the vial as they could damage the GC.

The prepared vials and those with the internal standard extraction solution were placed into the autosampler vials to begin GC analyses. If not

measured immediately, the extracts could be stored in a lab freezer at -15 °C for 14 days.

Haloacetic Acids (HAAs) Analysis

Calibration solutions and samples preparation. Prepare calibration solutions were prepared as follows. 25mL phosphate buffer 0.3mol/L and 1mL sodium sulfite 1mol/L were added in a 1L volumetric flask and fill with DI water to the mark. This solution was used to fill eight 100 mL volumetric flasks on the mark. A necessary amount of the calibration standard (20µg/mL) was injected into the solution by a gas tight syringe. The relevant volumes and concentrations are shown in the table below.

Table 2 Calibration conditions for HAA measurements

Calibration concentration	0µg/L	2.5µg/L	10µg/L	30µg/L	70µg/L	100µg/L
Calibration standard volume	0µL	12.5 µL	50 µL	150µL	350µL	500µL

20 mL aliquots from all calibration solutions were transferred into 40 mL clean glass vials, with two additional vials with matrix spike and matrix spike duplicates. Matrix spike (MS) and matrix spike duplicates (MSD) were prepared by adding 30µL calibration standard # 2 into 20 mL samples (labeled MS and MSD) prepared for determining HAAs recovery. As was the case with THMs, MS and MSD concentrations were expected have 30 µg/L more HAAs than same sample without injected calibration standard.

20µL of the acid surrogate additive standard (20µg/mL in MtBE) was injected into all 20 mL samples that included the selected calibration points,

samples and matrix spike samples. 1mL 98% H_2S0_4 added to all these samples following which the samples were capped and shaken.

Extraction

The extraction procedure was similar to that described above for THM analyses but MtBE was used as a solvent instead of pentane. In these procedures, 250 mL internal standard extraction solution (50µg/L internal standard in MtBE) was added to a bottle fitted with a dispenser and carefully pipetted to dispense 4mL internal standard extraction solution into the 20 mL vials. Two layers were formed, a MtBE top layer and an aqueous bottom layer. Their further processing with sodium sulfate and transfers were similar to those for THMs, with some differences described below.

Derivatization

Using a disposable glass Pasteur pipette, approximately 3 ml from the upper MtBE layer was transferred to a round-bottom centrifuge tube to which approximately ½ of a small round scoop of anhydrous, powdered magnesium sulfate $MgSO_4$ was added directly. 1mL 10% H_2SO_4/methanol solution was added to each round-bottom centrifuge tube which was capped and placed in a heating block maintained at 50°C and kept there for 2 hours. Following this, the centrifuge tubes were removed from the heating block and allowed to cool for 30 minutes before opening the cap.

4mL saturated sodium bicarbonate solution was added to each centrifuge tube which was shaken for two minutes to release the evolved CO_2. Using a disposable glass Pasteur pipette, approximately 1mL of the upper MtBE layer was transferred from centrifuge tube to an autosampler vial which was tightly

capped and crimped with a hand crimper. Unless analyzed immediately, the extracts could be stored in a lab freezer at -15 °C for 14days.

CHAPTER 3 EFFECTS OF BROMIDE ON ABSORBANCE AND FLUORESCENCE OF NOM AND FORMATION OF BROMINATED DISINFECTION BY-PRODUCTS

3.1 Changes of Absorbance of NOM Caused by Chlorination in the Presence of Bromide

Experiments described in this section address effects of chlorination carried out at varying bromide concentration on the changes of absorbance and fluorescence spectra of several sources of NOM. These include isolated Suwannee River fulvic acid (SRFA) and Lake Washington water sampled during the spring and summer 2012 respectively.

Prior research has shown that the absorbance of natural water at λ>250 nm is almost solely defined by the aromatic functional groups of humic substances. During disinfection (chlorination or chloramination) of NOM, chlorine tends to selectively attack activated aromatic rings in NOM, which are also the chromophores detected by absorbance measurements breaking them and decreasing the intensity of NOM absorbance.

The technique of differential absorbance spectroscopy has been proven to be useful for probing changes of NOM properties in many reactions, notably in chlorination (Korshin et al., 2002, 2007). And the differential absorbance when NOM-exiting natural water is chlorinated has several features, the values of differential absorbance are always negative, almost well-defined peaks are around 272 nm, and the intensity of absolute differential absorbance is monotonic increasing over time or increasing chlorine dose.

Effects of chlorination and bromination on the absorbance spectra of Suwannee River Fulvic acid (SRFA)

Absorbance spectra for SRFA (DOC 5mg/L) reacting with chlorine at varying contact times are shown in Figure 6. The Cl_2: DOC ratio in this experiments was 1.1, pH 7 and bromide concentrations varied from 0 to 40 mg/L. This range of bromide concentrations was used to cover an exhaustively wide range of possibly involved bromine species.

In all cases, the halogenation of SRFA was accompanied by consistent changes of the absorbance that became more prominent with increasing contact time. This decrease was most prominent in the wavelength range around 250-400 nm.

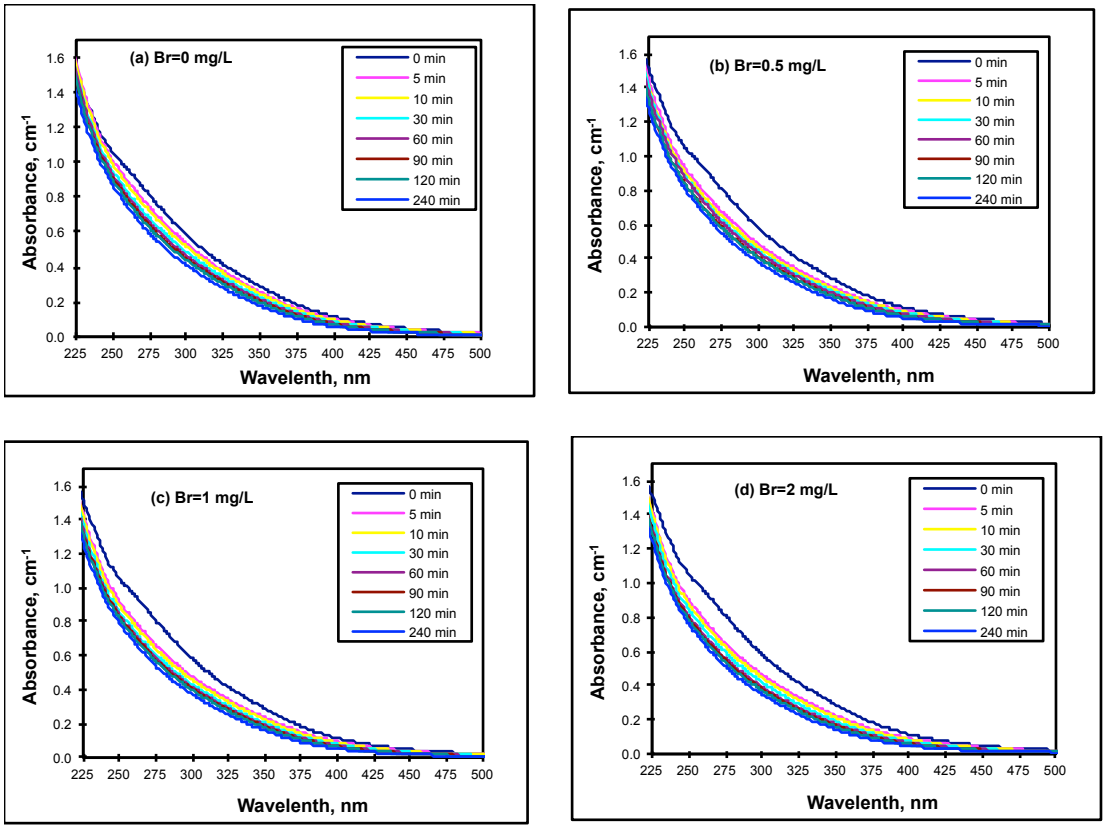

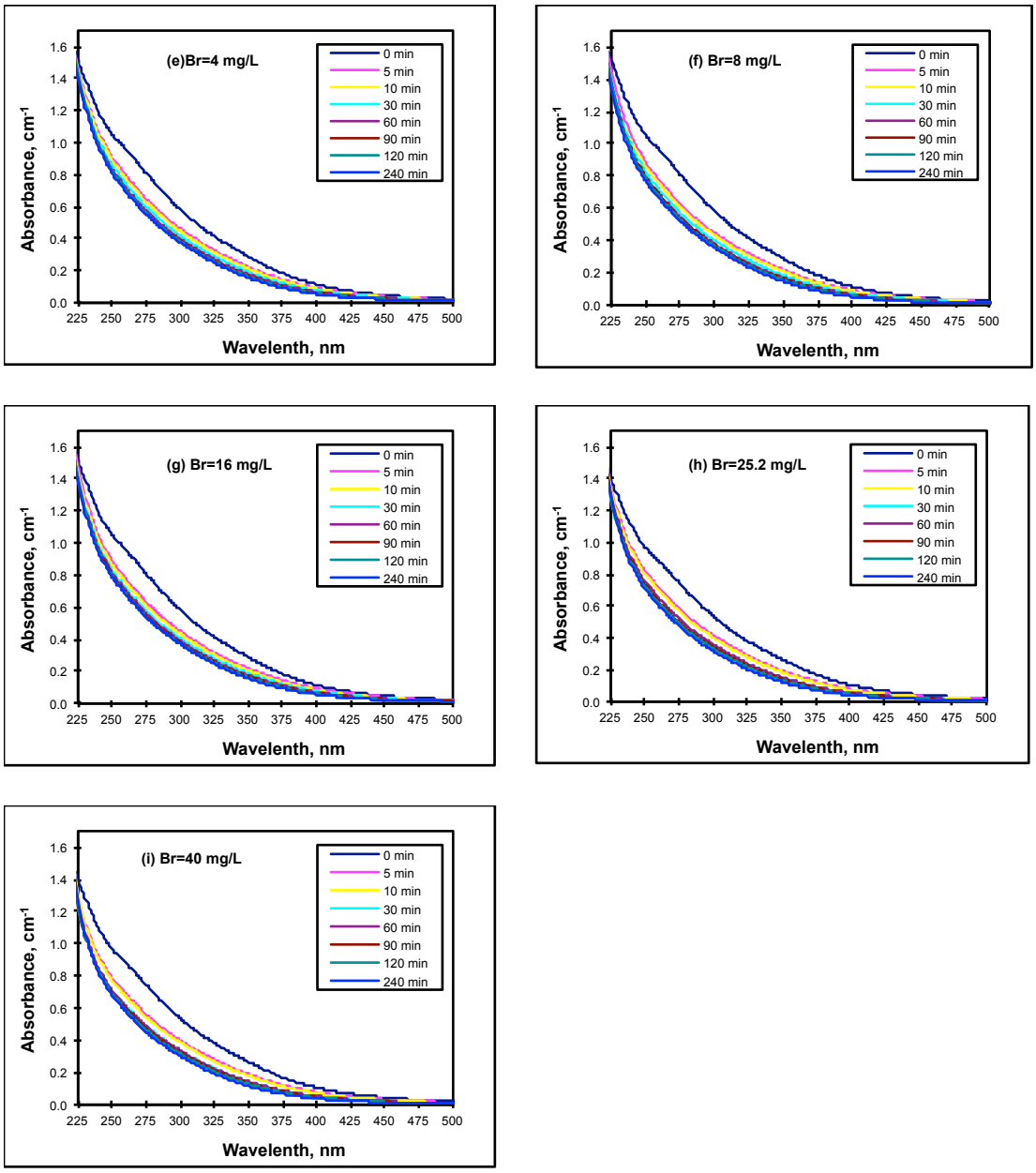

Figure 6 UV absorbance spectra of chlorinated SRFA chlorinated in the presence of varying bromide concentration, DOC 5 mg/L, chlorine to DOC ratios of 1.1 mg/mg, pH 7.0, reaction time from 5min to 4h, bromide concentrations: (a) 0 mg/L, (b) 0.5 mg/L, (c) 1 mg/L, (d) 2 mg/L, (e) 4 mg/L, (f) 8 mg/L, (g) 16 mg/L, (h) 25.2 mg/L, (i) 40 mg/L.

A set of differential absorbance spectra calculated for chlorinated SRFA using the data shown in Figure 6 are shown in Figure 7. The data show that the absolute values of differential absorbance (e.g., the intensity of the peak located at 265 nm) tended to increase somewhat as the bromide concentration increased but the overall

shape of the differential spectra did not undergo considerable changes. Kinetically, the intensity of differential absorbance relatively increased more rapidly in the initial phase of reaction (ca. initial 30 minutes) at increasing bromide dose but during the next phase of reaction effects of bromide were less obvious. As was mentioned above, the maximum of the differential spectra of SRFA was always located at ca. 265 nm.

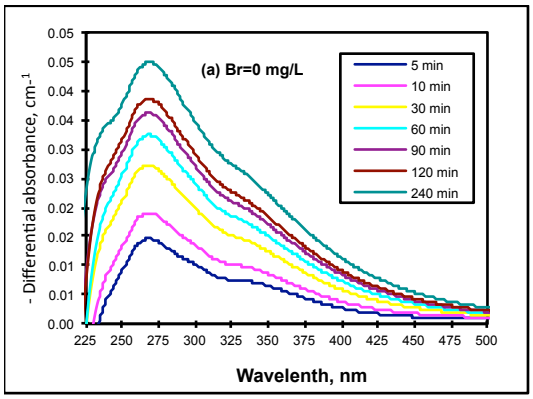

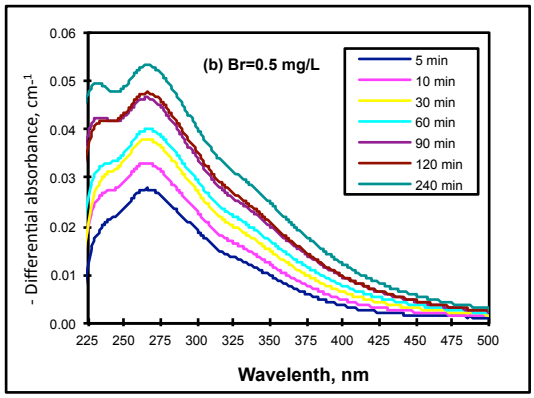

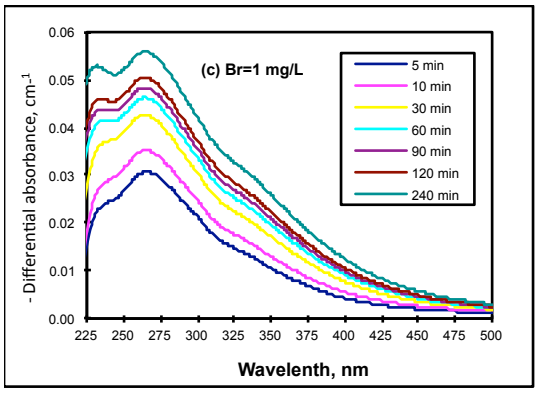

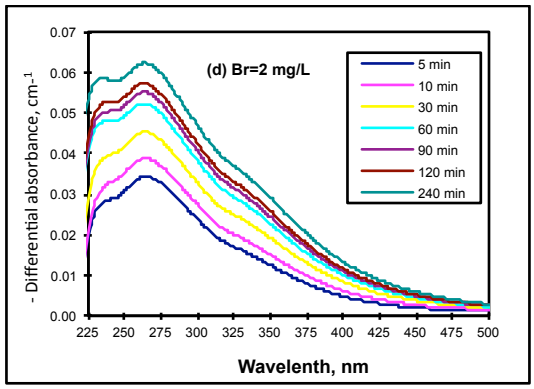

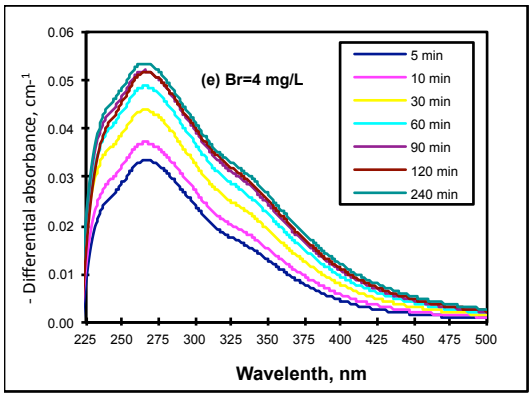

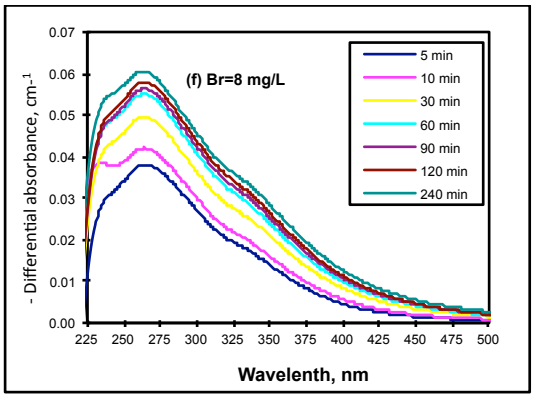

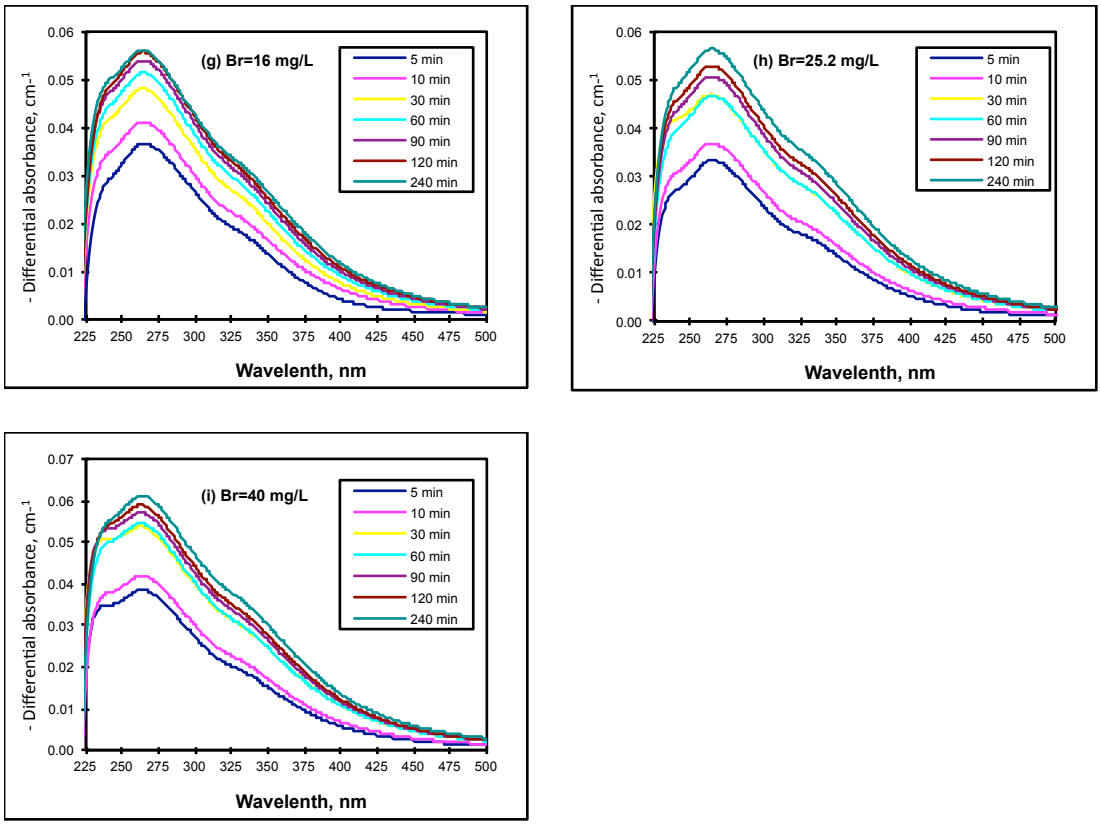

Figure 7 Differential absorbance spectra of chlorinated SRFA in the presence of varying bromide concentrations, DOC 5 mg/L, chlorine to DOC ratios of 1.1 mg/mg, pH 7.0, reaction time from 5min to 4h, bromide concentrations (a) 0 mg/L, (b) 0.5 mg/L, (c) 1 mg/L, (d) 2 mg/L, (e) 4 mg/L, (f) 8 mg/L, (g) 16 mg/L, (h) 25.2 mg/L, (i) 40 mg/L.

To examine effects of halogenation of the features of the absorbance spectra of SRFA that have lower initial intensities but are potentially more sensitive the changes of intrinsic SRFA chemistry brought about by its interactions with chlorine and/or bromine species, we used the method of differential log-processed spectra that calculates the value of $\ln(A/A_0)$. These values are zero if no change of absorbance takes place but they increase if the absorbance of SRFA (or any other NOM) at any selected wavelength changes relatively more prominently irrespective of its initial value. The method can examine a very wide range of absorbance values but its applicability depends on the precision of absorbance measurements which becomes critical in this case.

Figure 8 show the spectra calculated using this approach. These log-processed differential spectra show the presence of several features. The values of the log-transformed absorbance are positive (indicating an increase of absorbance) for wavelengths < 220 nm but this is caused by the presence of excess of sulfite used to quench chlorine. In the range of wavelengths ca. 230 to 270 nm, the values of differential logarithms of absorbance increase nearly linearly with the wavelength, and they exhibit a plateau for the range of ca. 270 to 320 nm. At higher wavelengths, the differential absorbance tends to increase linearly again. The data for wavelength > 400 nm are not shown in these figures due to an insufficient signal to noise ratio.

One important observations that be made based on the observation of the data shown in Figure 8 that while the magnitude of the log-transformed differential absorbance, especially that at wavelengths > 350 nm, tends to increase somewhat with the concentration of bromide, all the main features remain the same. On the other hand, the magnitude of differential $Ln(A/A_0)$ increased with increasing the reaction time similarly to the data for non-log transformed differential absorbance shown in Figure 7.

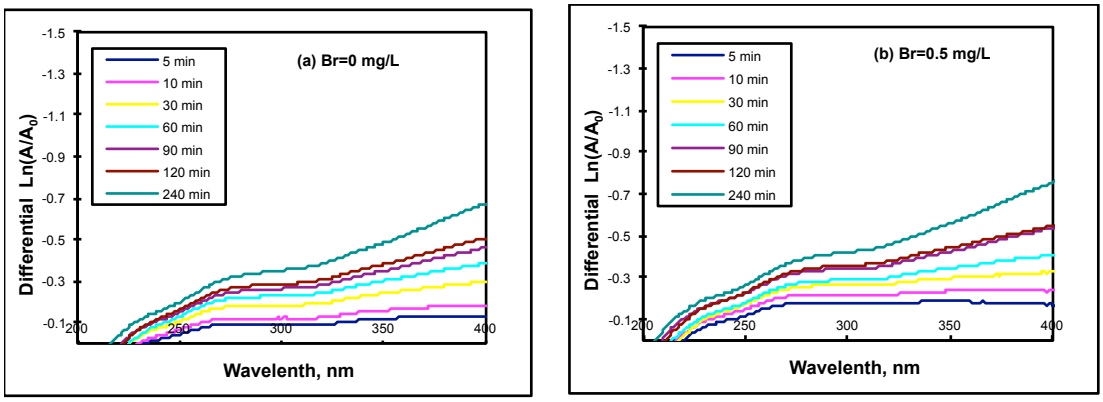

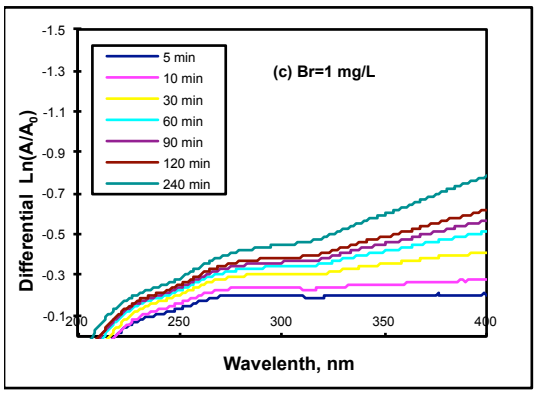
(c) Br=1 mg/L
5 min
10 min
30 min
60 min
90 min
120 min
240 min
Differential Ln(A/A0)
Wavelenth, nm

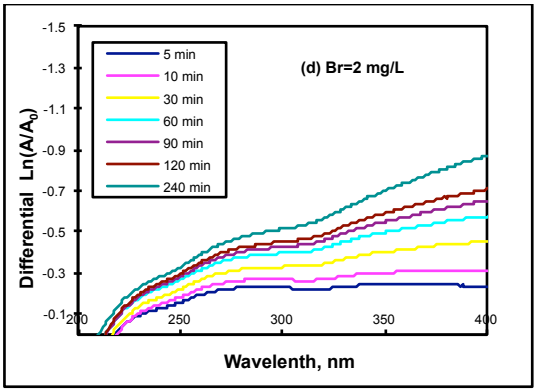
(d) Br=2 mg/L
5 min
10 min
30 min
60 min
90 min
120 min
240 min
Differential Ln(A/A0)
Wavelenth, nm

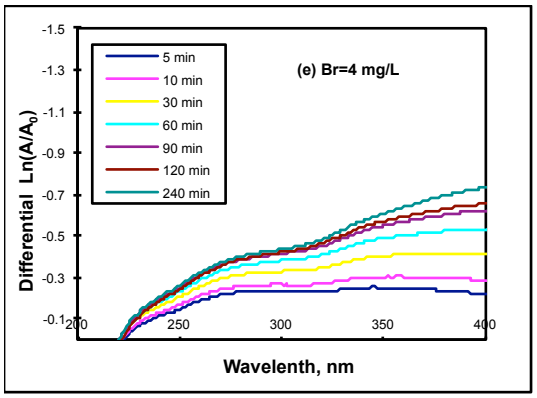
(e) Br=4 mg/L
5 min
10 min
30 min
60 min
90 min
120 min
240 min
Differential Ln(A/A0)
Wavelenth, nm

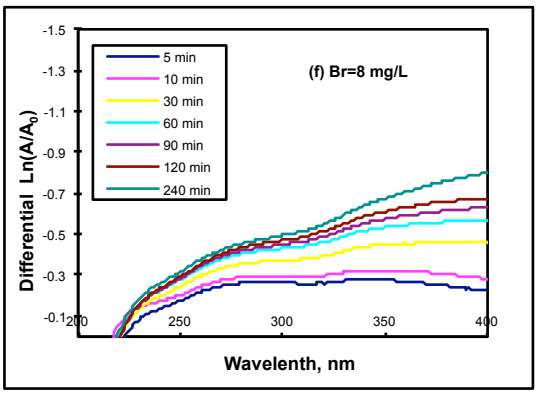
(f) Br=8 mg/L
5 min
10 min
30 min
60 min
90 min
120 min
240 min
Differential Ln(A/A0)
Wavelenth, nm

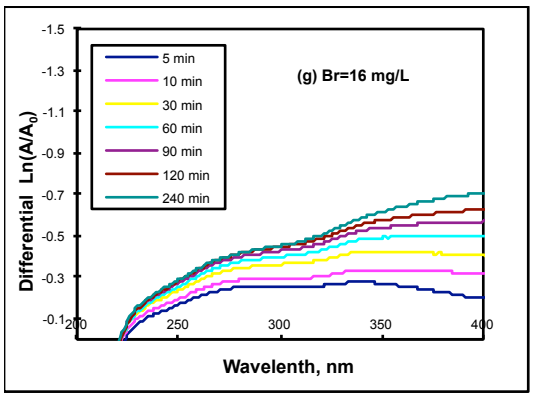
(g) Br=16 mg/L
5 min
10 min
30 min
60 min
90 min
120 min
240 min
Differential Ln(A/A0)
Wavelenth, nm

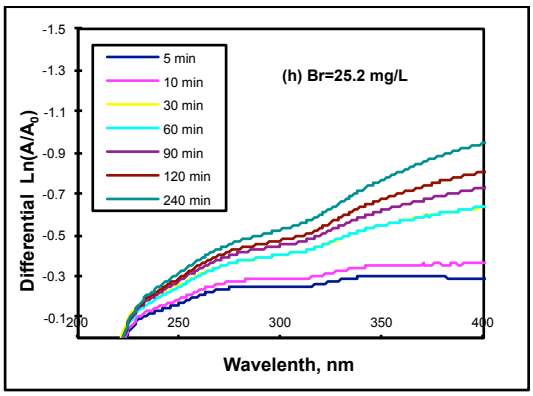
(h) Br=25.2 mg/L
5 min
10 min
30 min
60 min
90 min
120 min
240 min
Differential Ln(A/A0)
Wavelenth, nm

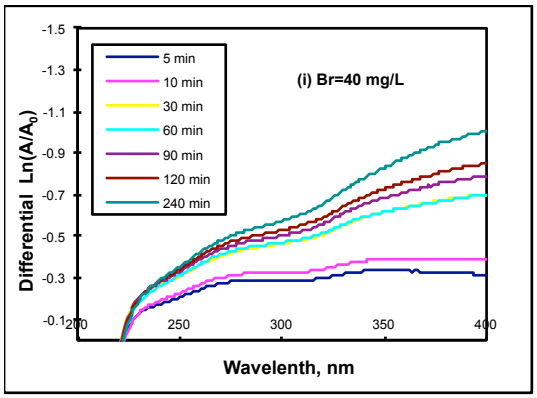
(i) Br=40 mg/L
5 min
10 min
30 min
60 min
90 min
120 min
240 min
Differential Ln(A/A0)
Wavelenth, nm

Figure 8 Differential Ln (A/A_0) of chlorinated SRFA in the presence of varying bromide concentrations, DOC 5mg/L, chlorine to DOC ratios of 1.1 mg/mg, pH 7.0, reaction time from 5min to 4h, bromide concentrations (a) 0 mg/L, (b) 0.5 mg/L, (c) 1 mg/L, (d) 2 mg/L, (e) 4 mg/L, (f) 8 mg/L, (g) 16 mg/L, (h) 25.2 mg/L, (i) 40 mg/L.

Effects of chlorination and bromination on the absorbance spectra of Lake Washington

Lake Washington was sampled twice in February and June 2012, and filtered through three filters, 5 µm, 1 µm and 0.45 µm respectively before chlorination. The DOC for these samples were 2.3 mg/L and 3.65 mg/L.

Absorbance results for Lk. Washington water sampled in February 2012

Halogenation experiments for this sample (DOC 2.3 mg/L, Cl_2/DOC ratio 1, pH 7) employed bromide concentrations ranging from 0 to 4mg/ L. Results of the relevant absorbance measurements are given in Figure 9. Comparison of these data with those for SRFA (Figure 6) show the presence on considerable similarities and also some differences. First, the magnitude of UV absorbance spectra of Lake Washington are lower than of SRFA. This is not surprising due to the lower DOC content and lower concentration chromophores present in Lk. Washington water. Still, halogenation of this water caused the absorbance to decrease, most noticeably in the range 250 to 400 nm, which is similar to what was observed for SRFA.

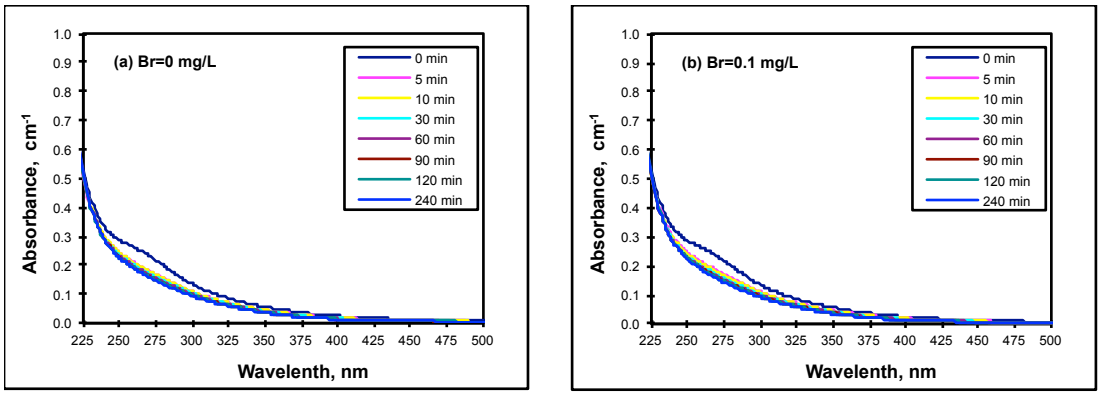

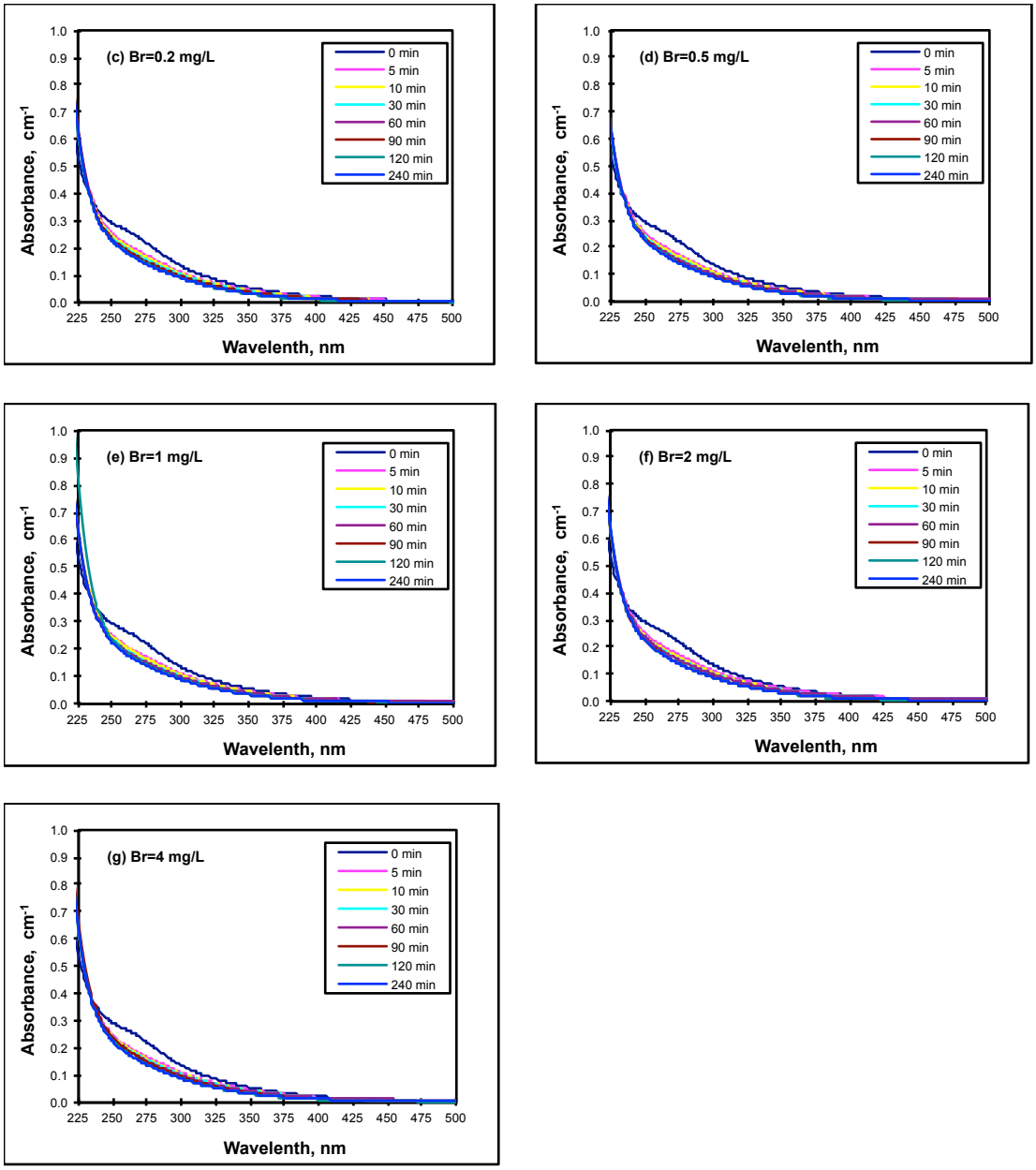

Figure 9 UV absorbance spectra of chlorinated Lake Washington (winter sampling) in the presence of varying bromide concentration, DOC 2.3mg/L, chlorine to DOC ratios of 1 mg/mg, pH 7.0, reaction time from 5min to 4h, bromide dose (a) 0 mg/L, (b) 0.1 mg/L, (c) 0.2 mg/L, (d) 0.5 mg/L, (e) 1 mg/L, (f) 2 mg/L, (g) 4 mg/L.

The differential absorbance spectra calculated for halogenated Lake Washington water behaved largely similar to those of SRFA, with their intensity consistently increasing with the reaction time. Increases of bromide were associated with some increases of the differential absorbance at 265 nm but this effects was not very prominent (Figure 10). The shape of the differential spectra of Lk. Washington

water was largely similar compared with that for SRFA but the band in the differential spectra in the former case was much narrower than in latter, and the shoulder located at ca. 350 nm that was fairly prominent in the differential spectra of SRFA was absence in the case of Lk. Washington water.

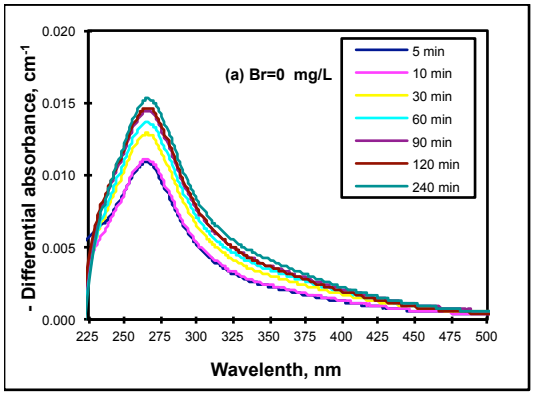

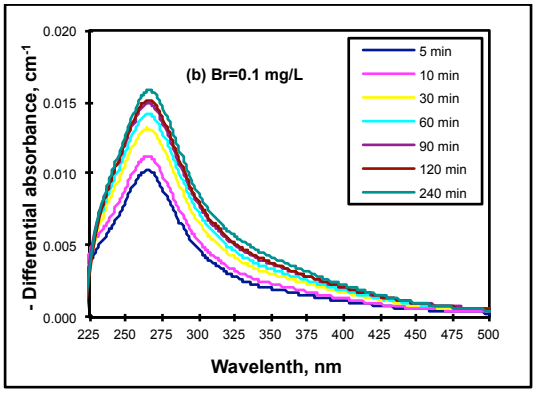

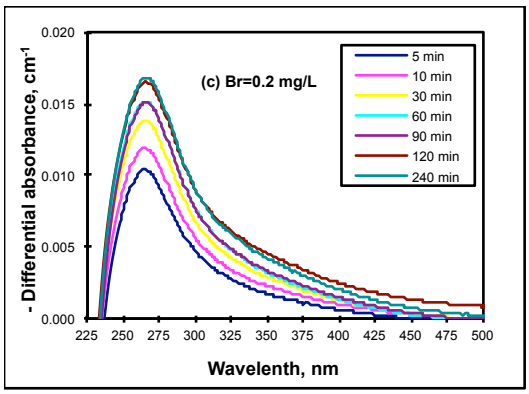

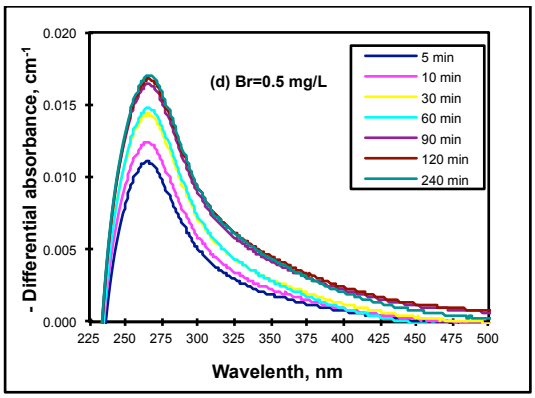

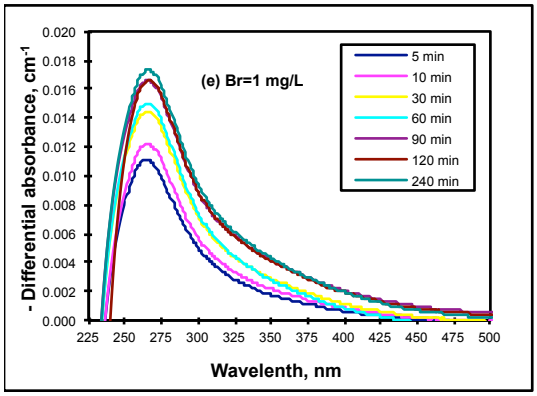

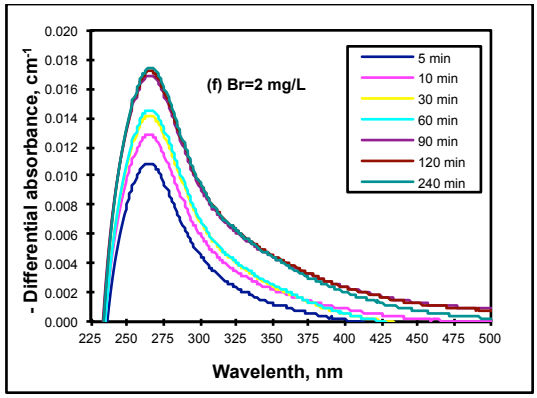

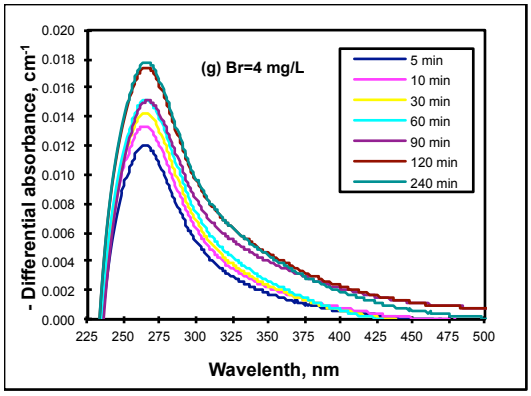

Figure 10 Differential absorbance spectra of chlorinated Lake Washington (winter sampling) in the presence of varying bromide concentrations. DOC 2.3mg/L, chlorine to DOC ratios of 1 mg/mg, pH 7.0, reaction time from 5min to 4h, bromide concentration (a) 0 mg/L, (b) 0.1 mg/L, (c) 0.2 mg/L, (d) 0.5 mg/L, (e) 1 mg/L, (f) 2 mg/L, (g) 4 mg/L.

Figure 11 shows the differential $\ln(A/A_0)$ spectra for Lk. Washington water obtained at varying reaction times and bromide doses. These spectra have largely the same characteristics as those of SRFA with the intensity of the differential Ln (A/A_0) spectra increased with increasing reaction time and higher bromide concentrations. However, the behavior of the log-transformed differential absorbance is less consistent at wavelengths > 350 nm – this is clearly caused by the limited precision of absorbance measurements for the relatively low DOC sample of Lk. Washington water. On the other hand, the peak of differential absorbance spectra at 265 nm shown in Figure 10 is also presence in the log-transformed spectra shown in Figure 11. It intensity is almost the same as that of the log-transformed spectra for wavelengths > 325 nm.

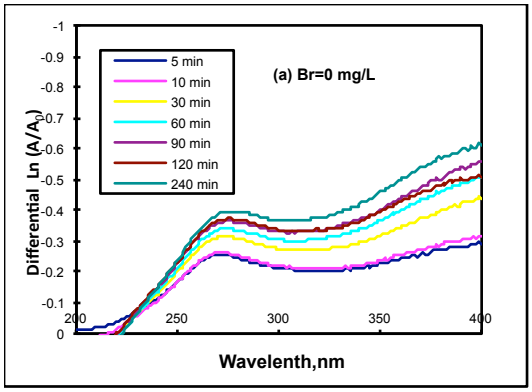
(a) Br=0 mg/L
5 min
10 min
30 min
60 min
90 min
120 min
240 min
Differential Ln (A/A0)
Wavelenth,nm

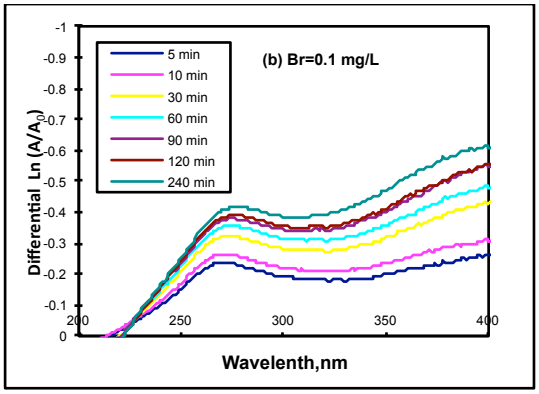
(b) Br=0.1 mg/L
5 min
10 min
30 min
60 min
90 min
120 min
240 min
Differential Ln (A/A0)
Wavelenth,nm

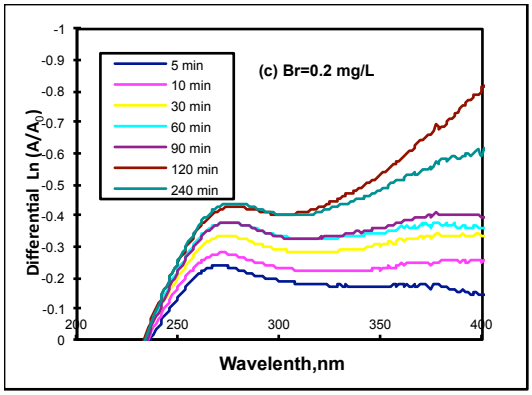
(c) Br=0.2 mg/L
5 min
10 min
30 min
60 min
90 min
120 min
240 min
Differential Ln (A/A0)
Wavelenth,nm

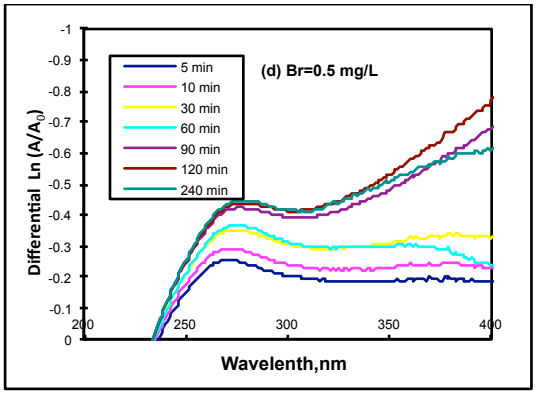
(d) Br=0.5 mg/L
5 min
10 min
30 min
60 min
90 min
120 min
240 min
Differential Ln (A/A0)
Wavelenth,nm

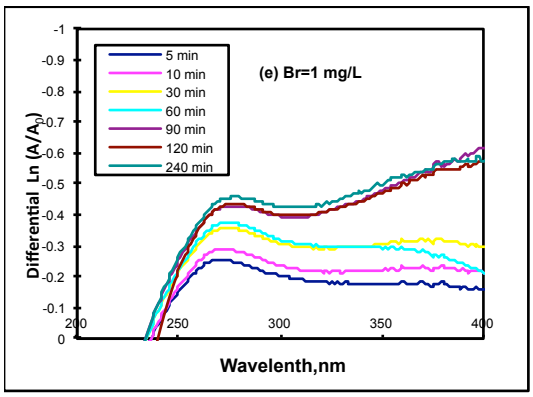
(e) Br=1 mg/L
5 min
10 min
30 min
60 min
90 min
120 min
240 min
Differential Ln (A/A0)
Wavelenth,nm

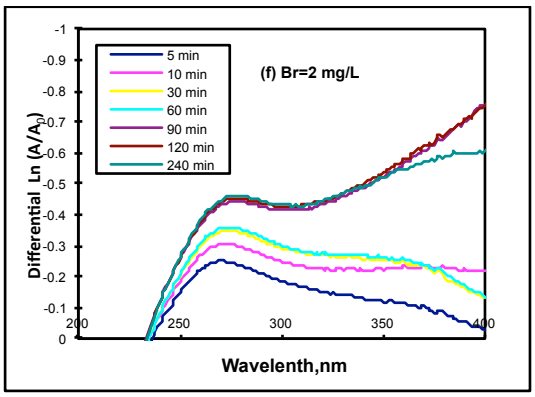
(f) Br=2 mg/L
5 min
10 min
30 min
60 min
90 min
120 min
240 min
Differential Ln (A/A0)
Wavelenth,nm

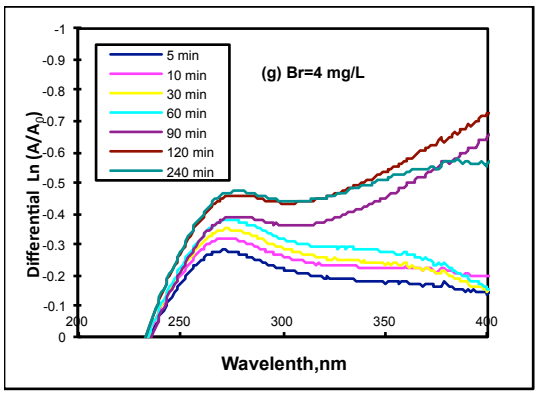
(g) Br=4 mg/L
5 min
10 min
30 min
60 min
90 min
120 min
240 min
Differential Ln (A/A0)
Wavelenth,nm

Figure 11 Differential Ln (A/A_0) of chlorinated Lake Washington (winter sampling) in the presence of varying bromide concentrations. DOC 2.3mg/L, chlorine to DOC ratios of 1 mg/mg, pH 7.0, reaction time from 5min to 4h, bromide dose (a) 0 mg/L, (b) 0.1 mg/L, (c) 0.2 mg/L, (d) 0.5 mg/L, (e) 1 mg/L, (f) 2 mg/L, (g) 4 mg/L.

Absorbance results for Lk. Washington water sampled in June 2012

Experiments with the summer samples of Lake Washington water (DOC 3.65 mg/L, Cl_2/DOC ratio 1, pH 7) were carried out using a narrower range of bromide, from 0 mg/L to 0.5 mg/ L. The resultant absorbance spectra are shown in Figure 12. Their features are largely the same as those for the other Lk. Washington sample with the main difference that absorbance in the summer sample are higher thus reflecting its higher DOC concentration.

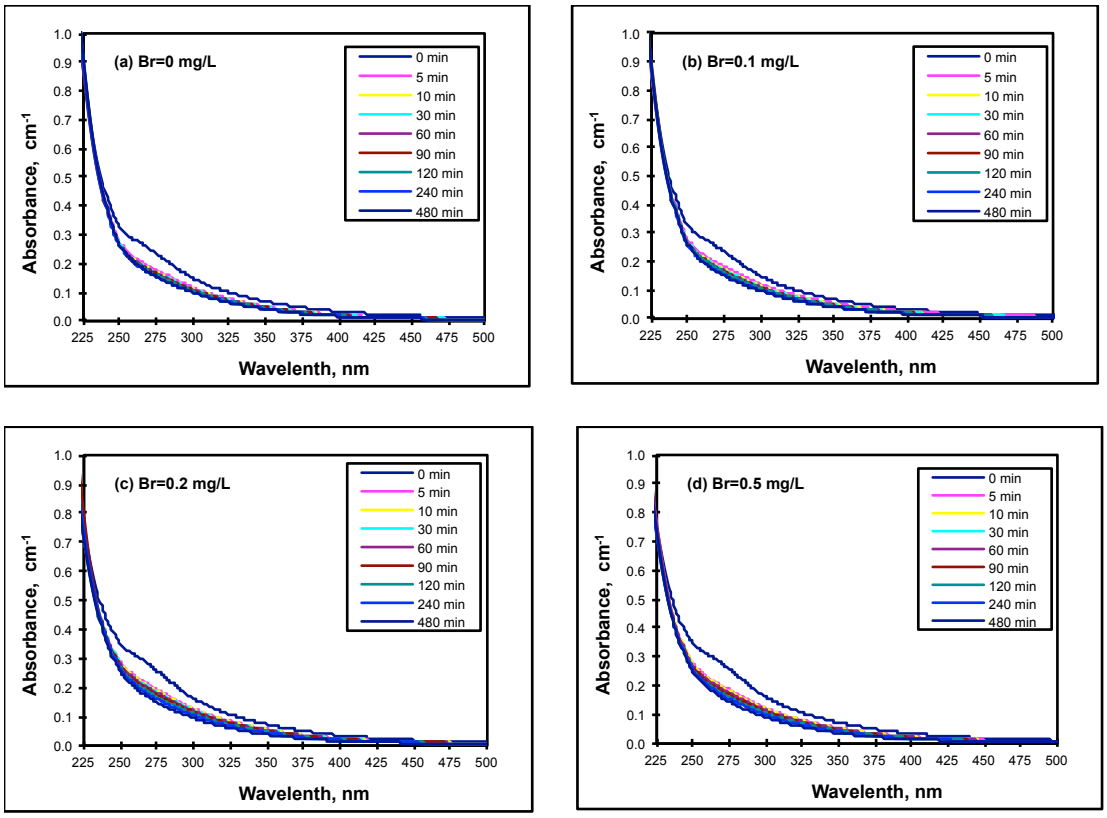

Figure 12 UV absorbance spectra of chlorinated Lake Washington (summer sampling) in the presence of varying bromide concentrations. DOC 3.65 mg/L, chlorine to DOC ratios of 2 mg/mg, pH 7.0, reaction time from 5min to 8h, bromide dose (a) 0 mg/L, (b) 0.1 mg/L, (c) 0.2 mg/L, (d) 0.5 mg/L.

Figure 13 shows differential absorbance spectra calculated using the data show in Figure 12. As was seen before for SRFA and the winter Lk. Washington sample, the intensity of differential absorbance increases as the concentrations of bromide increase. The shape of the differential spectra presented in Figure 12 is very similar to those shown in Figure 10. In both cases, they have important differences from the features seen in the differential spectra of SRFA thus revealing the site-specific nature of NOM chromophores affected by halogenation

.

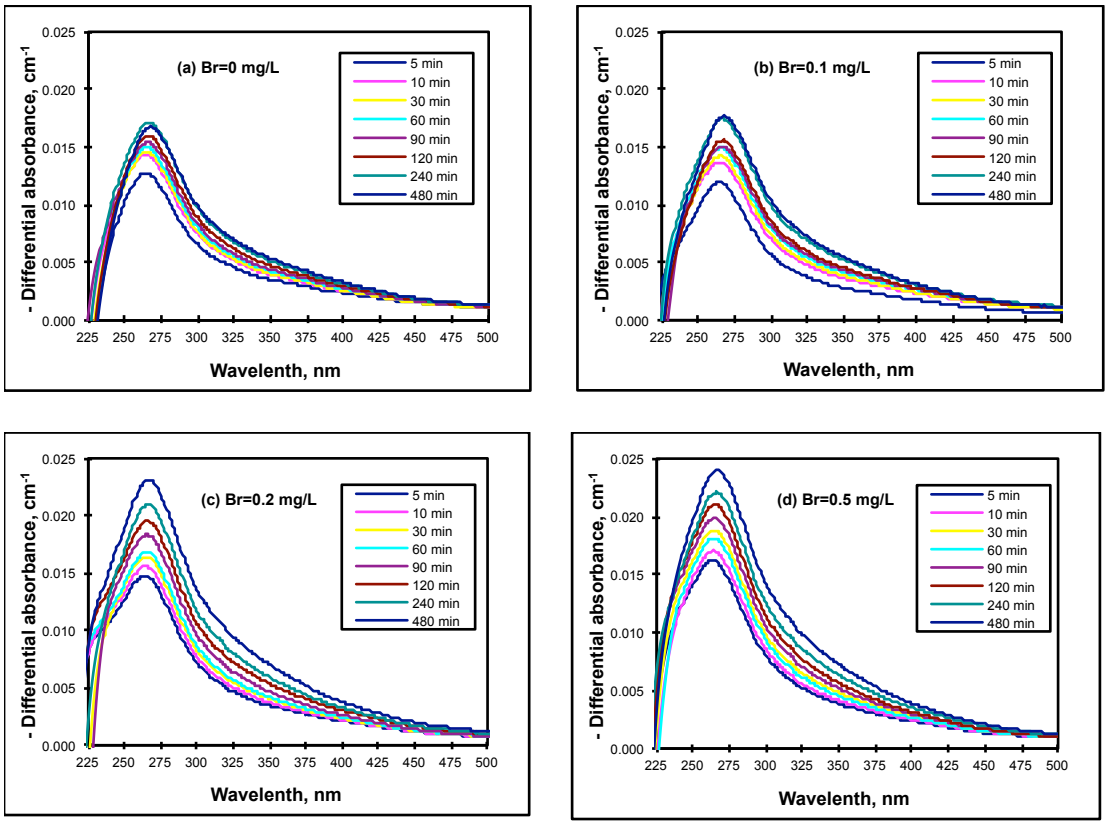

Figure 13 Differential absorbance spectra of chlorinated Lake Washington (winter sampling) in the presence of varying bromide concentration, DOC 3.65 mg/L, chlorine to DOC ratios of 1 mg/mg, pH 7.0, reaction time from 5min to 8h, bromide dose (a) 0 mg/L, (b) 0.1 mg/L, (c) 0.2 mg/L, (d) 0.5 mg/L.

Calculations of the log-processed differential $\ln(A/A_0)$ spectra for the summer sample of Lk. Washington water showed results similar to those presented in Figure 11. However, changes of the log-processes differential spectra in the winter sample

were consistent and prononounced, especially in the range of wavelengths > 300 nm (Figure 14). Otherwise, their shape remains quite consistent for varying reaction times and bromide concentrations. The data appear to indicate that chlorination and bromination of NOM cause largely identical changes of its absorbance spectra for a given NOM type.

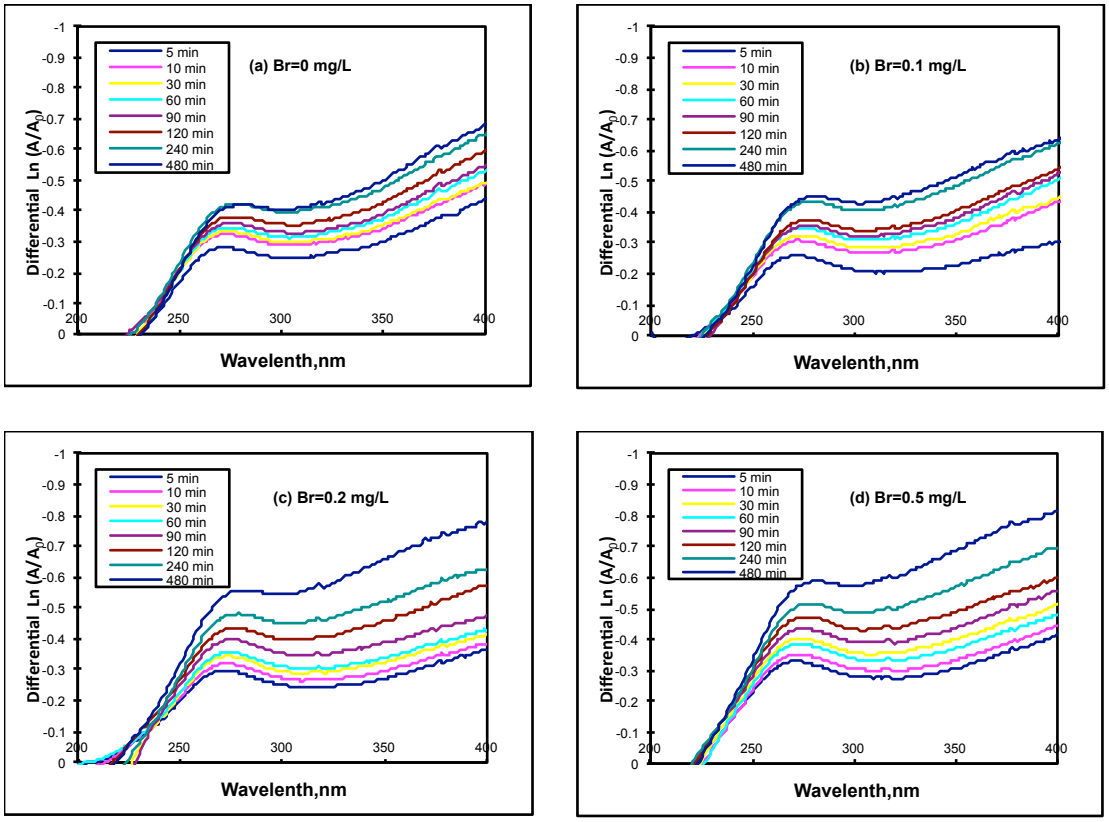

Figure 14 Differential Ln(A/A_0) spectra of chlorinated Lake Washington (winter sampling) in the presence of arying bromide concentrations. DOC 3.65 mg/L, chlorine to DOC ratios of 1 mg/mg, pH 7.0, reaction time from 5min to 8h, bromide dose (a) 0 mg/L, (b) 0.1 mg/L, (c) 0.2 mg/L, (d) 0.5 mg/L.

3.2 Changes of Fluorescence Caused by Chlorination in the presence of Varying Concentrations of Bromide

The utility of fluorescence as tool for monitoring reactions of NOM chlorination and correlating the observed changes of fluorscence with yields of DBPs has been examined in prior research but the relevant studies have been quite limited. In principle, fluorescence is NOM is expected to be highly sensitive to both the initial

NOM nature and its reactivity with halogen species, and to the extent of change of NOM fluorophores affected by chlorination or bromination. The purpose of this part of this study was to analyze in more detail main characteristics of the changes of NOM fluorescence associated with variation of bromide concentration, as was discussed for the absorbance spectra of NOM in the preceding section of this document.

In terms of general understanding of NOM fluorescence properties and halogenation effects, NOM is typically dominated by humic substances that have varying prominence of the polyhydroxyaromatic (PHA) moiety while their apparent molecular weights (AMW) range from <3000 to >10000 Da. The fluorophores in NOM are mostly associated with the activated aromatic units in PHA and halogenation is expected to consume them that thus decreases NOM fluorescence intensity, just as it has been observed in the measurements of NOM absorbance affected by chlorine and bromine species. However, these reactions also cause NOM molecules to be break down into smaller fragments, and emission yields of these smaller molecules may be higher than those of the original NOM substrate, mostly due to lower contributions of radiationless losses of energy in more rigid smaller molecules compared with their larger predecessors.

The occurrence of higher yields of fluorescence in humic molecules with lower AMW values has been reported in prior. In addition, changes of NOM fluorescence upon its halogenation can be affected by the incorporation of chlorine or bromine (or, in the case of iodination, iodide as will be discussed in the next section). The incorporation of these elements with widely different atomic weights (average atomic weightsof chlorine, bromine and iodine are 35.45, 79.90 and 126.90 g/mol, respectively) will also change the AMW values of NOM molecules that have reacted

with chlorine, bromine or iodine species. Both the presence of the heavy atoms such as bromine or iodine in structurally discrete NOM fluorophores and net increase of the molecular weights of NOM molecules containing these groups can cause the intensity of fluorescence to decrease (so called heavy atom effect on the emission of organic species. In all, the occurrence of these three processes can be associated with complex and non-monotonic changes of NOM emission intensity and overally fluorescence spectra at varying reaction times and bromide concentrations. To quantufy these changes, consistent measurements of the fluorescence of SRFA and Lk. Washington water (both spring and summer sampling) waters were carried out. Results of these measurements are discussed in the sections that folows.

Fluorescence data for Suwannee River Fulvic acid (SRFA)

Chlorination of SRFA was observed to cause complex changes of its fluorescence. In the absence of bromide, the intensity of fluorescence tended to increase rather than decrease with increasing reaction time (Figure 15 (a)). At the same time, the position of the maximum in the spectra is shifted towards a lower wavelength. Both processes appear to indicate that the breakdown of SRFA molecules caused by its chlorination cause relatively more prominent changes (increase) of its fluorescence intensity compared with effects possibly associated with the breakdown of SRFA fluorophores and/or chlorine incorporation into them.

However, the observed effects were strongly dependent on the presence of bromide (Figure 15). For SRFA chlorinated in the presence of 0.5 mg/L bromide, the absolute changes of fluorescence were almost negligible but the shape of the emission band underwent gradual changes that will be discussed in more detail below. For a 1 mg/L bromide concentration, the intensity fluorescence decreased almost immediately

after the start of reaction. Largely same effects were observed at increasingly higher bromide conditions and a constant chlorine dose but the absolute decrease of the SRFA fluorescence became very prominent. Given that the shape and overall intensity of the differential absorbance spectra of SRFA were almost identical in the same conditions, there is little doubt that the effects observed in SRFA fluorescence are not necessarily associated the degradation of the aromatic SRFA fluorophores but rather with the incorporation of bromine in them, with the attendant development of heavy atom effects prominent in the presence of bromine atoms incorporated into the organic substrate.

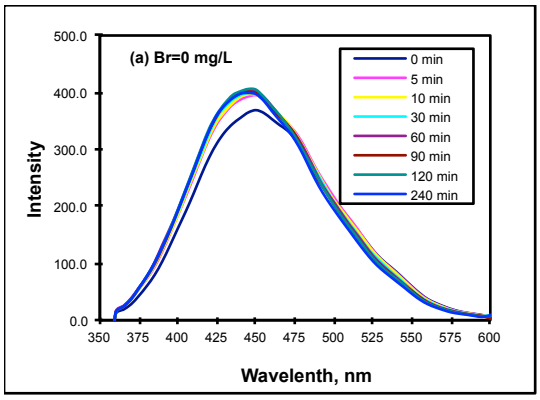

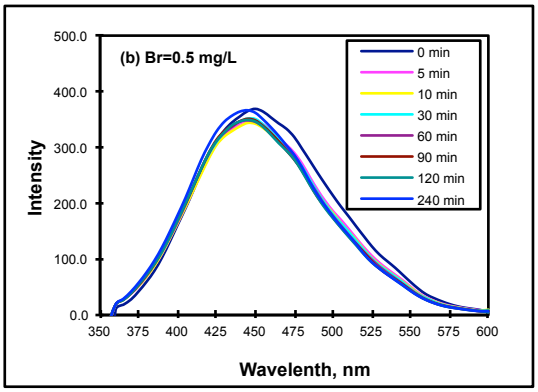

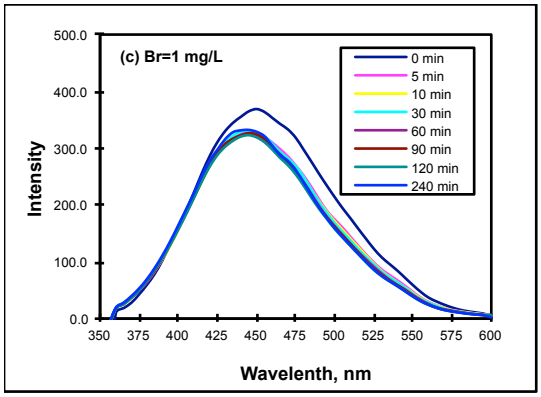

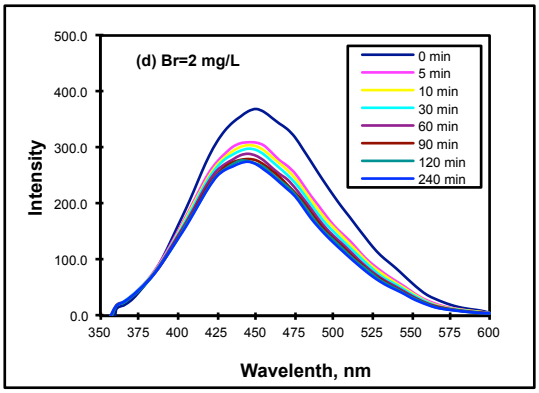

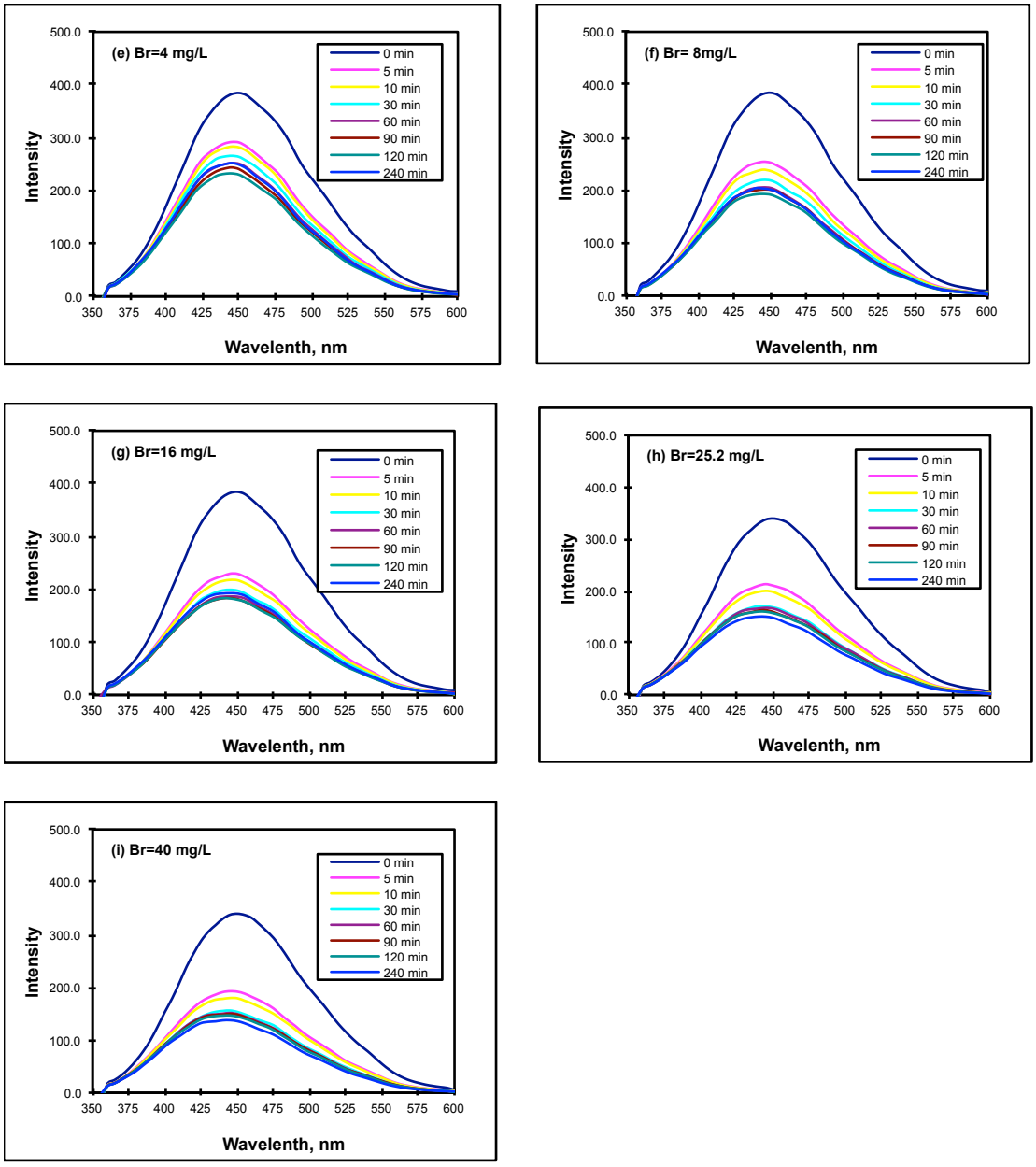

Figure 15 Fluorescence spectra of chlorinated SRFA in the presence of varying bromide concentrations. DOC 5mg/L, chlorine to DOC ratios of 1.1 mg/mg, pH 7.0, reaction time from 5min to 4h, bromide concentration (a) 0 mg/L, (b) 0.5 mg/L, (c) 1 mg/L, (d) 2 mg/L, (e) 4 mg/L, (f) 8 mg/L, (g) 16 mg/L, (h) 25.2 mg/L, (i) 40 mg/L.

To examine and compare the behavior of SRFA emission spectra at varying wavelengths, relative changes of the fluorescence intensities $(I_0-I_t)/I_0$ were calculated for the emissions measured in the range 400 to 575 nm. Emission data for lower and higher wavelengths were not used due to either to too low emission intensities or presence of effects of Raman scattering for high and low wavelengths, respectively.

This approach is similar to that used to examine relative changes of absorbance intensity via log-processed absorbance spectra (Figure 14). Results of calculations of the relative changes of emission intensities for SRFA are shown in Figure 16. These spectra have several consistent trends. For instance, SRFA data in the absence of bromide show that the intensity of emission decreases gradually at increasing reaction times and wavelengths above ca. 475 nm, while the emission intensities increase rather than decrease for lower wavelengths (Figure 16 a). This appears to be consistent with the view that the changes of SRFA emission caused by its chlorination are primarily related to the breakdown of SRFA molecules into smaller fragments since the maxima of the fluorescence intensities of NOM molecules with lower AWM values tend to shift to lower wavelengths

The observed relative changes of SRFA emission change gradually as the concentration of bromide increases. For a 0.5 mg/L bromide concentration (Figure 16 b), the behavior of relative changes of SFRA fluorescence shows a narrower range of negative value indicating that the effects of decreasing AWM of SRFA in the presence of bromide is counter-balanced by bromide incorporation in SRFA molecules with resultant increasing heavy atoms effects, that is the decrease of SRFA emission intensity. For bromide concentrations > 0.5 mg/L, the intensity of SRFA emission decreases in the entire range of wavelengths, and the absolute $(I_0-I_t)/I_0$ values increase practically immediately after the start of NOM halogenation in the entire range of emission wavelengths. This indicates the presence of increasingly strong heavy atom effects (bromide incorporation) on the emission of SRFA fluorophores.

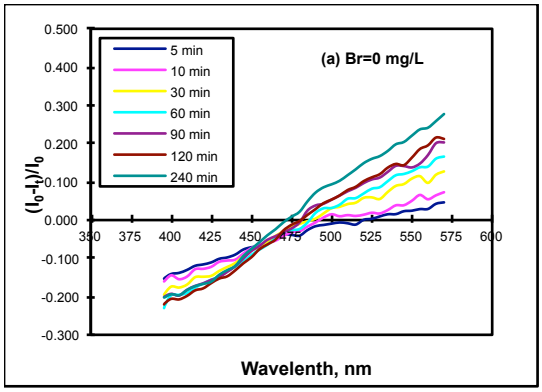
(a) Br=0 mg/L
5 min
10 min
30 min
60 min
90 min
120 min
240 min
$(I_0-I_t)/I_0$
Wavelenth, nm

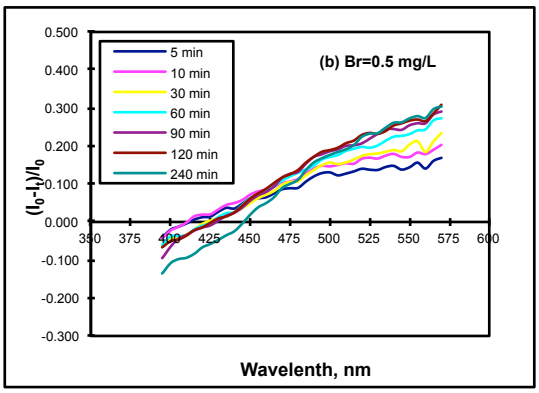
(b) Br=0.5 mg/L
5 min
10 min
30 min
60 min
90 min
120 min
240 min
$(I_0-I_t)/I_0$
Wavelenth, nm

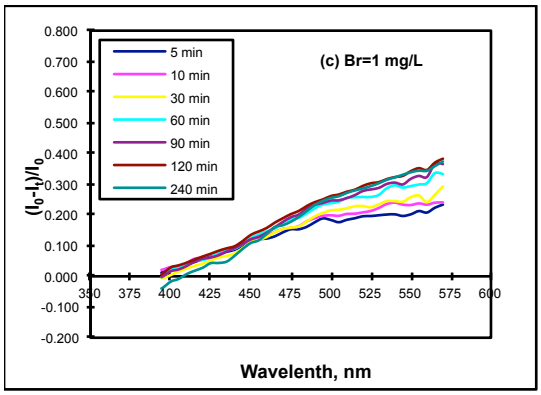
(c) Br=1 mg/L
5 min
10 min
30 min
60 min
90 min
120 min
240 min
$(I_0-I_t)/I_0$
Wavelenth, nm

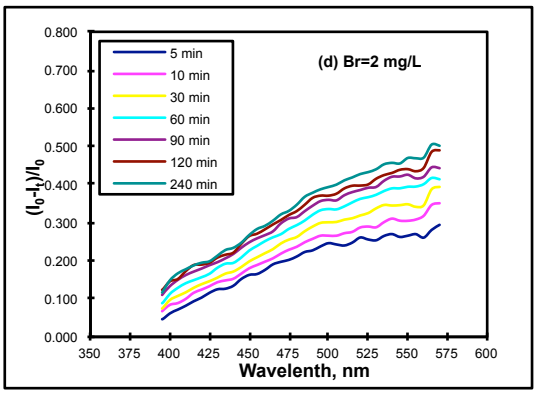
(d) Br=2 mg/L
5 min
10 min
30 min
60 min
90 min
120 min
240 min
$(I_0-I_t)/I_0$
Wavelenth, nm

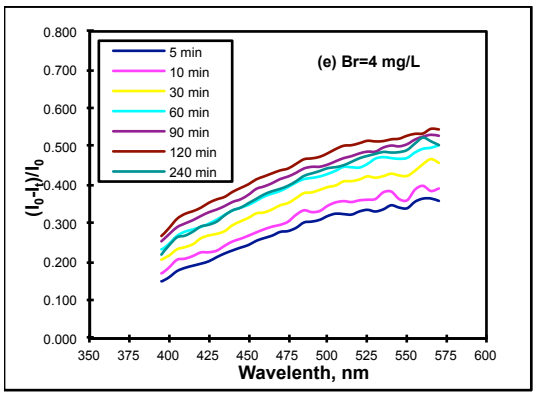
(e) Br=4 mg/L
5 min
10 min
30 min
60 min
90 min
120 min
240 min
$(I_0-I_t)/I_0$
Wavelenth, nm

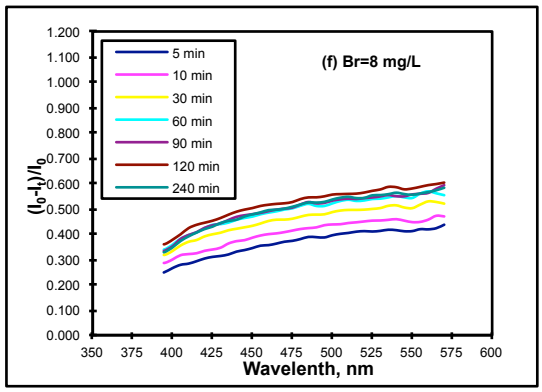
(f) Br=8 mg/L
5 min
10 min
30 min
60 min
90 min
120 min
240 min
$(I_0-I_t)/I_0$
Wavelenth, nm

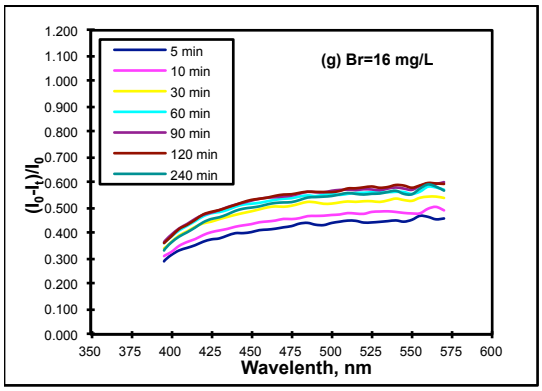
(g) Br=16 mg/L
5 min
10 min
30 min
60 min
90 min
120 min
240 min
$(I_0-I_t)/I_0$
Wavelenth, nm

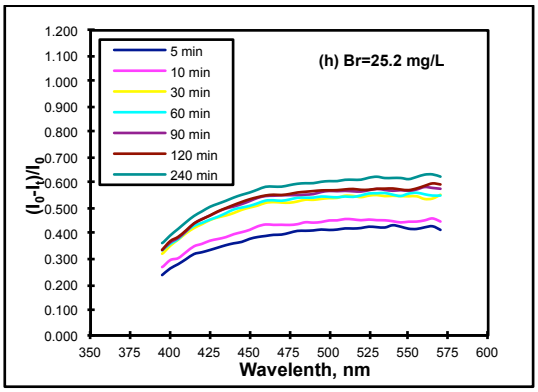
(h) Br=25.2 mg/L
5 min
10 min
30 min
60 min
90 min
120 min
240 min
$(I_0-I_t)/I_0$
Wavelenth, nm

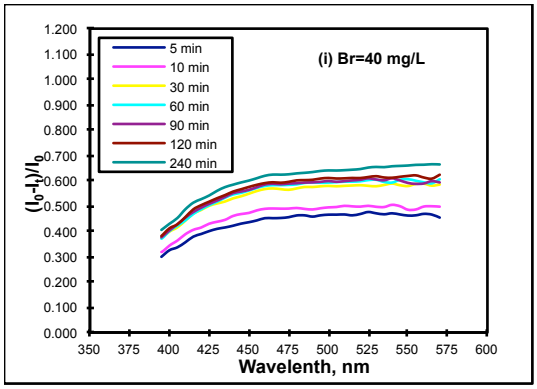

Figure 16 Differential relative changes of fluorescence spectra of SRFA chlorinated in the presence of varying bromide concentration. DOC 5mg/L, chlorine to DOC ratios of 1.1 mg/mg, pH 7.0, reaction time from 5min to 4h, bromide concentration (a) 0 mg/L, (b) 0.5 mg/L, (c) 1 mg/L, (d) 2 mg/L, (e) 4 mg/L, (f) 8 mg/L, (g) 16 mg/L, (h) 25.2 mg/L, (i) 40 mg/L.

Fluorescence data for Lake Washington water (winter 2012 sampling)

The fluorescence of Lk. Washington water chlorinated at somewhat different conditions compared with those reported above (a narrow range of reaction times and bromide concentrations) showed largely the same effects as those seen SRFA. In the absence of bromide, the fluorescence of Lk. Washington water changde non-monotonically (Figure 17 (a)). The emission at the maximum of the emission band (at ca. 430 nm) initially increased but for reaction times above 5 minutes it decreased and was not very different from that of the initial (unchlorinated) sample for reaction times exceeding 30 minutes. This appears to indicate that the initial phase of chlorination of Lk. Washington NOM caused its molecules to break down but then at least a part of the fluorophores was degraded by chlorine.

The behavior of emission intensities of Lk. Washington water chlorinated in the presence of bromide did not show trends as would be as clear as those for SRFA. However, in practically all cases the intensity of emission initially increased somewhat and then it undergo a decrease that was more noticeable for higher Br concentrations (Figure 17). This appears to show that bromide incorporation in Lk.

Washington NOM was also accompanied by decrease of its emission due to the heavy atom effect.

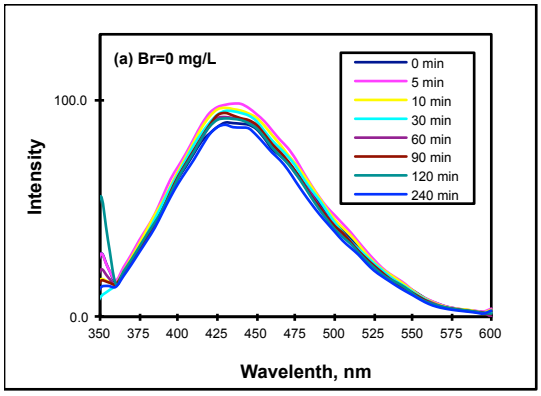

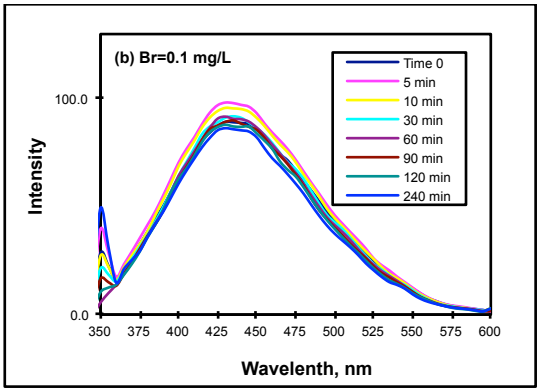

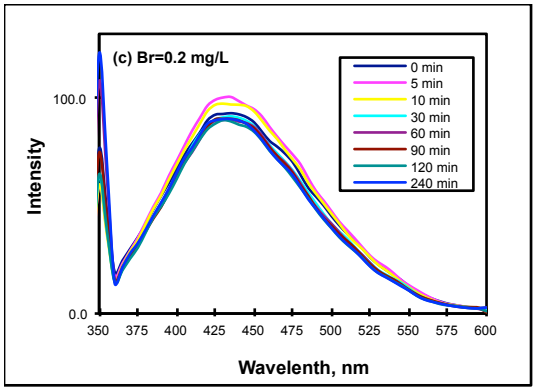

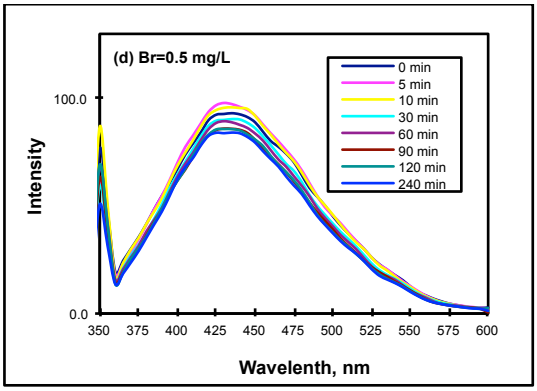

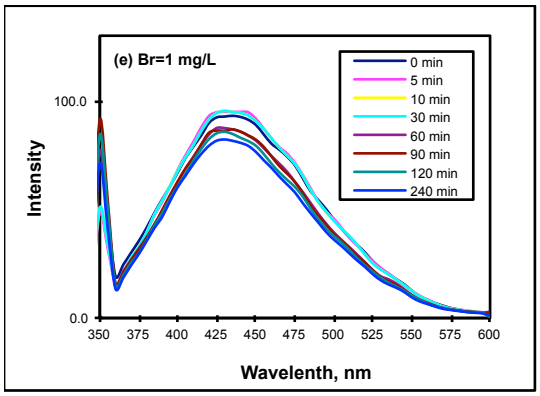

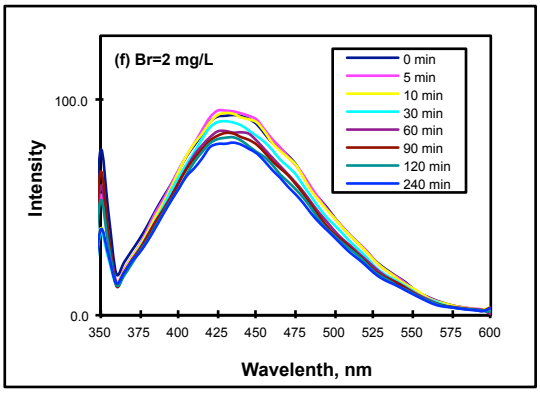

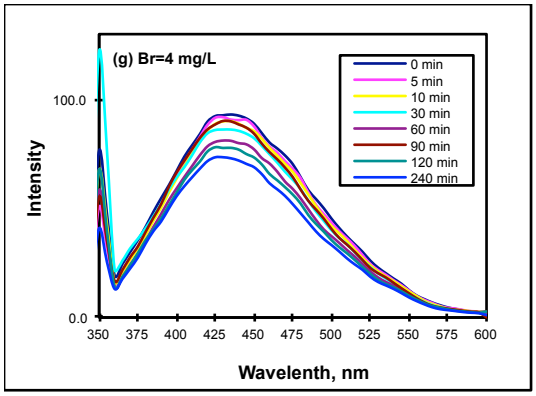

Figure 17 Fluorescence spectra of Lake Washington (winter sampling) chlorinated in the presence of varying bromide concentrations. DOC 2.3mg/L, chlorine to DOC ratios of 1 mg/mg, pH 7.0, reaction time from 5min to 4h, bromide concentrations (a) 0 mg/L, (b) 0.1 mg/L, (c) 0.2 mg/L, (d) 0.5 mg/L, (e) 1 mg/L, (f) 2 mg/L, (g) 4 mg/L.

This point can be further illustrated by the calculations of $(I_0-I_t)/I_0$ values shown in Figure 18. It demonstrates the presence of the effects similar to those seen for SRFA albeit the extent of effects is less pronounced. For instance, in the absence of bromide, relative changes of Lk. Washington emission are positive in the entire range of wavelengths for 5 and 10 minute reaction times. For longer reaction times, relative changes of the fluorescence become positive (that is, the fluorescence intensity decreases irrespective of its initial value) for wavelengths > 475 nm. A very similar behavior can be observed for 0.1 and 0.2 mg/L bromide concentration (Figure 18 b and c). Further increases of bromide levels are associated with the same pattern of changes that appear to be indicative on the heavy atom effect.

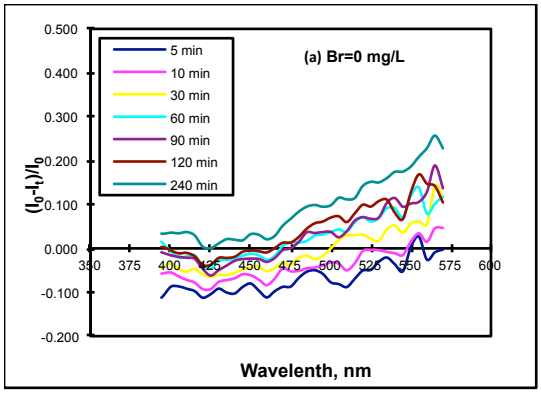
(a) Br=0 mg/L
5 min
10 min
30 min
60 min
90 min
120 min
240 min
$(I_0-I_t)/I_0$
Wavelenth, nm

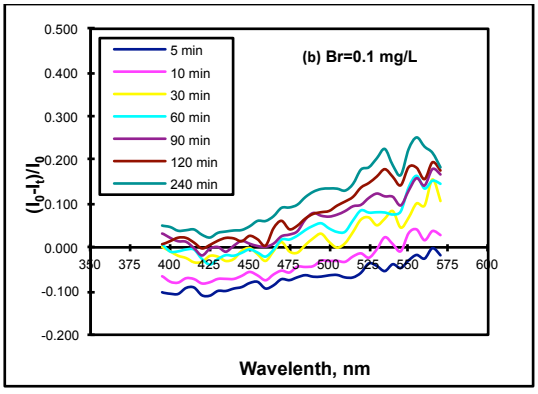
(b) Br=0.1 mg/L
5 min
10 min
30 min
60 min
90 min
120 min
240 min
$(I_0-I_t)/I_0$
Wavelenth, nm

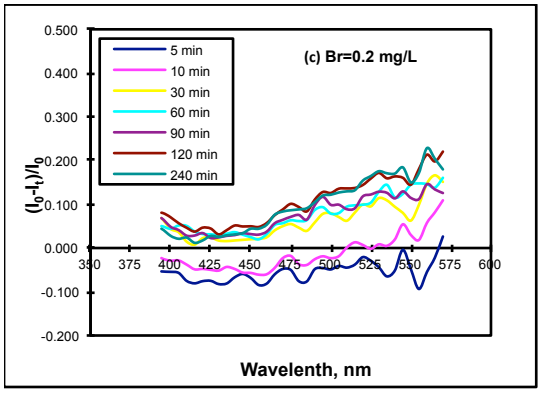
(c) Br=0.2 mg/L
5 min
10 min
30 min
60 min
90 min
120 min
240 min
$(I_0-I_t)/I_0$
Wavelenth, nm

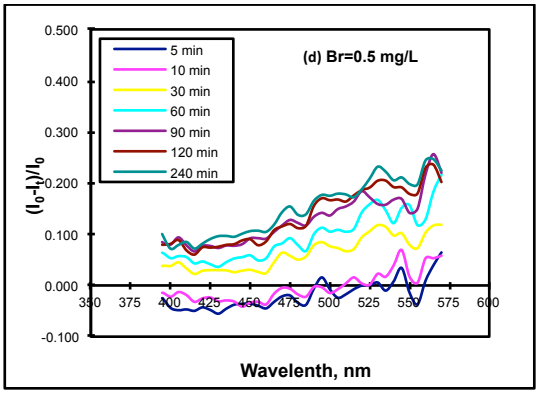
(d) Br=0.5 mg/L
5 min
10 min
30 min
60 min
90 min
120 min
240 min
$(I_0-I_t)/I_0$
Wavelenth, nm

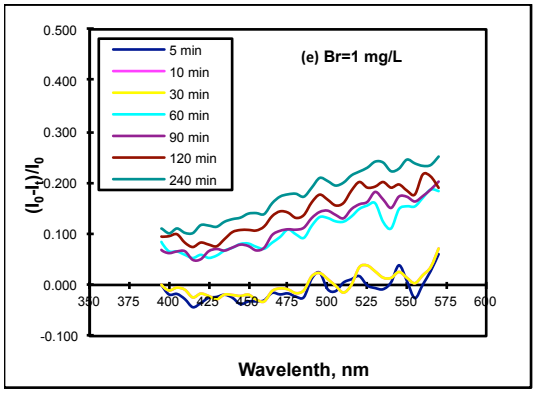
(e) Br=1 mg/L
5 min
10 min
30 min
60 min
90 min
120 min
240 min
$(I_0-I_t)/I_0$
Wavelenth, nm

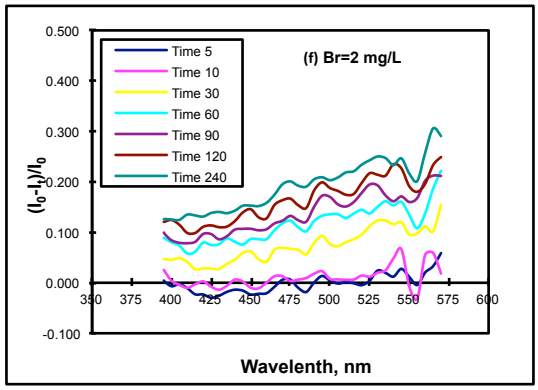
(f) Br=2 mg/L
Time 5
Time 10
Time 30
Time 60
Time 90
Time 120
Time 240
$(I_0-I_t)/I_0$
Wavelenth, nm

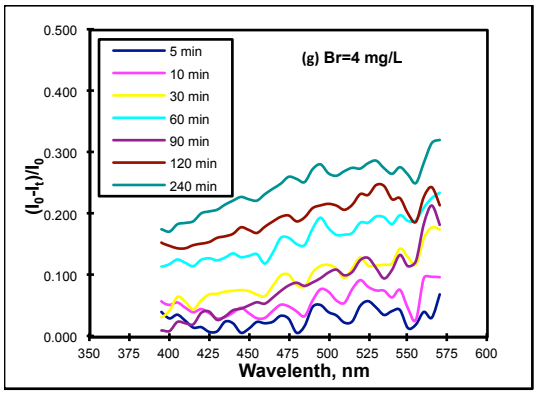
(g) Br=4 mg/L
5 min
10 min
30 min
60 min
90 min
120 min
240 min
$(I_0-I_t)/I_0$
Wavelenth, nm

Figure 18 Relative changes of fluorescence of Lake Washington chlorinated in the presence of varying bromide concentrations. DOC 2.3mg/L, chlorine to DOC ratios of 1 mg/mg, pH 7.0, reaction time from 5min to 4h, bromide concentrations (a) 0 mg/L, (b) 0.1 mg/L, (c) 0.2 mg/L, (d) 0.5 mg/L, (e) 1 mg/L, (f) 2 mg/L, (g) 4 mg/L.

Fluorescence data for the summer 2012 Lake Washington water sample

Effects of chlorination on the emission of Lake Washinton water sampled during the summer of 2012 were largely similar to those for the winter sample (Figure 19). (An increase of fluorescence intensity for wavelenghts < 360 nm in this data set is caused by an undercompensated Raman scattering. This difficulty existed due to an insufficient performance of the xenon lamp of the fluorimeter; this lamp had to be eventually replaced). Like in the case of Lk. Washington water obtained during the winter sampling, the intensity of emission initially increased at walenghts > 430 nm, but following this it underwent a decrease (Figure 19(a)). The introduction of higher bromide levels did not change this effect although the initial increase of the emission intensity disappeared.

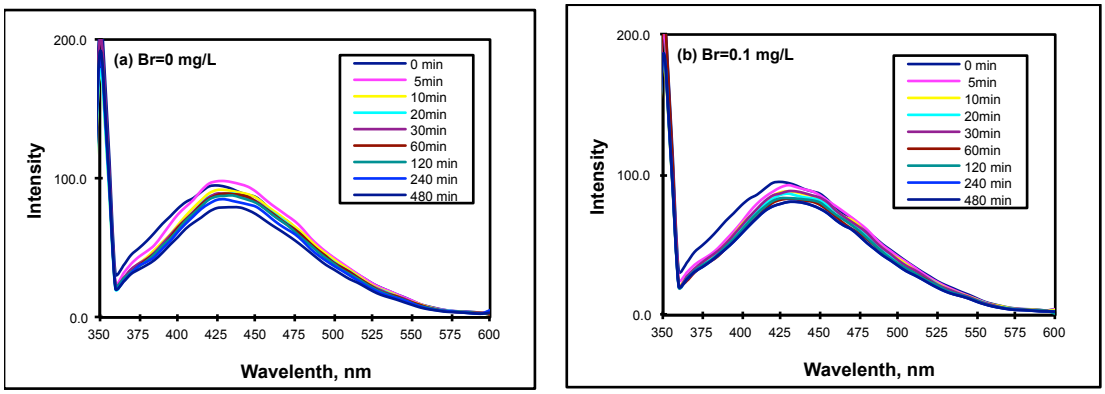

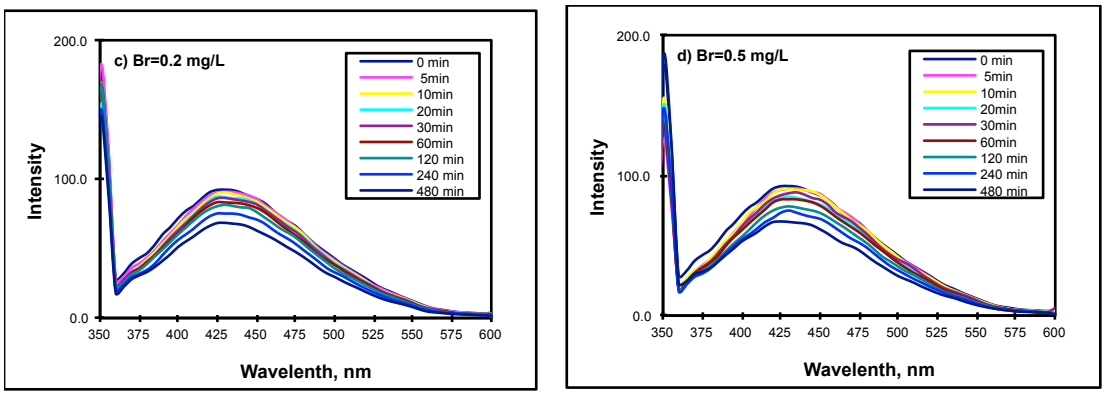

Figure 19 Fluorescence spectra of Lake Washington (summer sampling) chlorinated in the presence of varying bromide concentrations. DOC 3.65 mg/L, chlorine to DOC ratios of 1 mg/mg, pH 7.0, reaction time from 5min to 8h, bromide concentrations (a) 0 mg/L, (b) 0.1 mg/L, (c) 0.2 mg/L, (d) 0.5 mg/L.

Relative changes of the fluorescence intensity $(I_0-I_t)/I_0$ calculated using the data shown in Figure 19 are presented in Figure 20. Except the increases of the $(I_0-I_t)/I_0$ values below 425 nm caused by the presence of undercompensated Raman scattering in these samples, the behavior of the relative changes is similar to that found for the winter Lk. Washington sample and shown in Figure 18. The data confirm the presence of both the breakdown of molecules of Lk. Washington NOM and incorporation of bromide into them, as was seen for SRFA and the winter sample of this water source.

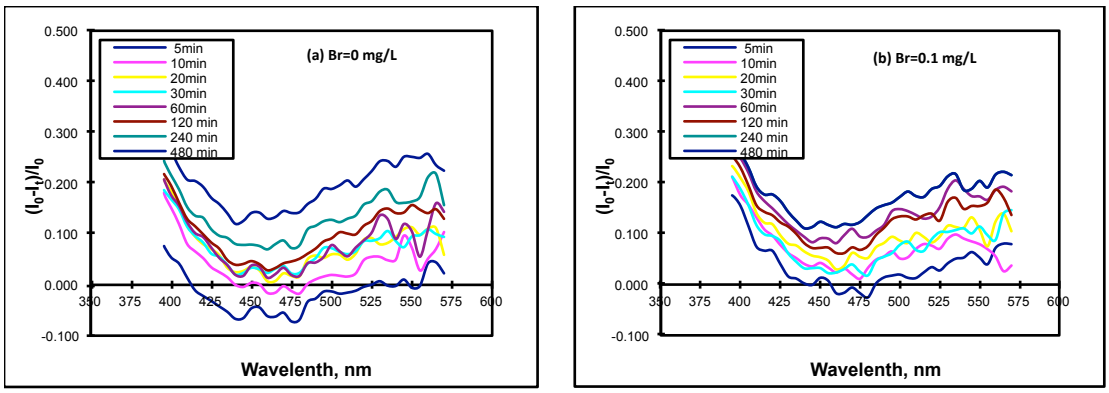

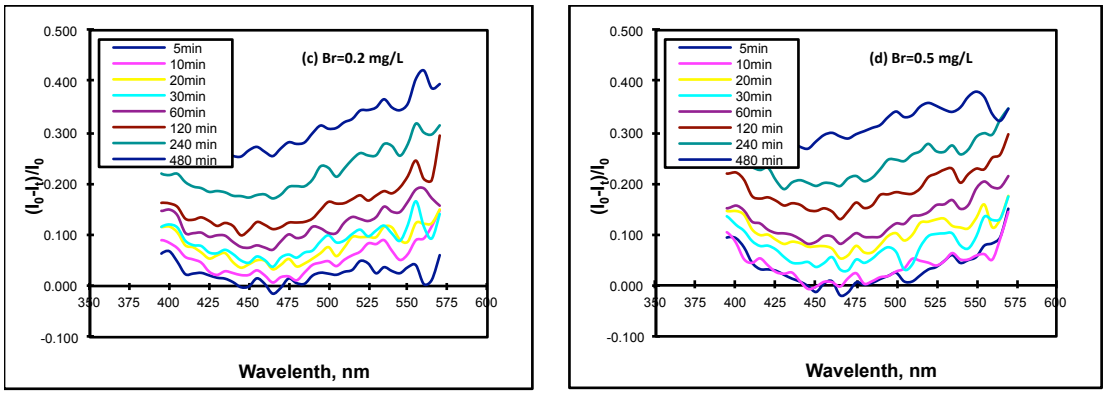

Figure 20 Relative changes of the fluorescence spectra of chlorinated Lake Washington (summer sampling) in the presence of varying bromide concentration,. DOC 3.65 mg/L, chlorine to DOC ratios of 1 mg/mg, pH 7.0, reaction time from 5min to 8h, bromide concentration (a) 0 mg/L, (b) 0.1 mg/L, (c) 0.2 mg/L, (d) 0.5 mg/L.

3.3 Disinfection by products

The data presented above indicated that while the differential absorbance spectra of the selected NOM sources are largely insensitive to the occurrence of parallel chlorination and bromination reactions (although the kinetics of the changes of differential absorbance is affected by bromide). In contrast, the fluorescence of NOM is affected by bromination in complex and non-monotonic ways although the use of the concept of relative changes of fluorescence intensities at high enough wavelengths (e.g. > 475 nm) allow tracking the extent of specific changes possibly associated with bromination, that is the occurrence of heavy atom effect.

The above data need to be examined and compared in the context of the formation of DBPs whose yields and speciation tend to undergo pronounced changes in the presence of bromide. In this section, we present DBP data for Lake Washington samples. It is no be noted that this water source does contain a small but measureable amount of bromide (ca. 50 µg/L). Accordingly, DBP measurements show that even when no bromide was added to the system, there was a considerable formation of Br-

containing DBPs which in this study were exemplified by the two most prominent groups, namely THMs and HAAs, It also needs to be noticed that the THM data generated in this study may be somewhat imprecise due to the partial loss of these species to the headspace formed in the reaction vessel as chlorination of the selected water proceeded. While this was corrected for using the Henry law formulas and these calculations show that losses of brominated THMs are relatively low, losses of chloroform may be more pronounced.

Figure 21 shows molar concentrations of individual THMs species for varying reaction times and bromide ion concentrations. The generation of the individual THM species was very fast for short reaction times (< 15 to 30 minutes) and following that incremental changes of THM concentrations were less prominent. This behavior is entirely consistent with the data of prior research. As expected, bromide ion concentration plays an important role in the production of DBPs. Indeed, the influence of bromide is quite striking for each compound. For instance, Figure 21 (a) shows that chloroform production decreased significantly when bromide concentration increased from from 0 mg/L to 0.5 mg/L. The formation of two mixed bromochloro THM species (bromodichloromethane and bibromochloromethane) tended to increase with higher bromide concentrations. The levels of bromoform increased strongly for bromide concentrations > 0.2mg/L.

The mass concentrations of the four THM are presented in Figure 22. These data show largely the same pattern as that shown in Figure 21.

Molar yields of total THM (TTHM) and the estimated concentration of bromine incorporated in these species are shown in Figure 23 and Figure 24 for molar and weight concentrations, respectively. These results are quite predictable:

increasing initial bromide levels resulted in substantial increases of the TTHM concentration and even more so for bromide incorporated in TTHM.

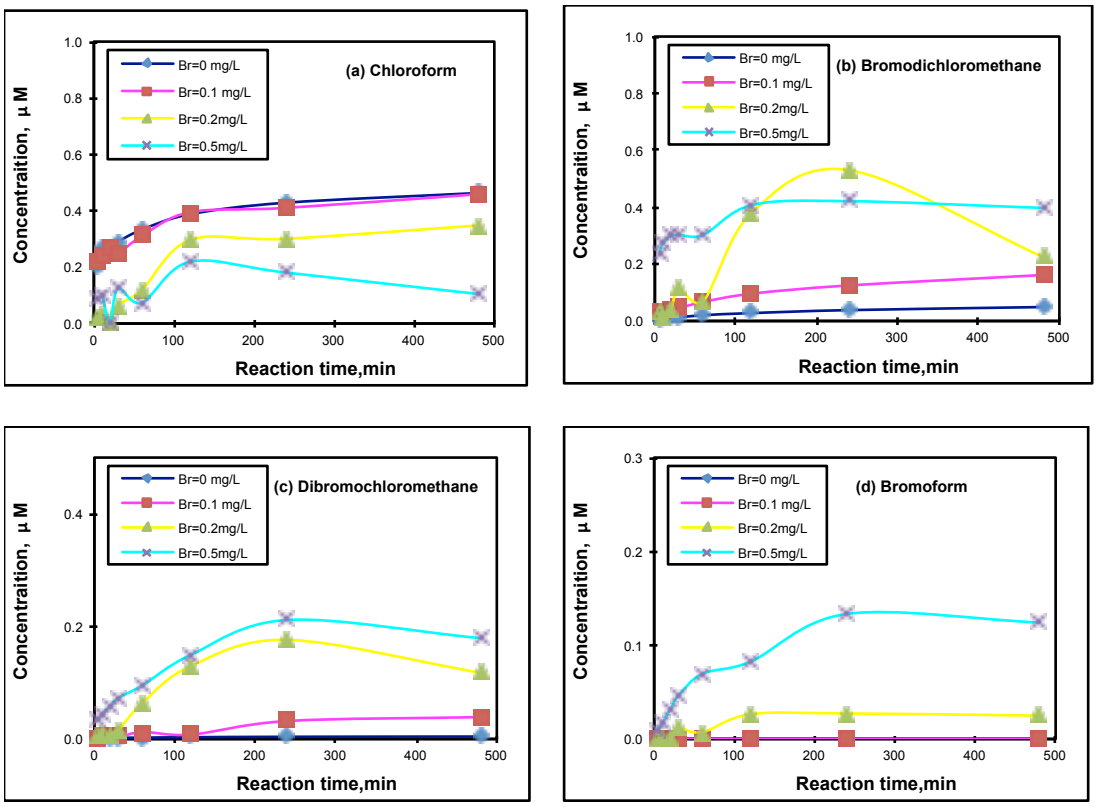

Figure 21 Molar concentrations of THM4 species formed at varying reaction time and initial bromide ion concentrations. pH=7, Lake Washington DOC=3.65mg/L, chlorine to DOC ratios of 1.0 mg/mg, (a) chloroform, (b) bromodichloromethane, (c) dibromochloromethane, (d) bromoform.

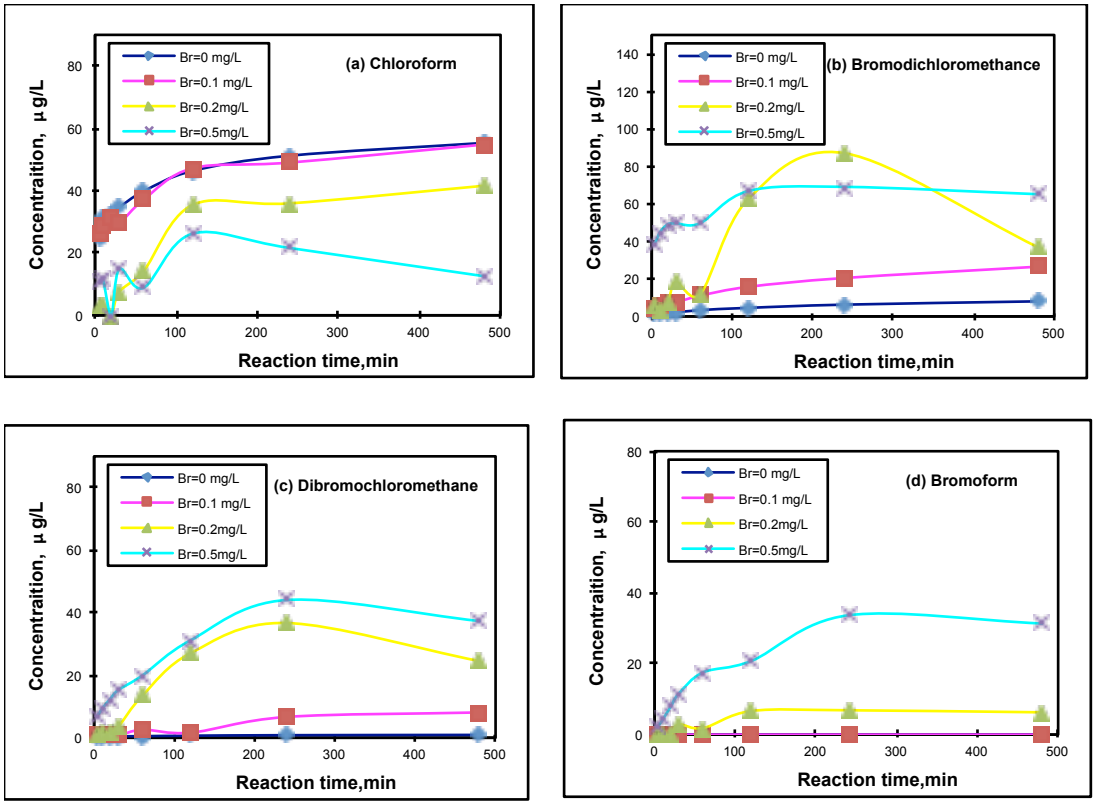

Figure 22 Mass concentrations of THM4 species formed at varying reaction times and initial bromide ion concentrations. pH=7, Lake Washington DOC=3.65mg/L, chlorine to DOC ratios of 1.0 mg/mg, (a) chloroform, (b) bromodichloromethane, (c) dibromochloromethane, (d) bromoform.

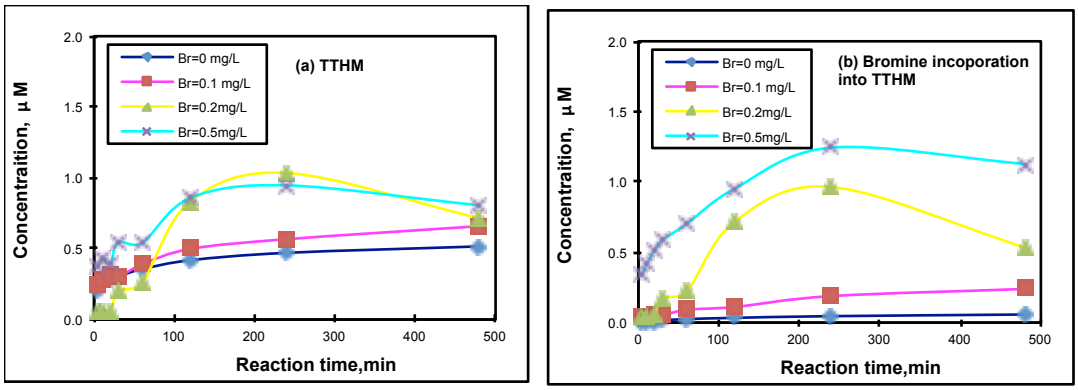

Figure 23 Molar concentrations of TTHM (a) and concentrations of bromine incorporated in TTHM (b) as function of chlorination reaction time and initial bromide ion concentration, pH=7, Lake Washington DOC=3.65mg/L, chlorine to DOC ratios of 1.0 mg/mg.

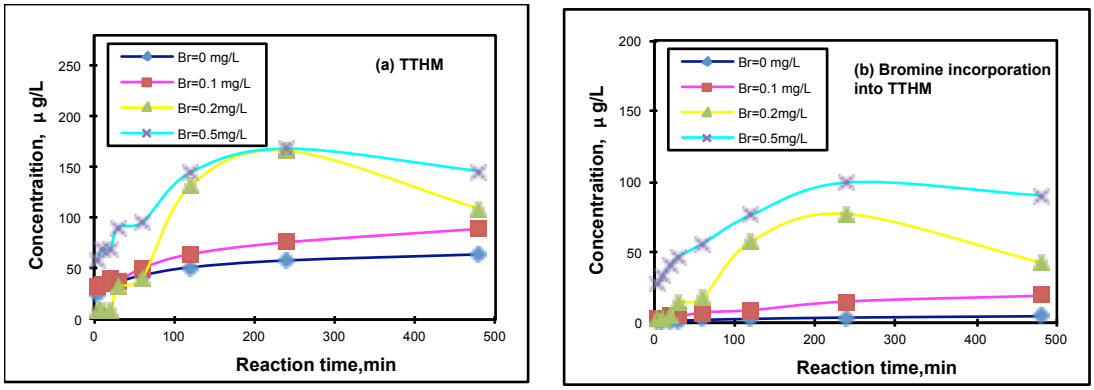

Figure 24 Mass concentrations of TTHM (a) and concentrations of bromine incorporated in TTHM (b) as function of chlorination reaction time and initial bromide ion concentration, pH=7, Lake Washington DOC=3.65mg/L, chlorine to DOC ratios of 1.0 mg/mg.

Distribution diagrams (that show contributions of the relevant species into their combined concentrations) of the THMs species produced from chlorination of Lake Washington water are shown in Figure 25 and Figure 26 for data presented for molar and weight fractional basis, respectively. The data show that the mole or weight fractions of chloroform declined somewhat with increasing reaction time and much more prominently for bromide concentration 0 mg/L to 0.5 mg/L. For instance, the contribution of chloroform measured at the end of the reaction time decreased from 0.89 to 0.13, while the molar fractions of bromodichloromethane, dibromochloromethane and bromoform increased in the same conditions to 0.4, 0.22 and 0.15 respectively. Mass fractional distribution of THMs species (Figure 26) exhibited similar trends.

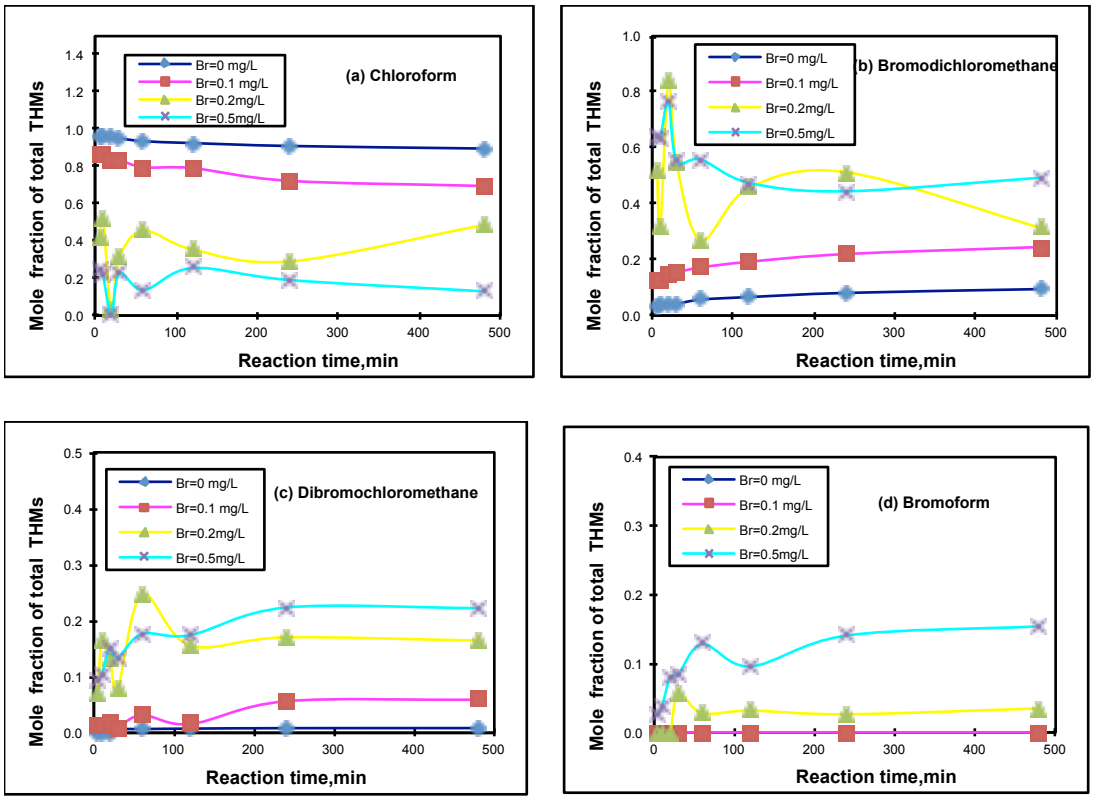

Figure 25 Molar fractions of THM species in TTHM concentrations as function of chlorination time and initial bromide ion concentration, pH=7, Lake Washington DOC=3.65mg/L, chlorine to DOC ratios of 1.0 mg/mg, (a) chloroform, (b) bromodichloromethane, (c) dibromochloromethane, (d) bromoform.

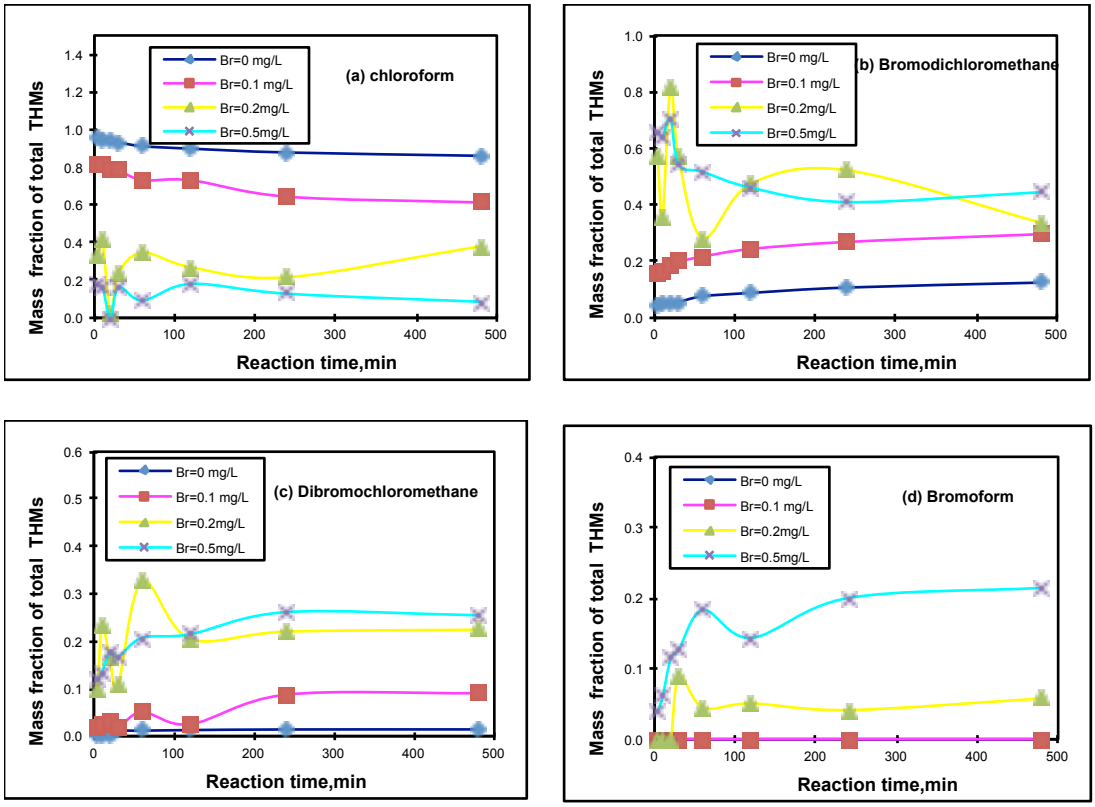

Figure 26 Mass fractions of THM species in TTHM concentration as function of chlorination time and initial bromide ion concentration, pH=7, Lake Washington DOC=3.65mg/L, chlorine to DOC ratios of 1.0 mg/mg, (a) chloroform, (b) bromodichloromethane, (c) dibromochloromethane, (d) bromoform.

Figure 27 summarizes these observations and illustrates the difference of species and concentration of THMs at varying concentratioins of bromide. Increasing the bromide concentration caused molar THM concentration to shift significantlytoward the domination of bromine containing THMs. The concentration of chloroform continuously declined with elevated bromide levels and was dramatically reduced for Br levels above 0.2 mg/L. The lower bromine-incorporated species bromodichlormethane increased with bromide concentration from 0 mg/L to 0.5 mg/L. Dibromochloromethane contains 2 mole bromide /mole THM, was rarely detected at bromide 0 mg/L and followed by a increase with increasing bromide ion concentration. The fromation of the highest bromine-containing specie bromoform was not reliably detected until bromide concentration was at a 0.5 mg/L level.

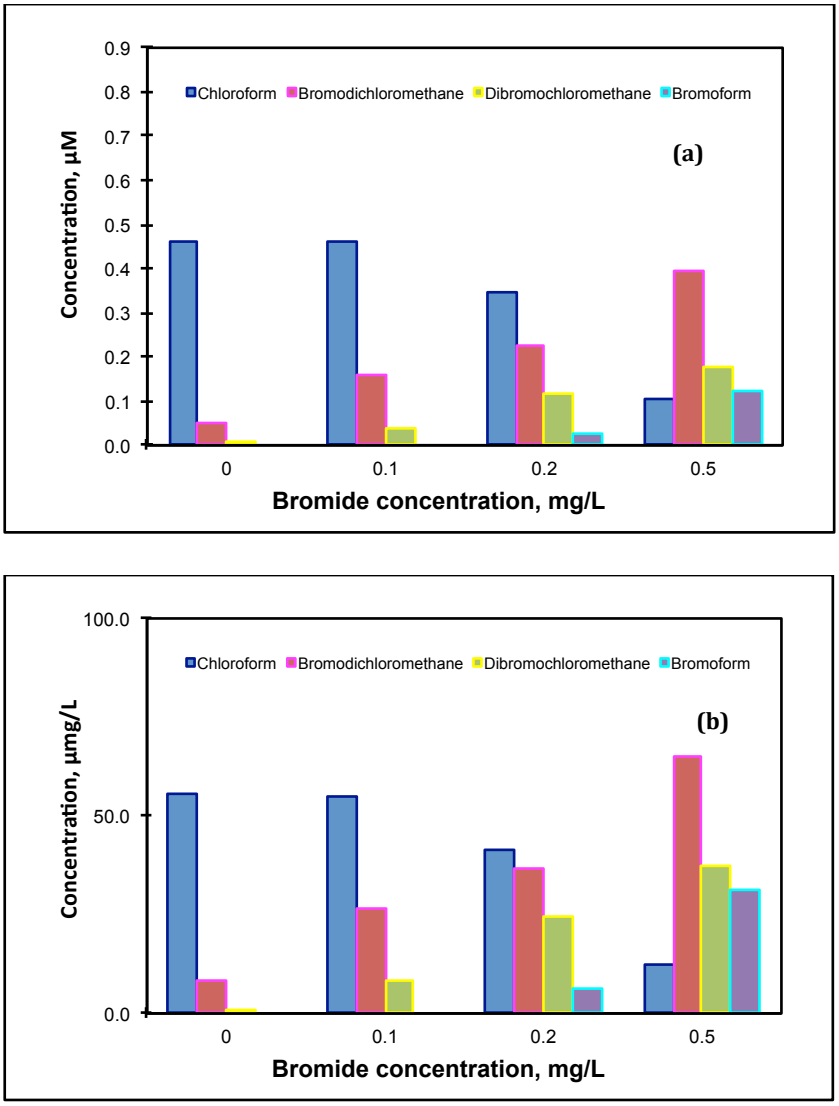

Figure 27 Effect of bromide on the molar yields (a) and mass yields (b) of individual THM species in chlorinated Lake Washington sampling DOC=3.65 mg/L, chlorine to DOC ratios of 1.0 mg/mg, reaction time 8 h, pH 7.

The speciation (or distribution) of the THM species produced from chlorinated Lake Washington water at pH 7 are shown in Figure 28 for both mole and mass fractional basis. At low bromide concentrations (< 0.2 mg/L), the prevalent THM speciation fractions generally follow the order: chloroform > bromodichloromethane > dibromochloromethane > bromoform. At intermediate to

high bromide concenentration, the order was changed: bromodichloromethane > dibromochloromethane > bromoform > chloroform

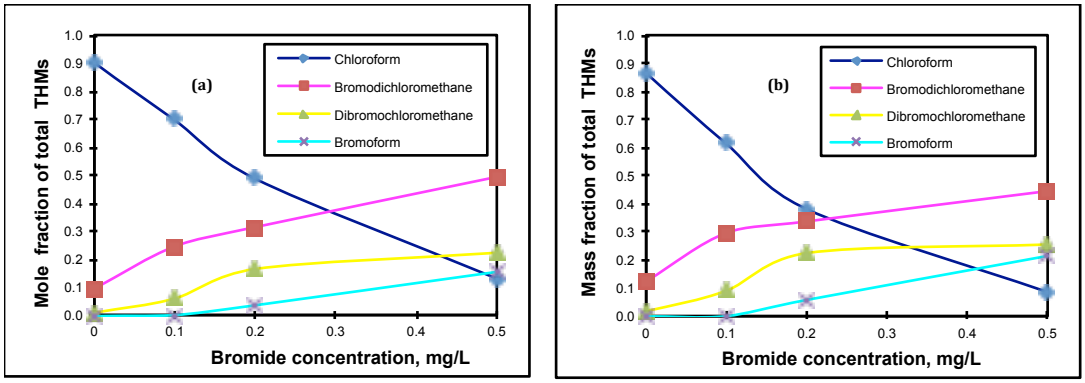

Figure 28 Distribution of individual THM species on a mole fractional basis (a) and on a mass fractional basis (b) in chlorinated Lake Washington sampling DOC=3.65 mg/L, chlorine to DOC ratios of 1.0 mg/mg, reaction time 8 h, pH 7.

Yields of individual HAA species as function of bromide concentration and reaction time are exhibited in Figure 29 and Figure 30 for molar and weight concentration units, respectively. The data show that, similarly to the THM data shown above, the molar or weight concentrations of each individual HAA species increased rapidly in the beginning of the reactions and then they exhibited less prominent incremental changes.

The data show that the bromide concentration plays a critical role in HAAs speciation and distribution. The yields of DCAA and TCAA that contain only chlorine were reduced significantly for elevating bromide concentrations. At the same time, the concentrations BCAA and BDCAA and all the other bromine-containing HAAS increased rapidly and consistently. The only exception was the formation of TBAA which was not reliably detected until the concentration of bromide reached a 0.5 mg/L level. However, the rapid change of TBAA concentration in these

conditions may be an artifact since TBAA may undergo hydrolysis releasing bromoform.

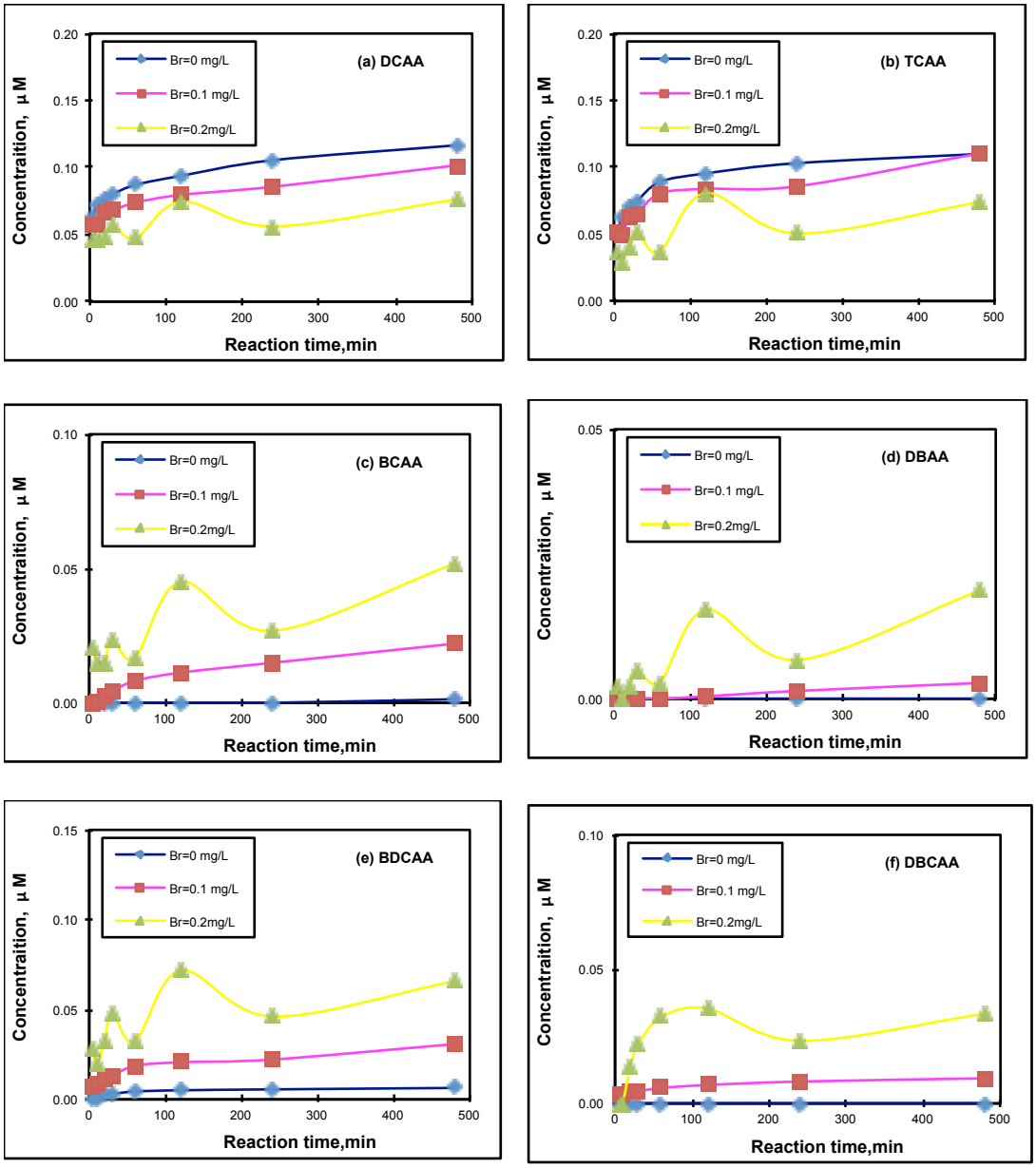

Figure 29 Molar concentration of HAAs species formed at varying chlorination times and initial bromide ion concentration, pH=7, Lake Washington DOC=3.65mg/L, chlorine to DOC ratios of 1.0 mg/mg, (a) DCAA, (b) TCAA, (c) BCAA, (d) DBAA, (e) BDCAA, (f) DBCAA,.

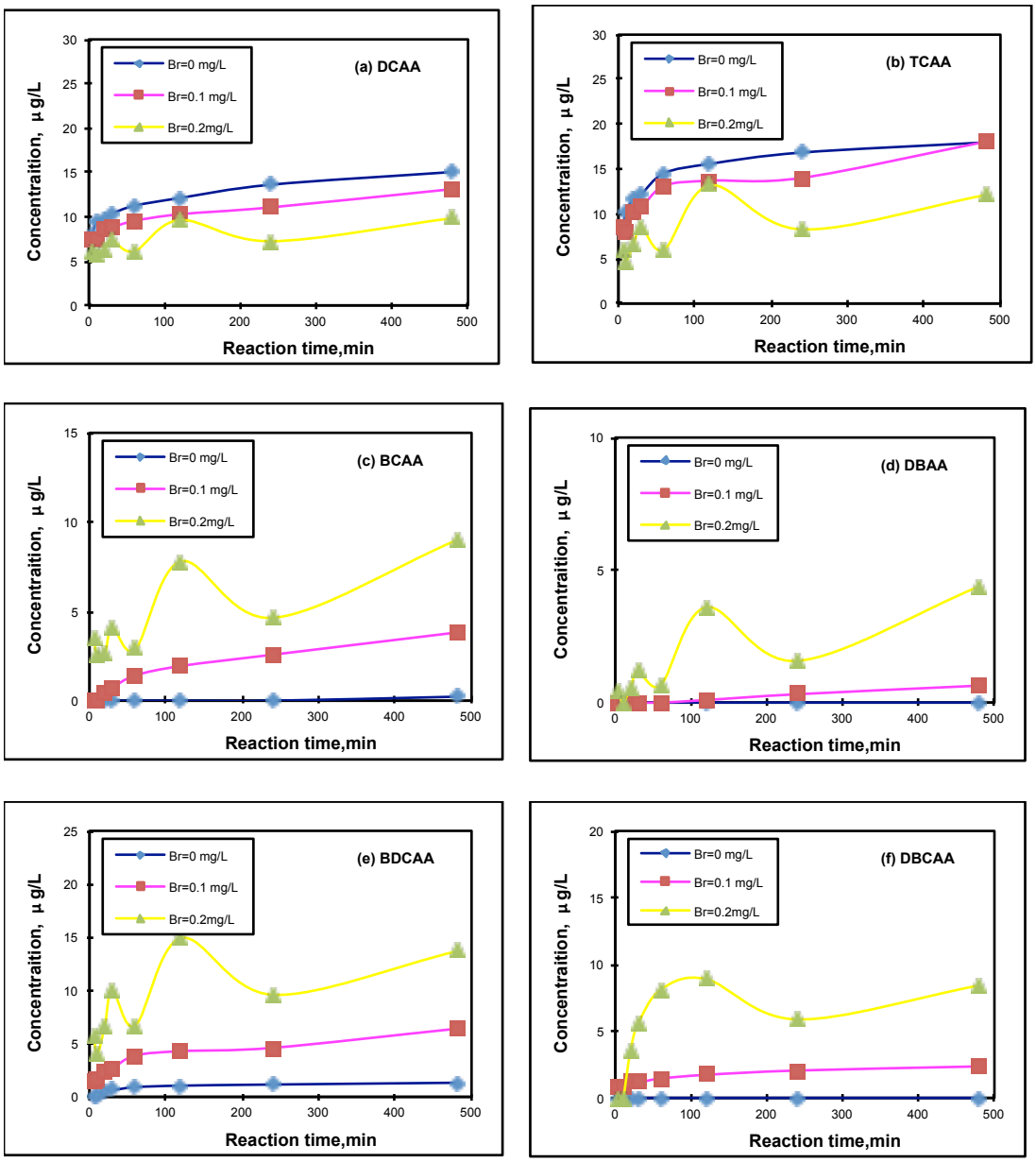

Figure 30 Mass concentrations of HAAs species formed as function of varying chlorination time and initial bromide ion concentration, pH=7, Lake Washington DOC=3.65mg/L, chlorine to DOC ratios of 1.0 mg/mg, (a) DCAA, (b) TCAA, (c) BCAA, (d) DBAA, (e) BDCAA, (f) DBCAA,.

Molar and weight concentration of THAA and the concentrations of bromine incorporated in them are shown in Figure 31 and Figure 32, respectively. The data show that the yields of HAA species increase until bromide concentrations were 0.5 mg/L. But THAA concentrations increased dramatically for a 0.5 mg/L bromide concentration, mostly due to the sudden increase of TBAA levels. However, given

that this contradicts the trend seen for the other employed conditions, this may be an artifact.

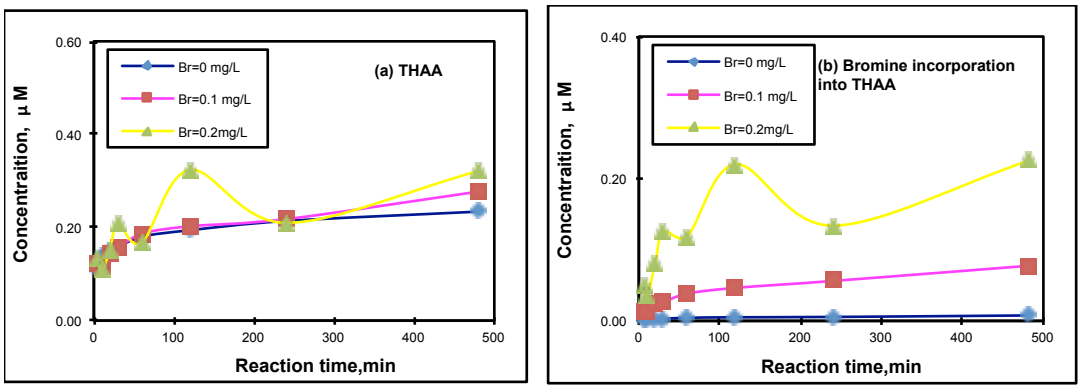

Figure 31 Molar concentrations of THAA (a) and overall bromine incorporated in the HAA species (b) as function of chlorinated reaction time and initial bromide ion concentration, pH=7, Lake Washington DOC=3.65mg/L, chlorine to DOC ratios of 1.0 mg/mg.

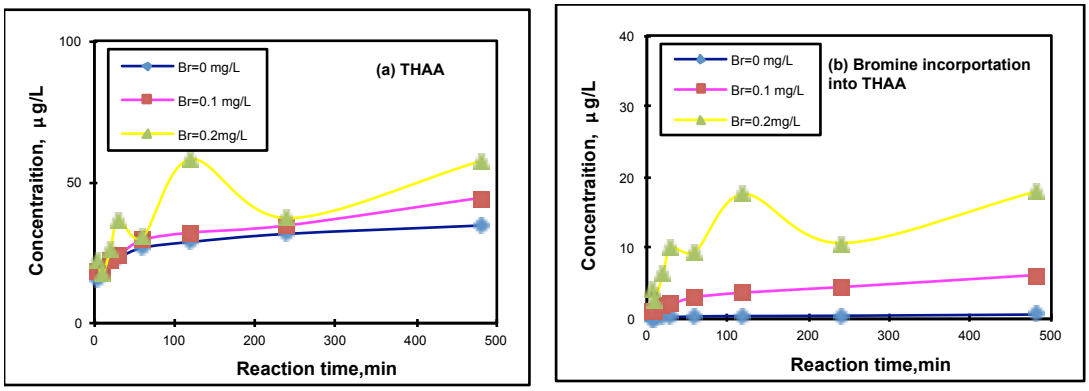

Figure 32 Mass concentrations of THAA (a) and overall bromine incorporated in the HAA species (b) as function of chlorinated reaction time and initial bromide ion concentration, pH=7, Lake Washington DOC=3.65mg/L, chlorine to DOC ratios of 1.0 mg/mg.

Figure 33 and Figure 34 illustrate the distribution of individual HAA species as a function of contact time and initial bromide levels expressed as molar and weight concentration fractions, respectively. As expected, the molar fractions of the chlorine-containing species DCAA and TCAA declined markedly when the bromide concentration increased from 0 mg/L to 0.5 mg/L. The contributions of BCAA and BDCAA containing a atom of bromine per molecule increased gradually at higher

bromide level until bromide reached 0.5 mg/L. The fractional contributions of DBAA DBCAA that have 2 atoms of bromine per molecule showed a more rapid increase trends with increasing bromide concentrations. Finally, considerable contributions of TBAA were observed for the bromide level of 0.5 mg/L only.

.

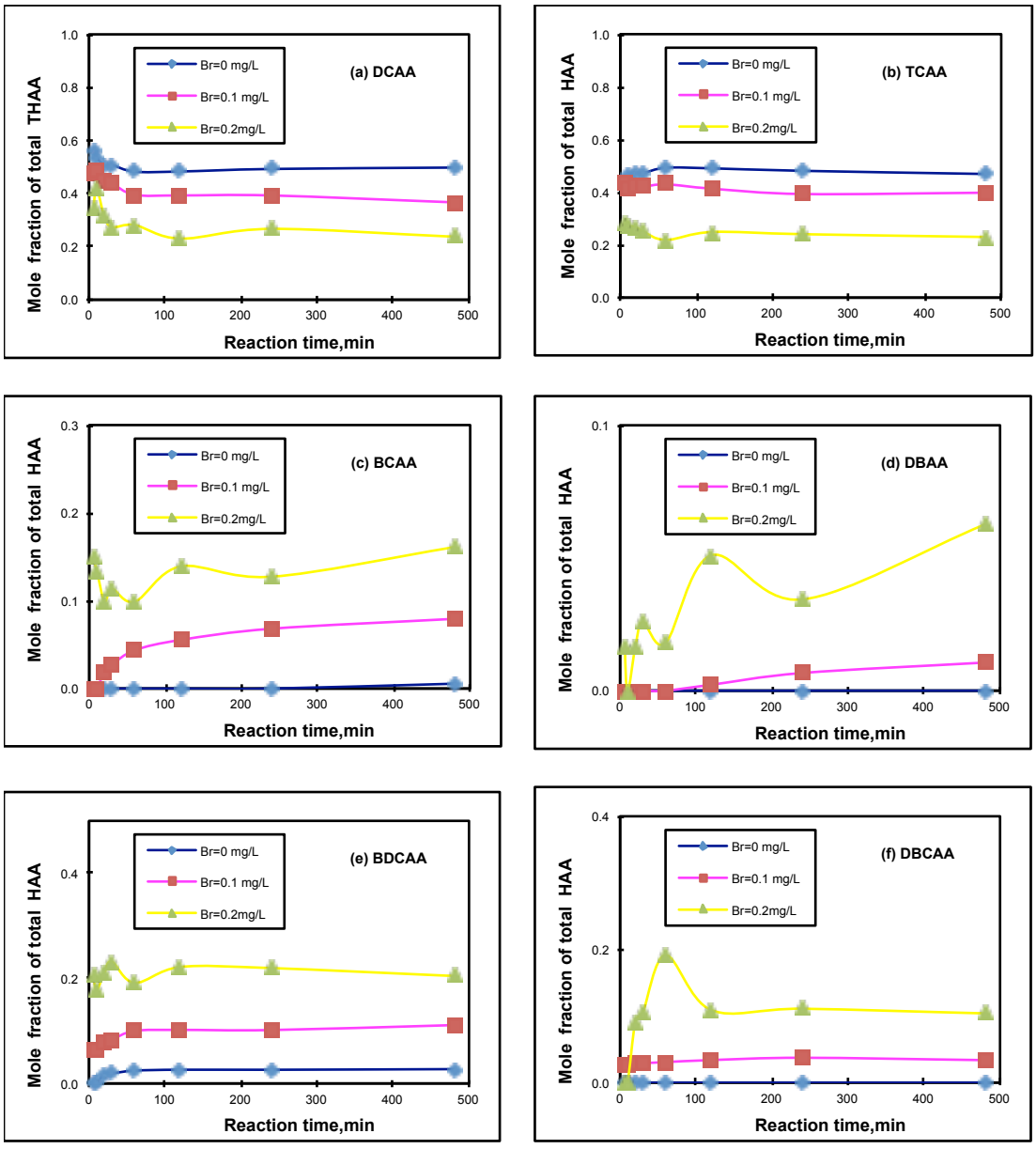

Figure 33 Molar fractions of individual HAAs species in THAA as a function of chlorination time and initial bromide ion concentration, pH=7, Lake Washington DOC=3.65mg/L, chlorine to DOC ratios of 1.0 mg/mg, (a) DCAA, (b) TCAA, (c) BCAA, (d) DBAA, (e) BDCAA, (f) DBCAA.

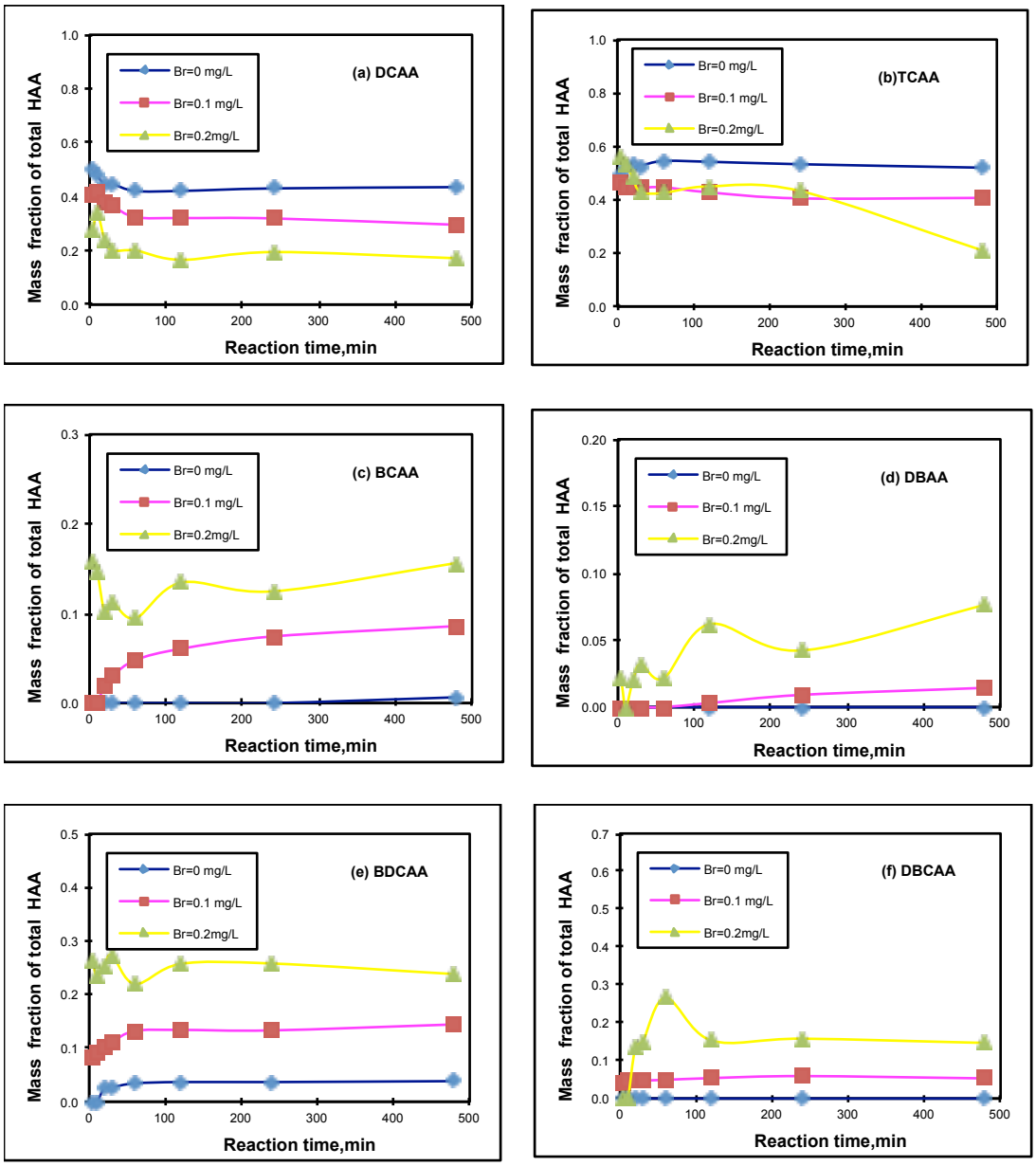

Figure 34 Weight fractions of individual HAAs species in THAA as a function of chlorination time and initial bromide ion concentration, pH=7, Lake Washington DOC=3.65mg/L, chlorine to DOC ratios of 1.0 mg/mg, (a) DCAA, (b) TCAA, (c) BCAA, (d) DBAA, (e) BDCAA, (f) DBCAA.

Changes of the HAAs speciation and overall concentrations in chlorinated with Lake Washington water as a function of varying bromide concentrations are summarized in Figure 35. In general, increasing bromide concentration tended to cause molar THAA concentrations to increases, and also to significantly shift the speciation of HAAs from predominantly chlorinated species to mixed bromochloro

species and to solely brominated species. The reduction in DCAA and TCAA yields occurred simultaneously with increases of contributions of BCAA and BDCAA which were observed to gradually rise with bromide concentrations varying from 0 mg/L up to 0.5 mg/L. This trend is qualitatively similar to that for THMs.

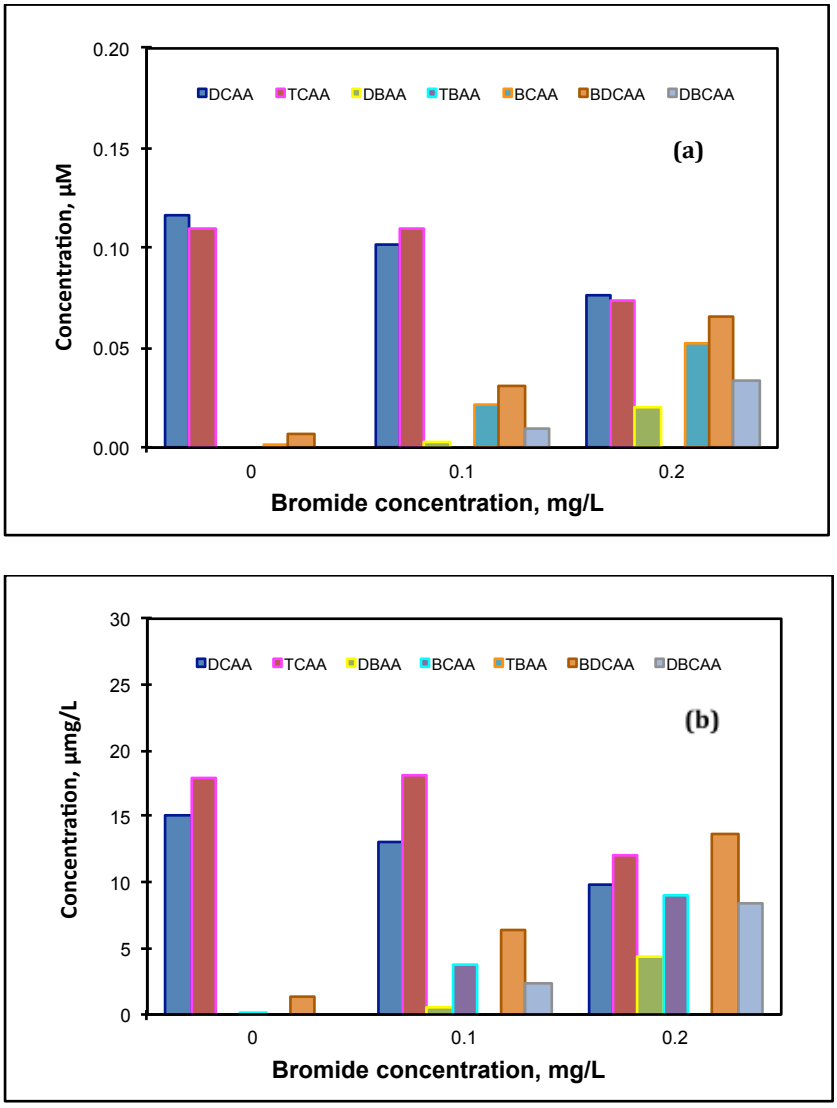

Figure 35 Effect of bromide on the molar (a) and mass yields (b) of individual HAA species in chlorinated Lake Washington water. DOC=3.65 mg/L, chlorine to DOC ratios of 1.0 mg/mg, reaction time 8 h, pH 7.

The contributions of individual HAA species at varying bromide concentration expressed using both molar and mass fractional basis are presented in Figure 36. At

low bromide concentration (< 0.2 mg/L), the relative contributions of HAA species were in the order: TCAA > DCAA > BDCAA > BCAA > DBCAA > DBAA > TBAA. Above 0.2 mg/L, the order changed, at for the highest utilized bromide concentration (0.5 mg/L), the speciation order was nearly opposite that that observed at a 0 mg/L bromide: DBCAA > BDCAA > TBAA > BCAA > DBAA > TCAA > DCAA.

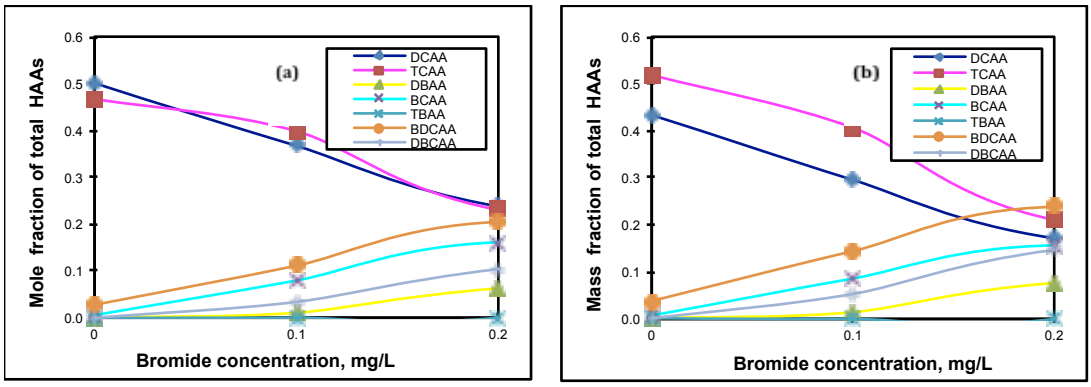

Figure 36 Fractional contributions of individual HAA species expressed using mole fractional basis (a) and on mass fractional basis (b) in chlorinated Lake Washington sampling DOC=3.65 mg/L, chlorine to DOC ratios of 1.0 mg/mg, reaction time 8 h, pH 7.

Figure 37 shows the impacts of bromide concentration on the yields of THMs and selected HAAs (HAA5) in chlorination water. The HAA5 represent the sum of MCAA, MBAA, DCAA, DBAA, TCAA. Of those, MCAA and MBAA tend to acount for less 5% of THAA; these species were not detected in this study. Otherwise, eincreases of bromide concentrations were observed to be accompanied by substancial increases of TTHM concentrations; these increases were in the range of 27%-56% of the TTHM concentration in the absence of added bromide. The yield of HAA9 also increased in these conditions by 18%-80% (although the latter number may be an artifact) resulted in increasing initial bromide levels. However, HAA5

concentrations decreased, mostly because of the increasing contributions of the HAA species that are not included in HAA5.

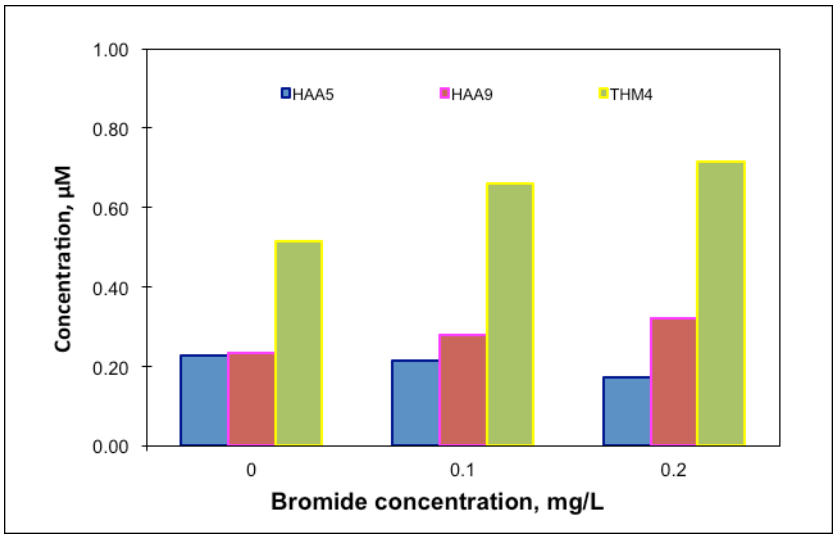

Figure 37 Effect of bromide on the molar yields of THMs and HAAs in chlorinated Lake Washington sampling DOC=3.65 mg/L, chlorine to DOC ratios of 1.0 mg/mg, reaction time 8 h, pH 7.

CHAPTER 4 EFFECT OF IODINATION ON THE ABSORBANCE AND FLUORESCENCE OF NOM

Recent changes in the regulations concerning maximum concentrations of DBPs in drinking water have necessitated an increased interest in using chloramine as a secondary disinfectant. The use of chloramine instead of chlorine allows maintaining a stable residual throughout the distribution system yet it greatly suppresses the formation of THMs and some HAAs (notable, trihalogenated HAA species). Among other consequences, the increased use of chloramine has caused more interest in the formation of iodine-containing DBPs. This is because while iodide is relatively stable in freshwater although it can be partially oxidized to iodate IO_3^-, it is virtually completely oxidized to inactive iodate in the presence of chlorine. Thus, the formation of iodine-containing DBPs in chlorinated water is largely prevented. However, during chloramination iodide can be oxidized to hypoiodous acid HOI which readily react with NOM forming I-DBPs. While iodide concentrations tend to be at least 10 times less than those of bromide in fresh water, toxicities of I-DBPs are much higher than those of Br-DBPs and Cl-DBPs.

In many studies, UV absorbance has been proven to be a very good indicator with which to estimate the amount of DBPs precursors present in any water, mostly due to the presence of UV-absorbing activated aromatic structures (i.e., phenolics and aromatic amines) attacked by oxidants (Harrington et al., 1996a; Reckhow et al., 1990). Other studies have shown that reliable and simple relationships exist between changes of UV absorbance and concomitant formation of DBP (Korshin et al., 1997a, 1999; Li et al., 1998). As was discussed above, this is because in the range of wavelengths > 250 nm the absorbance of NOM is defined by the presence of

unsaturated double bonds and π-π electron interactions in aromatic compounds. These functional groups and interactions decrease as a result of chlorine attack on electron-rich sites in NOM (Li et al., 1998, 2000).

Several studies have found that hydrophobic NOM samples or fractions tend to have higher light absorbance because such samples are relatively rich in aromatic carbon in general and phenolic structure, conjugated double bonds and larger molecule sizes in particular. Hydrophilic NOM tends to contain more aliphatic carbon and nitrogen-containing groups and is characterized by a smaller molecule sizes or AMWs.

Some studies found that hydrophobic NOM contains more precursors of DBPs (Harrington et al., 1996b; Liang and Singer, 2003). One study (Reckhow, 2007) was specifically focused on the relationships between the formations of DBP and properties of hydrophobic and hydrophilic NOM during chlorination and chloramination. This study observed that hydrophobic and high AMW (>5000 Da) NOM produced more TOX and THM than hydrophilic and low AMW (<5000 Da) NOM during chlorination. However, the separation into hydrophobic and hydrophilic NOM fractions had little impact on the formation of TOX while the formation of THM and HAA was more favorable from the hydrophilic rather than hydrophobic NOM during chloramination (Hua and Reckhow, 2007b).

4.1 Changes of absorbance of NOM caused by chloramination in the presence of iodide

Given that iodine species, similarly to those of chlorine or bromine, are likely to interact with the aromatic groups in NOM and these reactions can be well tracked using the fluorescence and/or absorbance methods, the goal of this section is to

examine in detail the changes of NOM absorbance caused by NOM interaction with chloramine at varying iodide concentrations and reaction times.

In this section, NOM from a Nordic reservoir (NNOM) was used. This is a standard sample of NOM and its properties are expected to be similar to those of SRFA.

Absorbance spectra of NNOM (DOC 5mg/L) reacting with chloramine at varying reaction times are shown in Figure 38. Iodide levels in these experiments were 0 mg/L to 4mg/L. The spectra are largely similar to those of SRFA or Lk. Washington water except that there is a conspicuous at 225 nm, with its intensity increasing at higher iodide concentrations. In fact, the peak at 225 nm was determined to be proportional to the concentration of iodide present in the solution, as was established by measuring UV absorbance of KI in the absence of NOM and chloramine.

It is important to realize that the spectra shown in Figure 38 reflect the absorbance of chloraminated NNOM after chloramine had been reduced by Na_2SO_3, which was used as a chloramine-quenching agent. This caused the HOI present in the sample to be reduced back to iodide. Accordingly, the changes of the peak at 225 nm reflect the consumption of iodide during the chloramination of NNOM (Awtrey and Connick, 1951). While the decrease of iodide concentration can be associated with both its incorporation into the NOM substrate, I-DBPs and also oxidation to iodate, it is relevant to assume conceptually that this decrease may related to the changes of the absorbance of NNOM caused by iodine species interactions with the chromophores (and fluorophores, as discussed in the next section).

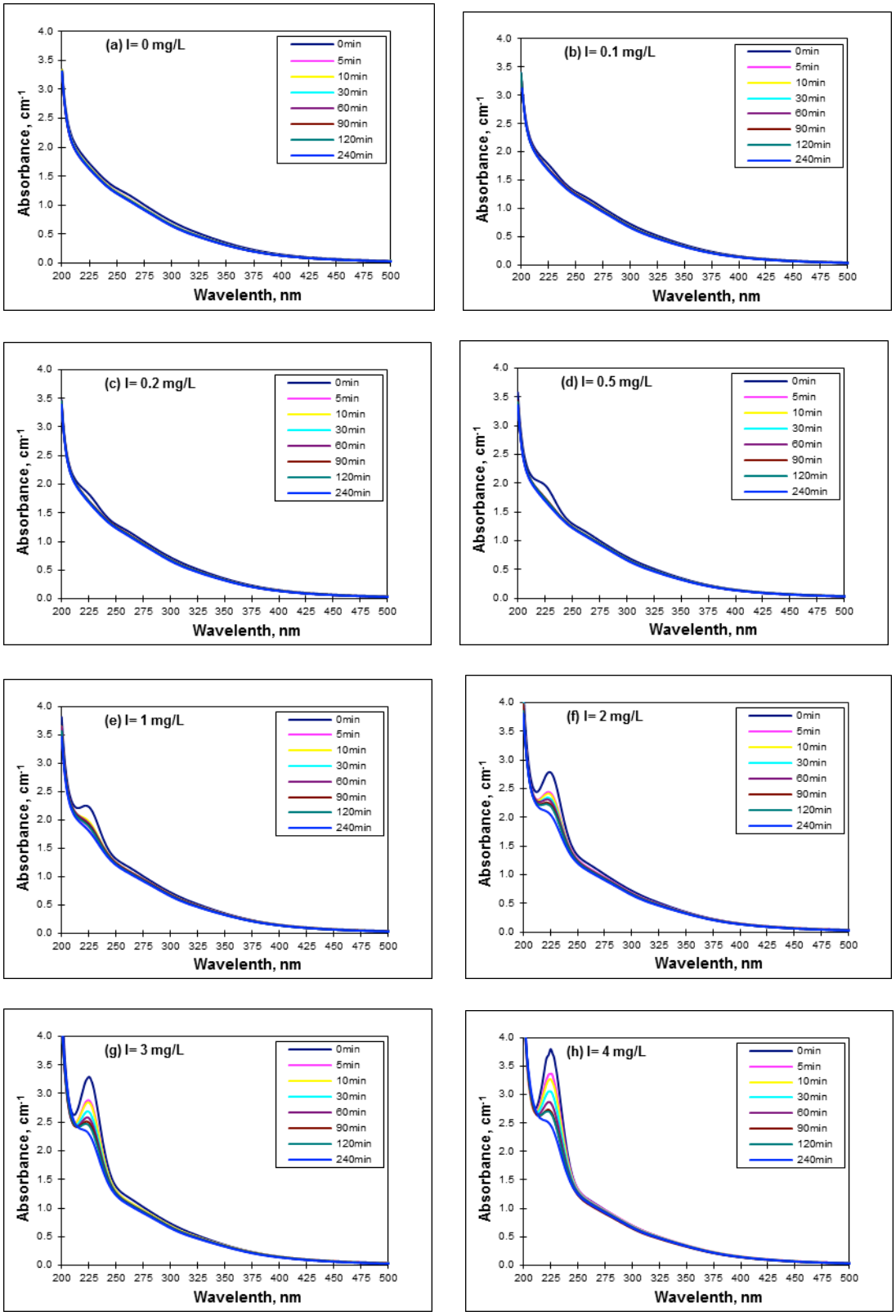

Figure 38 Absorbance spectra of Nordic NOM recorded at varying iodide concentrations in the presence of chloramine. DOC 5mg/L, chlorine to DOC ratios of 1.5 mg/mg, NH_4^+ to chlorine ratios of 1.5 mol/mol, pH 7.0, reaction time from 5min to 4 h, iodide concentration (a) 0 mg/L, (b) 0.1 mg/L, (c) 0.2 mg/L, (d) 0.5 mg/L, (e) 1 mg/L, (f) 2 mg/L, (g) 3 mg/L, (h) 4 mg/L.

Figure 38 does not show pronounced changes of NNOM other than the consistent changes of the peak at 225 nm. However, effects of chloramination and iodination can be tracked in much more detail using the differential approach. Figure 39 and Figure 40 show the differential spectra resulting from chloramination of Nordic NOM with enhancing iodide concentration over time. The difference between these figures is that

Figure 39 shows the data for the range of wavelengths 200 to 500 nm that are frequently predominated by the band at 225 nm. Figure 40 excludes the region of wavelengths < 250 nm and thus shows the changes of NOM absorbance in the range of wavelengths typical for differential spectroscopy of NOM.

In the absence of iodide, chloramination caused the initial absorbance of NOM to decrease at virtually all wavelengths (Figure 40A). The differential spectra observed to the chloramination of NNOM were similar to those observed in the case of chlorination of SRFA (Figure 7), but their intensity was much lower and the shoulder located at ca. 300 nm was relatively more prominent.

Increases of iodide concentration resulted in a strong enhancement of the structure at 225 nm and also of its changes as a function of time; this behavior is clearly indicative of the consumption of iodine species during chloramination (Figure 39). However, in the range outside of the strong peak at 225 nm, the differential spectra of NNOM became weaker for iodide concentrations up to 0.5 mg/L while retaining or rather enhancing the prominence of the peak at ca. 305 nm that was not clearly observed during the chlorination or bromination of SRFA (Figure 40). Further increases of iodide concentrations resulted in the enhancement of the differential absorbance at wavelengths < 260 nm although this may be caused by the strong increases of the adjacent band at 225 nm. At the same time, the differential absorbance in the range of wavelength > 325 nm decreased or even became positive at increasing iodide concentrations indicating that the absorbance of NNOM slightly increases in this range of wavelength rather than decreases (Figure 40). This behavior

was never seen for chlorination or bromination of NOM and this appears to be indicative of specific effects of iodine incorporation into NNOM or related effects.

Kinetically, the intensity of differential absorbance increased monotonically with increasing contact times in the absence of iodide but this behavior became increasingly complex for higher iodide concentrations, as especially evident for the differential spectra of NNOM at wavelengths > 325 nm for iodide levels 2 to 4 mg/L. In this case, the differential absorbance initially become positive and then negative indicating the occurrence of potentially complex transformations of NNOM. However, in all cases the iodination of NOM appears to proceed through an initial fast reaction that takes place within 30 minutes, and a slower reaction phase during which incremental changes of NNOM absorbance are less prominent.

The differential log-transformed spectra of chloraminated NNOM $Ln(A/A_0)$ are shown in Figure 41. This figure shows trends that are similar to and consistent with those shown in Figure 39 and Figure 40. However, the increase rather than decrease of the absorbance of NNOM at wavelengths > 325 nm, relatively short reaction times and high iodide concentrations is more clearly seen in Figure 41.

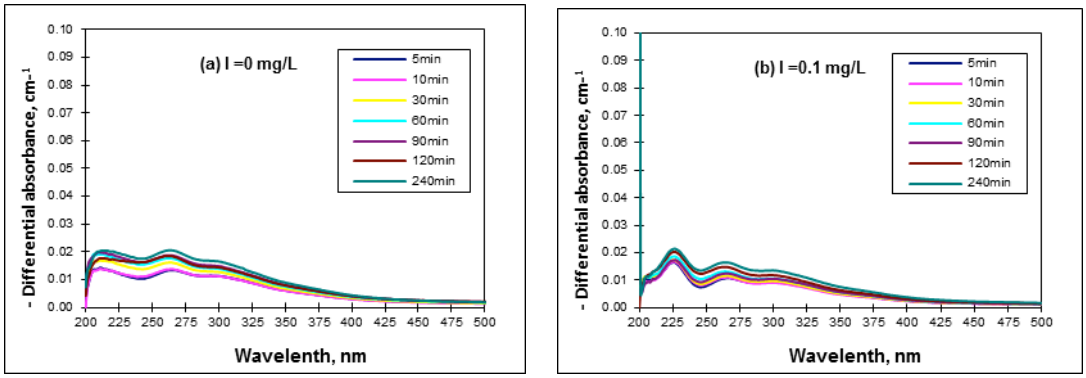

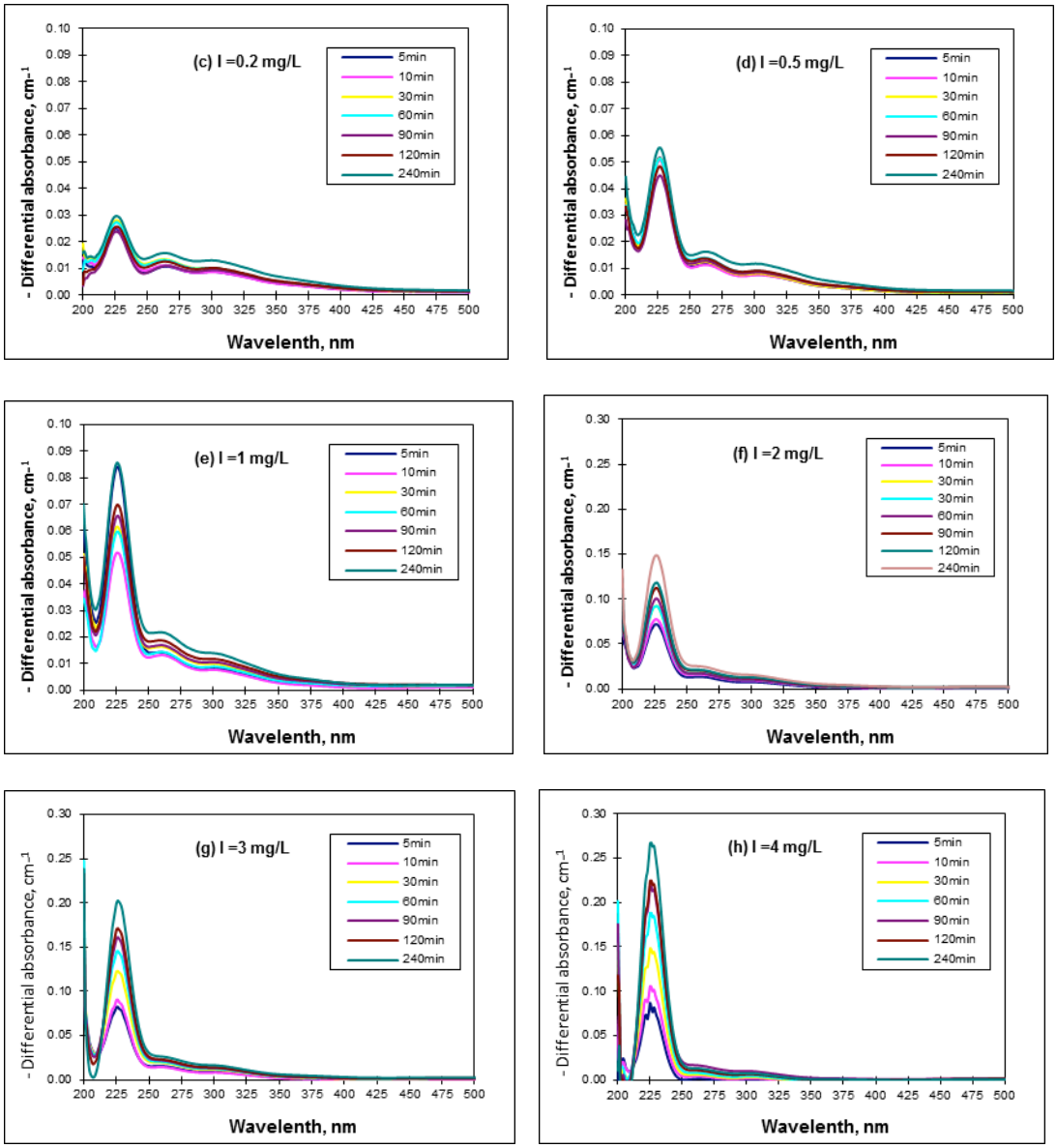

Figure 39 Differential absorbance spectra of Nordic NOM obtained for varying iodide concentrations in the presence of chloramine. DOC 5mg/L, chlorine to DOC ratios of 1.5 mg/mg, NH_4^+ to chlorine ratios of 1.5 mol/mol, pH 7.0, reaction time from 5min to 4h, iodide dose (a) 0 mg/L, (b) 0.1 mg/L, (c) 0.2 mg/L, (d) 0.5 mg/L, (e) 1 mg/L, (f) 2 mg/L, (g) 3 mg/L, (h) 4 mg/L.

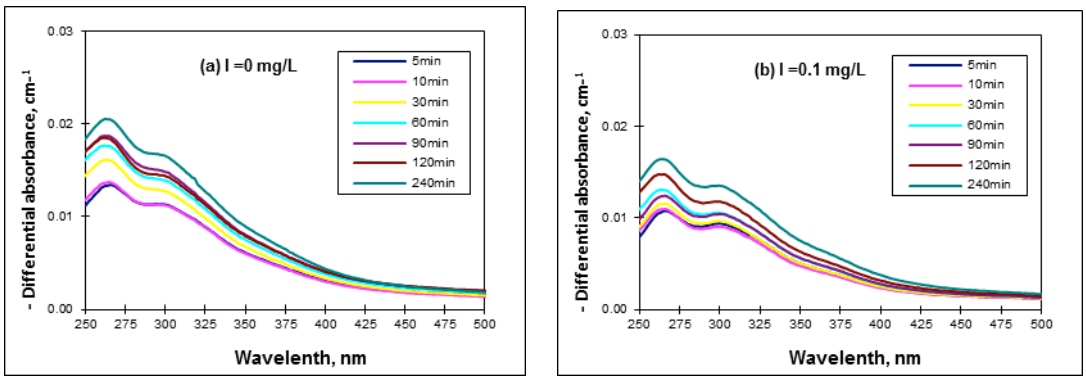

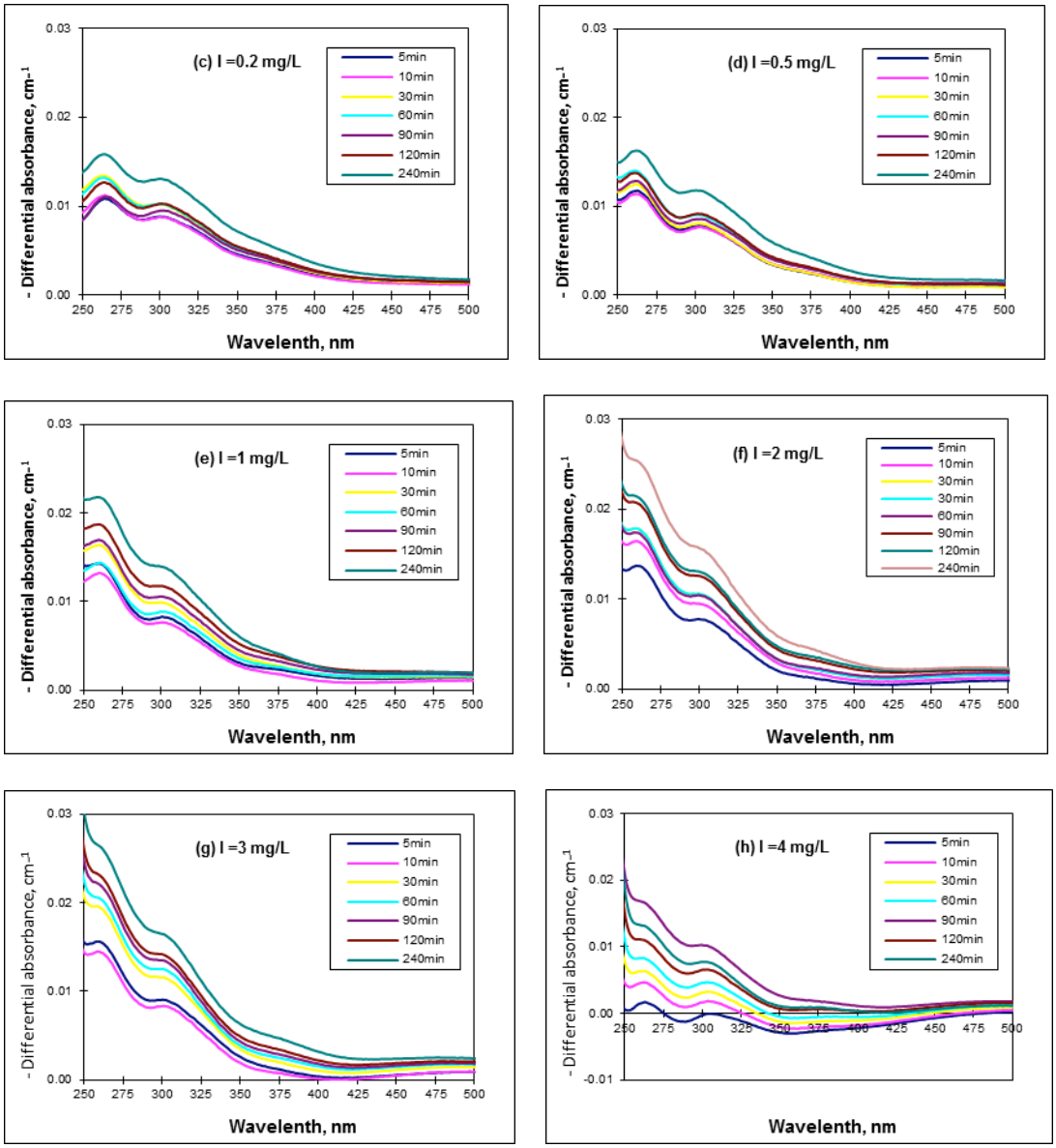

Figure 40 Differential absorbance spectra of Nordic NOM, in a region of 250 to 500 nm at varying iodide concentration in the presence of chloramine. DOC 5mg/L, chlorine to DOC ratios of 1.5 mg/mg, NH_4^+ to chlorine ratios of 1.5 mol/mol, pH 7.0, reaction time from 5min to 4h, iodide dose (a) 0 mg/L, (b) 0.1 mg/L, (c) 0.2 mg/L, (d) 0.5 mg/L, (e) 1 mg/L, (f) 2 mg/L, (g) 3 mg/L, (h) 4 mg/L.

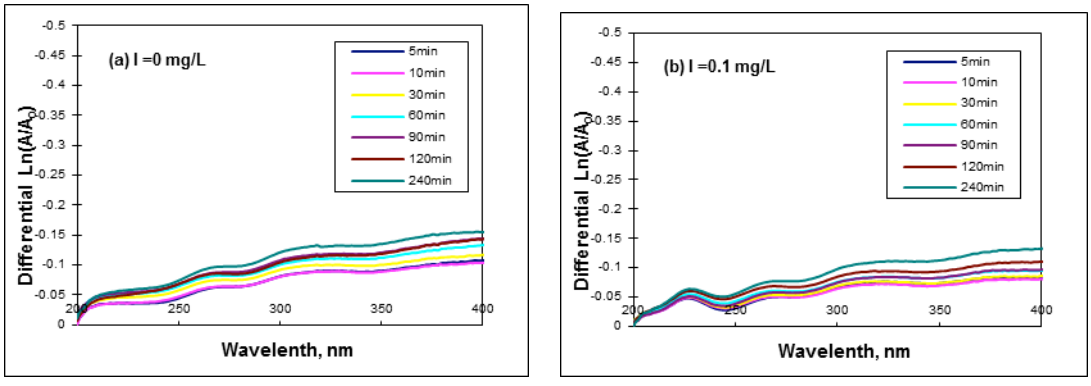

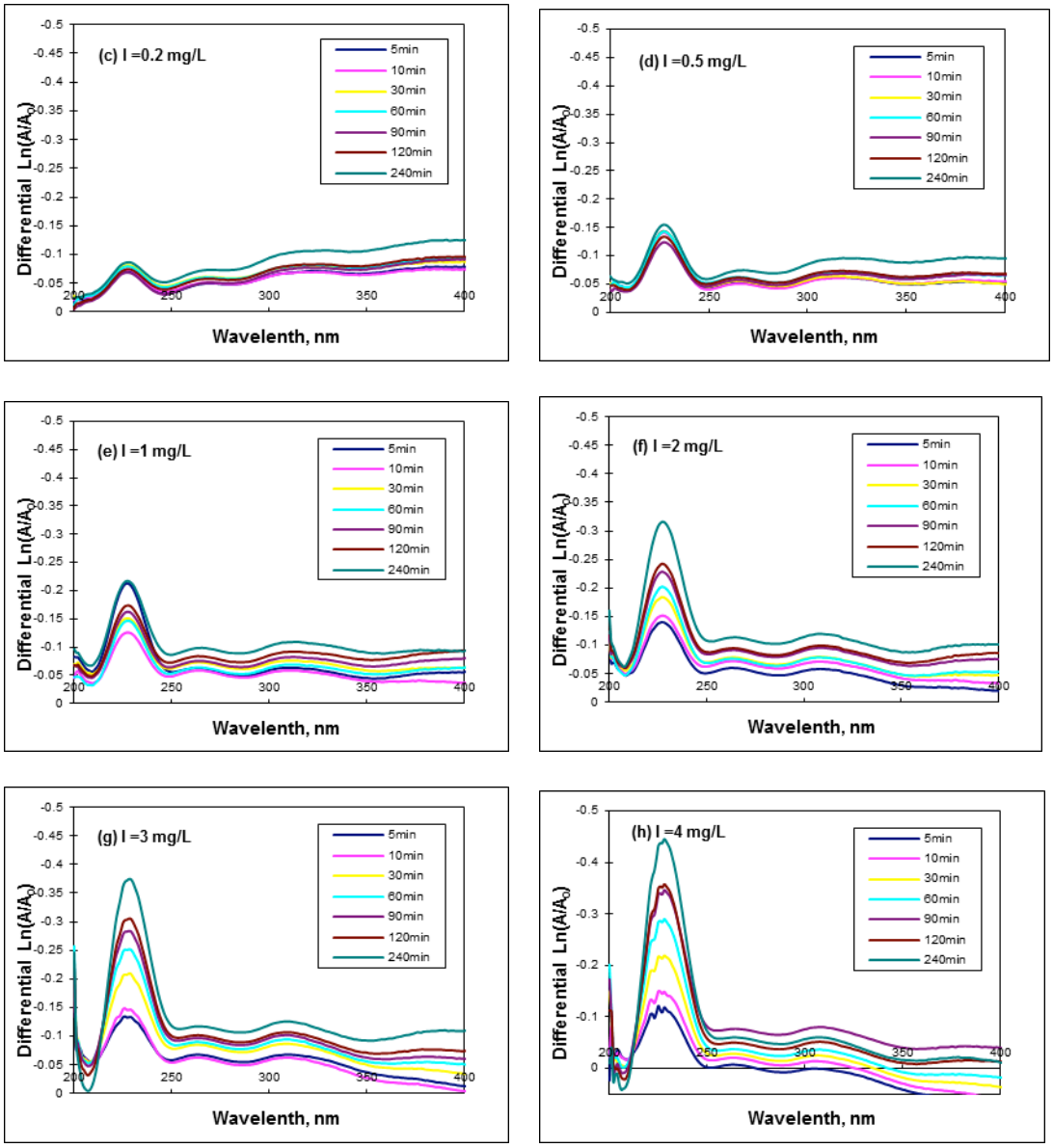

Figure 41 Differential Ln(A/A$_0$) spectra of Nordic NOM obtained for varying iodide concentrations in the presence of chloramine. DOC 5mg/L, chlorine to DOC ratios of 1.5 mg/mg, NH_4^+ to chlorine ratios of 1.5 mol/mol, pH 7.0, reaction time from 5min to 4h, iodide dose (a) 0 mg/L, (b) 0.1 mg/L, (c) 0.2 mg/L, (d) 0.5 mg/L, (e) 1 mg/L, (f) 2 mg/L, (g) 3 mg/L, (h) 4 mg/L.

Effects of iodide concentration effect on the changes of the absorbance of NNOM in during chloramination are further compared in Figure 42 and Figure 43 that present the relevant data for a fixed contact time but varying iodide levels. The intensity of differential absorbance (Figure 42) can be seen to increase at 225 nm for higher iodide levels. As was discussed above this indicates that both changes of

iodide concentration can be tracked in situ and that the consumption of iodide increases at its higher levels. Figure 43 presents the log-transformed differential $Ln(A/A_0)$ They show a similar trend in the range of 200 to 325 nm while there is a conspicuous phenomenon for $\lambda > 325$nm possibly associated, as discussed above, with the specific effects of iodine incorporation into NNOM.

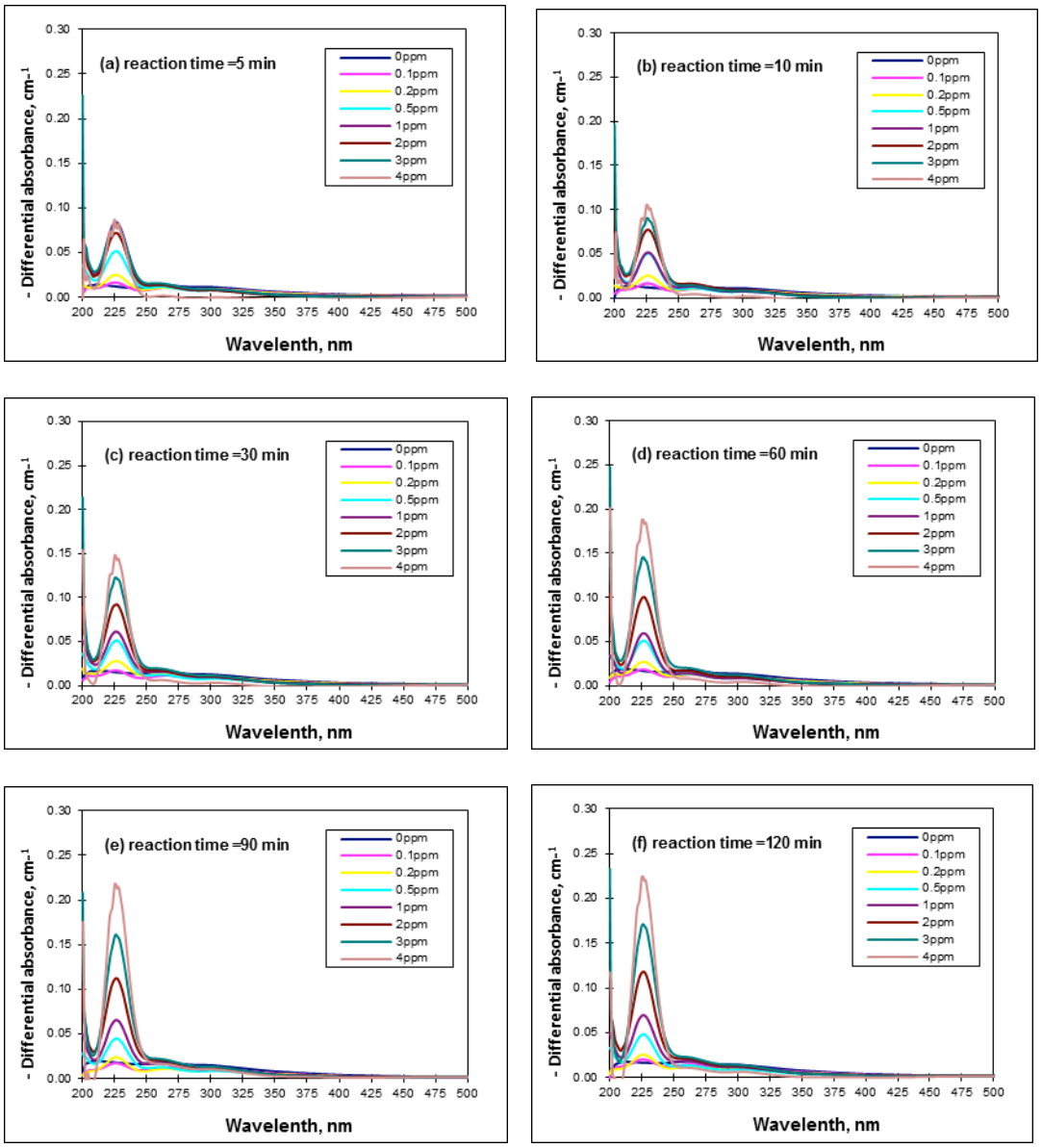

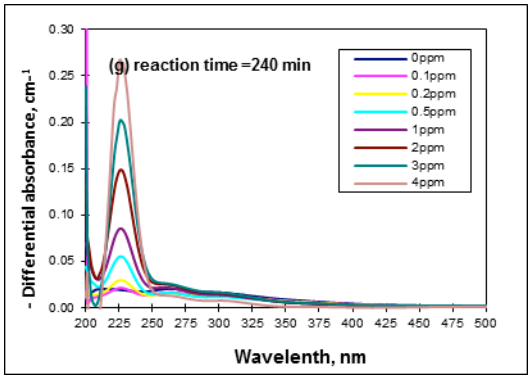

Figure 42 Effects of iodide on the differential absorbance spectra of Nordic NOM recorded for fixed chloramination times. DOC 5mg/L, chlorine to DOC ratios of 1.5 mg/mg, NH_4^+ to chlorine ratios of 1.5 mol/mol, pH 7.0, iodide concentration from 0 to 4mg/L, reaction time (a) 5 min, (b) 10min, (c) 30min, (d) 60min, (e) 90min, (f) 120min, (g) 240min.

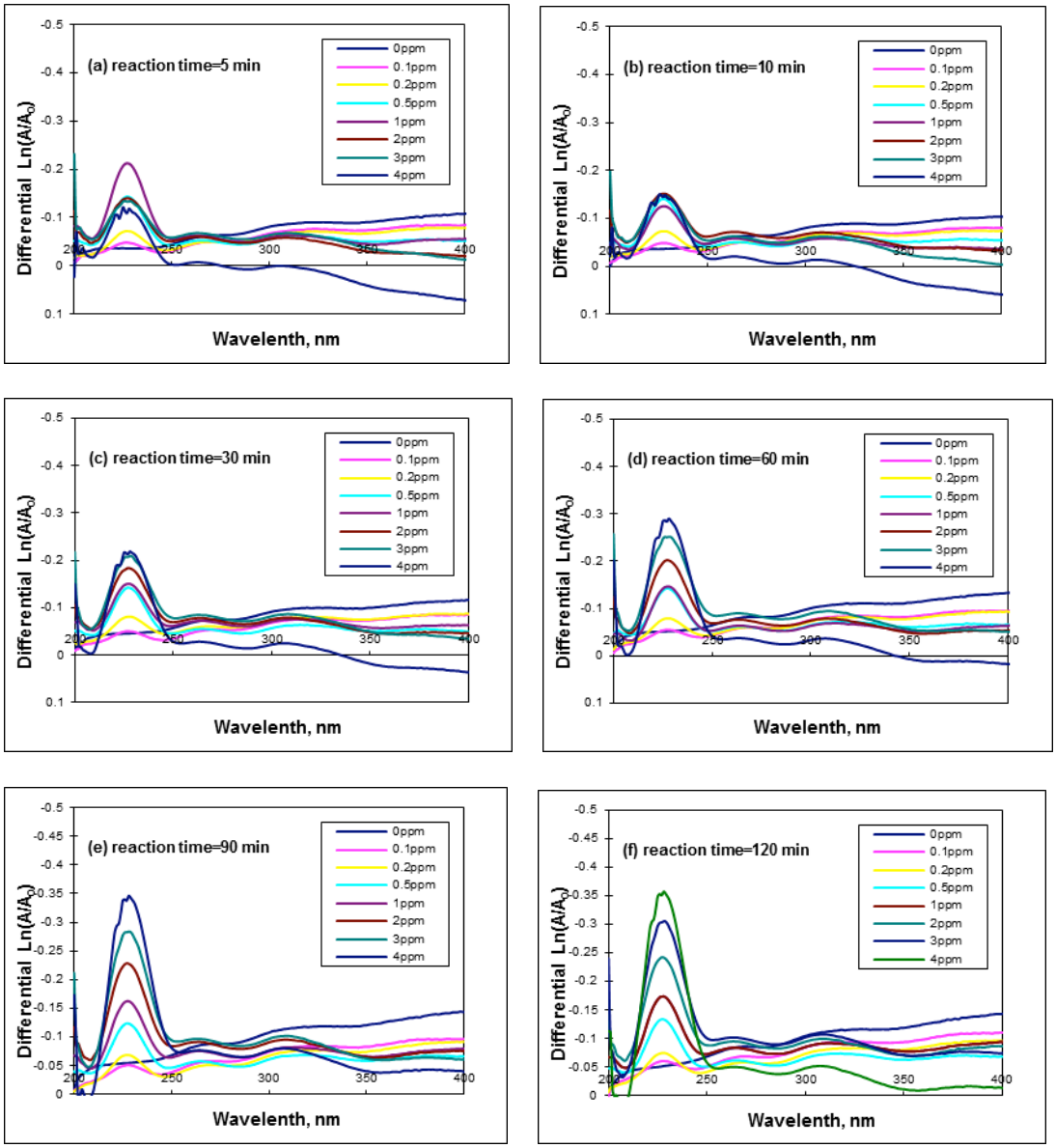

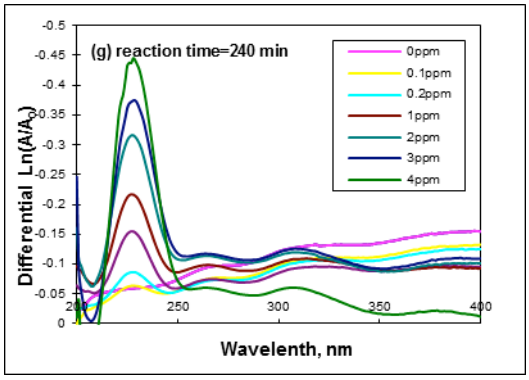

Figure 43 Effects of iodide on the log-transformed differential absorbance spectra of Nordic NOM recorded for fixed chloramination times. DOC 5mg/L, chlorine to DOC ratios of 1.5 mg/mg, NH_4^+ to chlorine ratios of 1.5 mol/mol, pH 7.0, iodide concentration from 0 to 4mg/L, reaction time (a) 5 min, (b) 10min, (c) 30min, (d) 60min, (e) 90min, (f) 120min, (g) 240min.

Figure 44 presents a compilation of changes of the differential spectra of NNOM at two fixed wavelengths (225 and 425 nm) that correspond to the specific effects associated with iodide consumption (at 225 nm) and, conceptually, iodine incorporation as well as the breakdown of NNOM chromophores (at 425 nm). Both dataset demonstrate the presence of the fast and slow NNOM chloramination and iodination reactions as well as the presence of complex effects of iodine on NOM chromophores. These can be examined in more detail based on the fluorescence data obtained for NNOM.

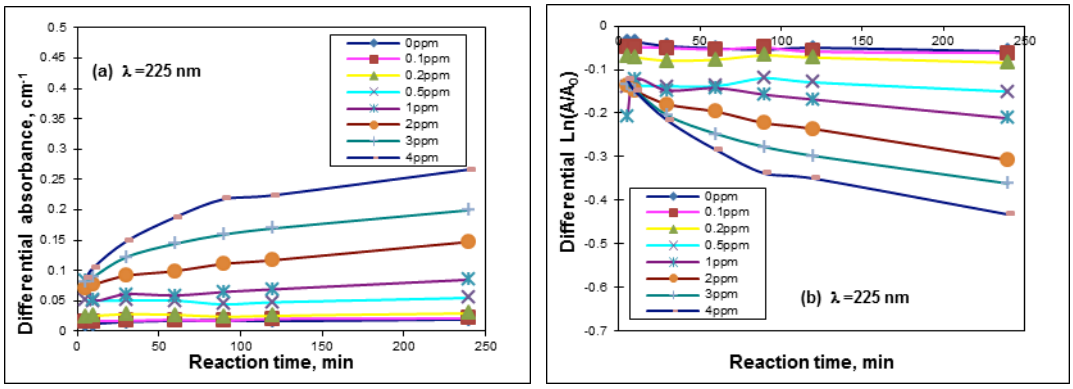

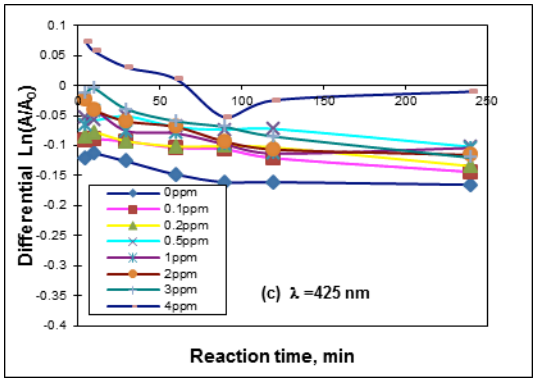

Figure 44 Differential Ln (A/A_0) and differential absorbance of Nordic NOM at a fixed wavelength with varying iodide dose, DOC 5mg/L, chlorine to DOC ratios of 1.5 mg/mg, NH_4^+ to chlorine ratios of 1.5 mol/mol, pH 7.0, (a) differential absorbance at 225nm, (b) differential Ln (A/A_0) at 225nm, (c) differential Ln (A/A_0) at 425nm.

4.2 Changes of fluorescence of NOM caused by chloramination in the presence of iodide

Fluorescence spectroscopy reveals the existence of mostly aromatic fluorophore groups which form a subset of chlromophores in NOM. Humic substance and protein-like species that are present in NOM have been ascertained as the most prominent fluorophore groups (Coble, 1996; Mopper and Schultz, 1993), and these classes of NOM functional groups represented by the relevant fluorophores are likely to be related to DBP formation (Reckhow et al., 1990). Several recent studies have evaluated the relationships between the changes of fluorescence intensity and levels of DBP formation in the case of chlorination. These studies have suggested multiple fluorescence indexes (FI) to examine such relationships. Examples of FI include changes of the ratio of fluorescence intensities at fixed wavelengths $\Delta(I_{500}/I_{400})$ and changes of the position of half the maximum fluorescence intensity $\lambda_{0.5}$ (Fabbricino and Korshin, 2004; Roccaro et al., 2009).

In this section, we examine in detail the behavior of NNOM fluorescence spectra during its chloramination and evaluate effects of iodide concentration and reaction time on the observed phenomena.

Figure 45 shows the fluorescence spectra of chloraminated NNOM at varying iodide doses and reaction times. In the absence of iodide, the behavior of the emission of NNOM is somewhat similar to that of SRFA chlorinated in the absence of bromide (Figure 15): the intensity of emission increases immediately after the start of the reaction but its further changes are relatively inconspicuous. Increase of iodide concentration do not case very pronounced changes of the fluorescence emission and for a 0.5 mg/L iodide concentration the emission spectra hardly changes throughout the reaction. However, at higher iodide concentrations, the intensity of emission decreases immediately after the onset of the reaction somewhat similarly to the data shown for the chlorination/bromination of SRFA (Figure 15). This is very likely to be caused by the heavy atom effects, as was discussed above.

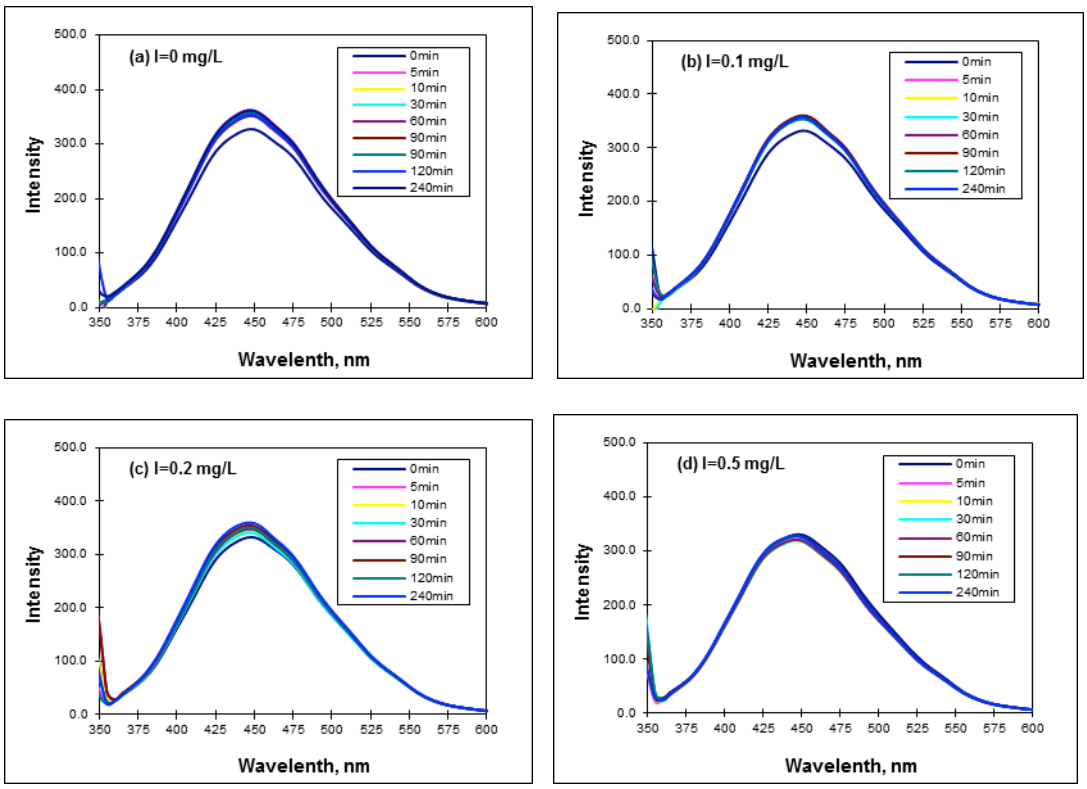

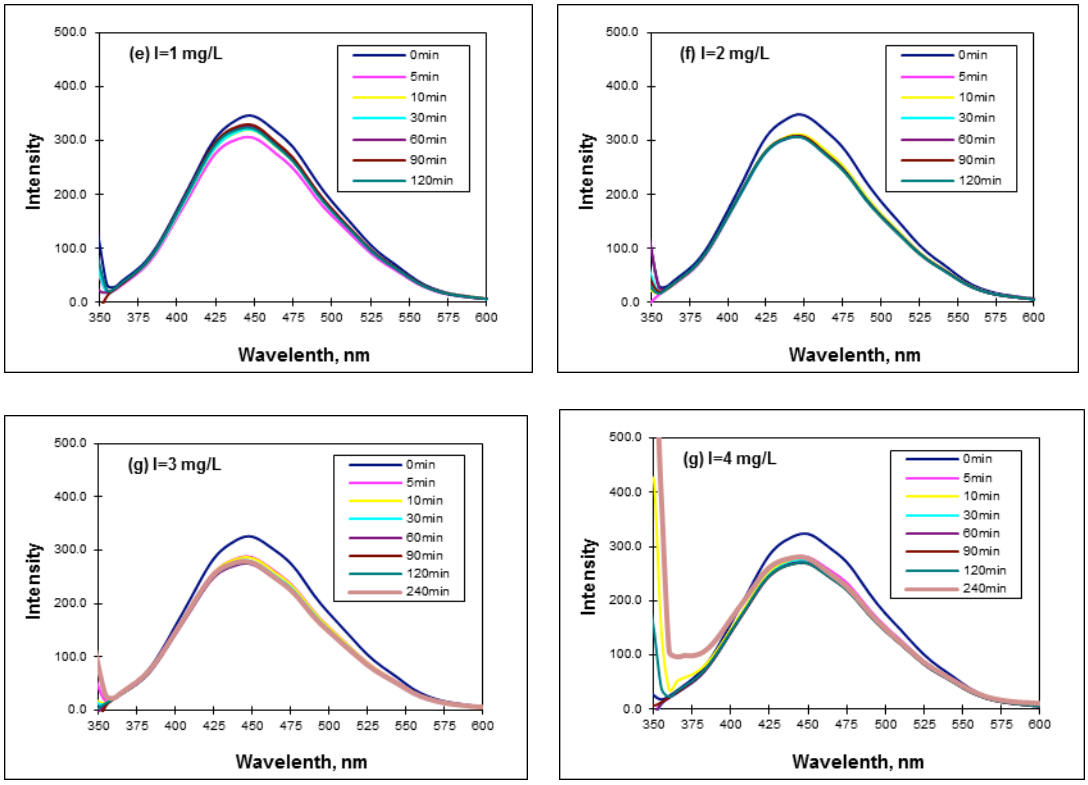

Figure 45 Fluorescence spectra of Nordic NOM obtained for varying iodide concentration in the presence of chloramine. DOC 5mg/L, chlorine to DOC ratios of 1.5 mg/mg, NH_4^+ to chlorine ratios of 1.5 mol/mol, pH 7.0, reaction time from 5 min to 4 h, iodide dose (a) 0 mg/L, (b) 0.1 mg/L, (c) 0.2 mg/L, (d) 0.5 mg/L, (e) 1 mg/L, (f) 2 mg/L, (g) 3 mg/L, (h) 4 mg/L.

Given the presence of relatively small changes of the absolute values of the emission of NNOM, we utilized the differential approach to calculate differential fluorescence spectra that are shown in Figure 46. These data confirm and enhance the above observations that changes of the iodide concentrations are associated with subtle and complex yet consistent changes of NNOM emission, notably its enhancement at virtually all wavelengths as a result of chloramination in the absence of iodide, and gradual prevalence of a decrease of NNOM emission, especially for wavelengths > 425 nm in the presence of increasing concentrations of iodide. This point is further enhanced by the data shown in Figure 47 that compared the differential intensities measured for varying iodide levels fixed reaction times. The figure clearly demonstrate the prevalence of a decrease rather than increase of NNOM

emission intensity at the concentration of iodide increases. This is clearly indicative of the incorporation of iodine in NNOM molecules and attendant manifestations of the heavy atom effects.

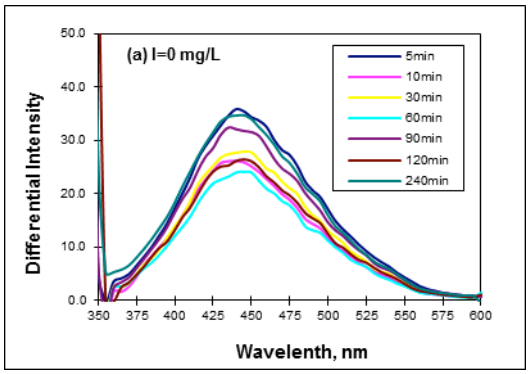

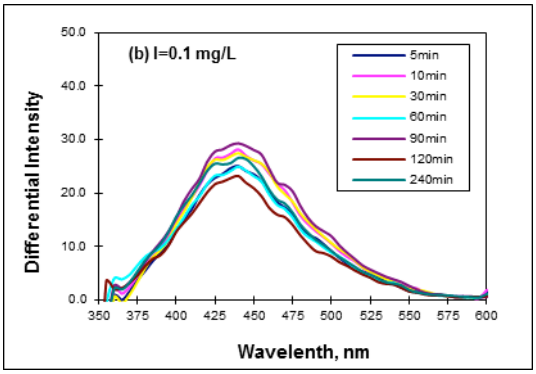

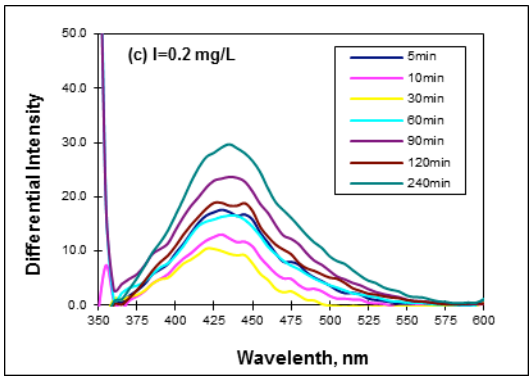

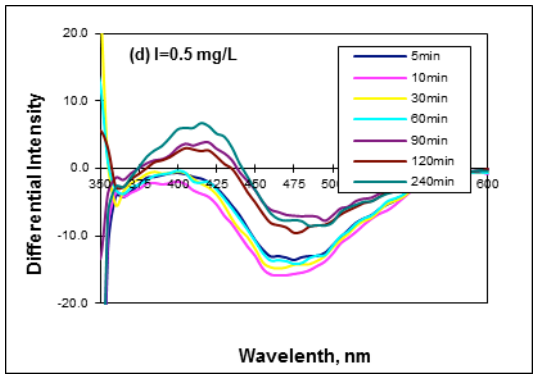

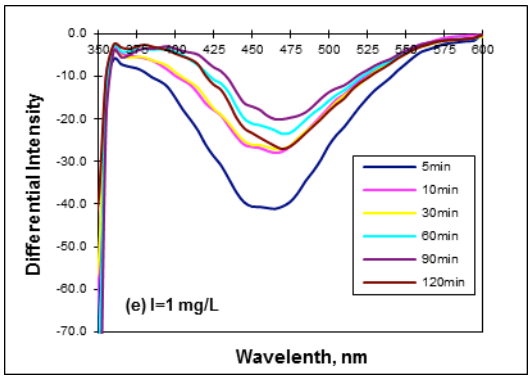

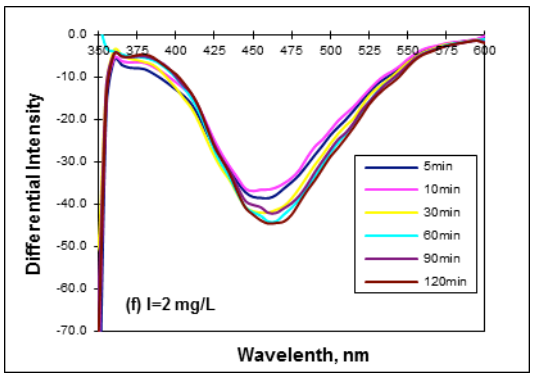

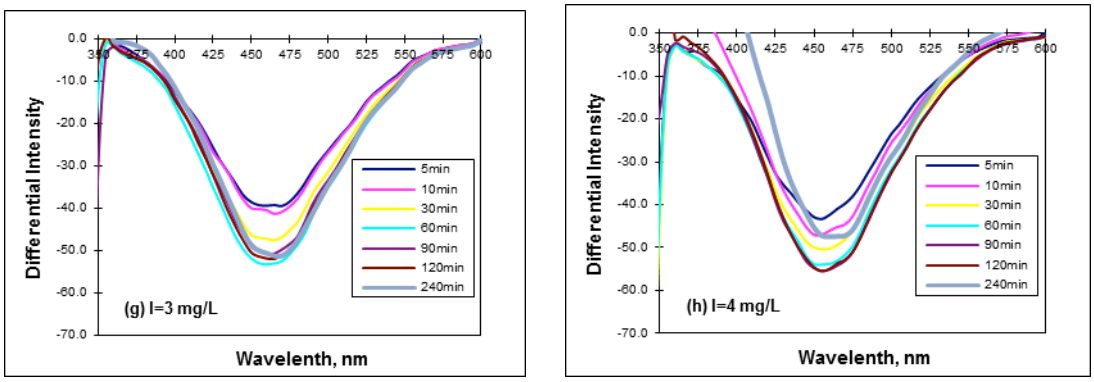

Figure 46 Differential fluorescence spectra of Nordic NOM obtained for varying iodide concentration in the presence of chloramine. DOC 5mg/L, chlorine to DOC ratios of 1.5 mg/mg, NH_4^+ to chlorine ratios of 1.5 mol/mol, pH 7.0, reaction time from 5min to 4h, iodide dose (a) 0 mg/L, (b) 0.1 mg/L, (c) 0.2 mg/L, (d) 0.5 mg/L, (e) 1 mg/L, (f) 2 mg/L, (g) 3 mg/L, (h) 4 mg/L.

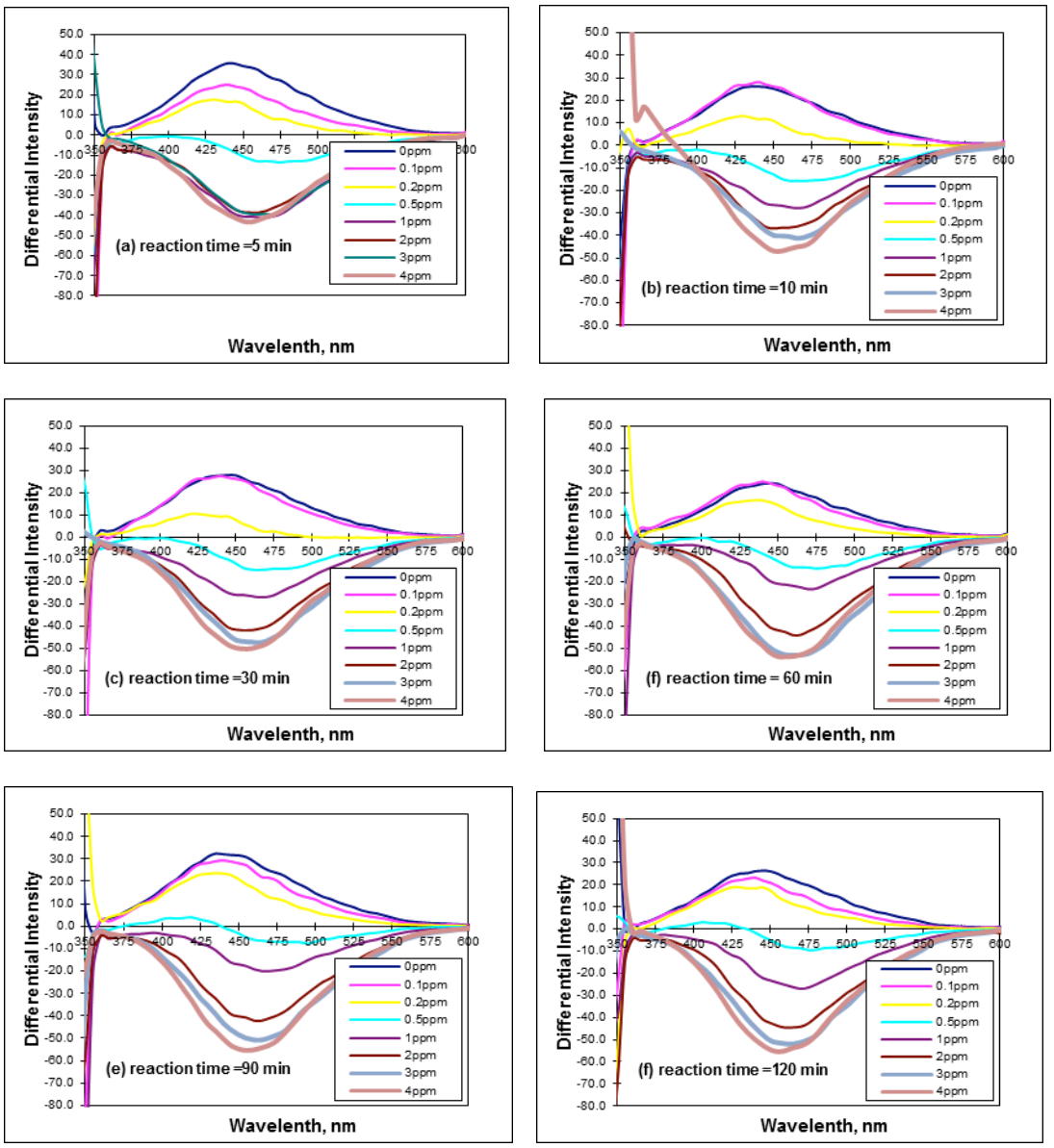

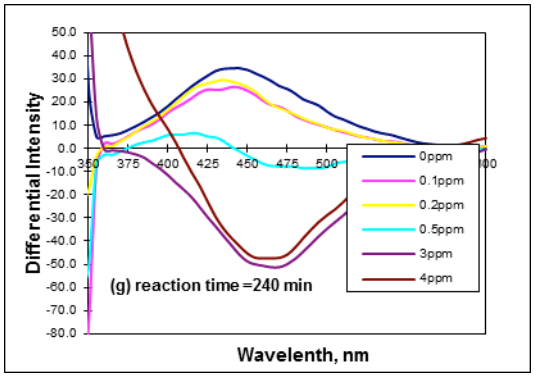

Figure 47 Effects of iodide on the differential fluorescence spectra of Nordic NOM recorded for fixed chloramination times. DOC 5mg/L, chlorine to DOC ratios of 1.5 mg/mg, NH_4^+ to chlorine ratios of 1.5 mol/mol, pH 7.0, iodide concentration from 0 to 4mg/L, reaction time (a) 5 min, (b) 10min, (c) 30min, (d) 60min, (e) 90min, (f) 120min, (g) 240min.

The notion that the consumption of iodide affects the fluorescence of NNOM can be clearly demonstrated by the data shown in Figure 48. The figure shows that increases of iodide consumption that are proportional to the differential absorbance of NNOM at 225 nm are also strongly correlated with the changes of NNOM emission at 460 nm. The decrease of the latter parameter was suggested in the discussion above to be caused by the incorporation of iodine into NNOM molecules while its increase may be caused by some oxidation and ensuing breakdown of NNOM molecules that appears to be characteristic for NNOM chloramination in the absence of iodide (Figure 45 and Figure 46). The data shown in Figure 48 demonstrate that small values of differential absorbance at 225 nm correspond to a relatively low incorporation of iodine into the organic substrate while gradually increasing values of differential absorbance at 225 nm are accompanied by a pronounced increase of the relative changes of NNOM emission which then stabilize and reach a plateau. This phenomenon may be explained by the existence of a maximum level of iodine incorporation into the organic substrate and further changes of the concentration of iodine species during chloramination may be caused by processes other than iodine

incorporation. The nature of such processes as well as associations between the phenomena observed for the absorbance and emission spectra of chloraminated and/or iodinated NOM will need to be explored in future studies.

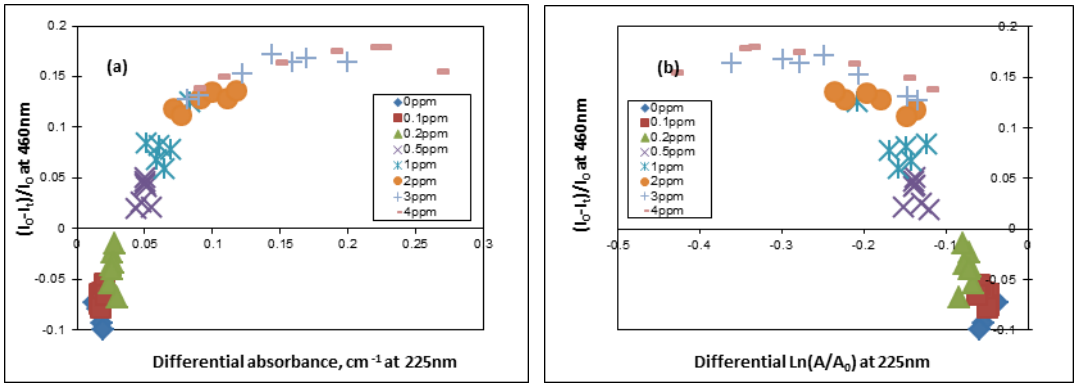

Figure 48 Relationships between differential absorbance of NNOM at 225 nm and changes of the fluorescence intensity at 460 nm at varying reaction times and initial iodide concentrations. (a) differential slop $(I_0-I_t)/I_0$ at 460nm with differential absorbance at 225nm, (b) differenial slop $(I_0-I_t)/I_0$ at 460nm with differential Ln(A/A0) at 225 nm.

Conclusions

This study demonstrated that the technique of differential absorbance and fluorescence spectroscopy can be successfully used for probing interactions of NOM in its reactions with chlorine, bromine and iodine species.

Experiments with varying bromide concentrations were carried out with SRFA and Lake Washington (winter and summer samples) which were chlorinated at a constant pH 7.0 and varying reaction times. These experiments showed that the magnitude of differential UV absorbance of SRFA increased with increasing bromide concentration and reaction time, and in all cases the differential spectra had a maximum in the wavelength range around 265 nm. The intensity of log-processed differential spectra of SRFA increased nearly linearly with the wavelength ca. 230 to 270 nm and then at wavelengths > 320 nm. Changes of the absorbance of Lake Washington water had a lower intensity due to a lower DOC of this water but most albeit not all of their features were similar to those of SRFA. Except the changes of the intensity and kinetics of the changes of the absorbance spectra of SRFA and Lake Washington NOM, bromination was not observed to exhibit specific effects. This can be explained by assuming that both chlorine and bromine selectively attack activated NOM chromophores (which are signatures of the aromatic rings NOM) and cause them to break down. While reactions of bromine species with these sites are faster than those of chlorine, they appear to follow the same reaction pathway.

In contrast with the lack of specific effects of bromination in the absorbance of NOM, NOM fluorescence was affected by varying bromide concentrations. In the absence of bromide, the intensity of SRFA fluorescence increased immediately after the start of chlorination but it decreased, very significantly at higher bromide

concentrations during bromination. The fluorescence spectra and relative changes of emission intensity of Lk Washington water showed effects similar to those characteristic for SRFA. The predominant reason of the observed effects in NOM fluorescence is likely to be related to two different processes. Namely, decreases of AWM of NOM caused by chlorination appear to be counter-balanced by bromide incorporation into the organic substrate (e.g., by reactions with putative polyhydroxyphenolic structures), with incrementally increasing heavy atoms effect and fluorescence quenching caused by them at higher bromide levels.

DBP formation in Washington summer sample was also measured at varying bromide concentration and chlorination reaction time. Increasing the bromide concentration caused molar TTHM concentration to increase and shift towards the predominance of bromine-containing THM species. Similar effects were detected for HAA species. The observed effects were highly consistent, however their relationship with changes of the absorbance and fluorescence of NOM remain to be explored in more detail.

In addition to NOM bromination studies, extensive experiments were carried out to examine changes of NOM absorbance and fluorescence during iodination. This was done for the case of chloramination of Nordic Reservoir NOM (NNOM) in the presence of different iodide concentrations. Iodide concentrations were varied in these experiments while other conditions were similar to those used in mixed chlorination/bromination experiments.

The measurements showed that changes of the absorbance spectra NNOM were similar to those of SRFA or Lk. Washington water except that there was a conspicuous peak at 225 nm. The intensity of this peak increased at higher iodide concentrations. This peak was determined to be proportional to the concentration of

iodide present in the solution and changes of this peak's intensity were concluded to reflect the consumption of iodide during the chloramination of NNOM. The differential absorbance of NNOM around 225nm increased with enhancing iodide concentration and chlorination reaction time. For log-transformed differential $Ln(A/A_0)$, there was a conspicuous structure located at $\lambda > 325$nm. It appeared immediately after the start of chloramination in the presence of iodide. Its intensity increased at higher iodide concentration but decreased as the reaction progressed. A possible explanation of this result is that iodine incorporation into NOM is accompanied by the formation of iodinated intermediates with spectroscopic properties different from those in the case of NOM chlorination or bromination.

Fluorescence spectra of chloraminated NNOM obtained at varying iodide doses and reaction times were examined as well. In the absence of iodide, their behavior was largely similar to that of SRFA or Lake Washington water chlorinated in the absence of bromide. In the presence of iodide, fluorescence intensity decrease similarly to but less conspicuously than what was observed in the case of bromination. Differential fluorescence spectra showed the presence of complex but consistent changes appearing to be indicative of the incorporation of iodine in NNOM molecules. Increases of iodide consumption during chloramination that are proportional to the differential absorbance of NNOM at 225 nm were strongly correlated with the changes of NNOM emission at 460 nm. The reason for this result is that the observed decreases of iodide concentration are in large extent caused by the incorporation of iodine into the NOM substrate with ensuing formation of I-DBPs (which were not measured in this study). Accordingly, the observed changes of the absorbance and fluorescence of NNOM were attributable to iodination of its chromophores and fluorophores. Future research will examine correlations between the formation of I-

DBPs and the specific effects seen in the behavior of the absorbance and fluorescence of NOM.

References

Acero, J.L., Piriou, P., and von Gunten, U. (2005). Kinetics and mechanisms of formation of bromophenols during drinking water chlorination: Assessment of taste and odor development. Water Research *39*, 2979–2993.

Ates, N., Yetis, U., and Kitis, M. (2007). Effects of bromide ion and natural organic matter fractions on the formation and speciation of chlorination by-products. Journal of Environmental Engineering *133*, 947–954.

Awtrey, A.D., and Connick, R.E. (1951). The Rate Law and Mechanism of the Reaction of Iodine with Thiosulfate Ion: The Formation of the Intermediate S2O3I-. J. Am. Chem. Soc. *73*, 1341–1348.

Beggs, K.M.H., Summers, R.S., and McKnight, D.M. (2009). Characterizing chlorine oxidation of dissolved organic matter and disinfection by-product formation with fluorescence spectroscopy and parallel factor analysis. Journal of Geophysical Research *114*, G04001.

Bellar, T.A., Lichtenberg, J.J., and Kroner, R.C. (1974). The occurrence of organohalides in chlorinated drinking waters. Journal (American Water Works Association) 703–706.

Bichsel, Y., and Von Gunten, U. (1999). Oxidation of iodide and hypoiodous acid in the disinfection of natural waters. Environmental Science & Technology *33*, 4040–4045.

Bichsel, Y., and Von Gunten, U. (2000). Formation of iodo-trihalomethanes during disinfection and oxidation of iodide-containing waters. Environmental Science & Technology *34*, 2784–2791.

Bull, R.J., Krasner, S., Daniel, P., and Bull, R. (2001). Health effects and occurrence of disinfection by-products (AWWA Research Foundation and American Water Works Association).

Cancho, B., Fabrellas, C., Diaz, A., Ventura, F., and Galceran, M.T. (2001). Determination of the odor threshold concentrations of iodinated trihalomethanes in drinking water. Journal of Agricultural and Food Chemistry *49*, 1881–1884.

Chang, E.E., Lin, Y.P., and Chiang, P.C. (2001). Effects of bromide on the formation of THMs and HAAs. Chemosphere *43*, 1029–1034.

Chellam, S., and Krasner, S.W. (2001). Disinfection Byproduct Relationships and Speciation in Chlorinated Nanofiltered Waters. Environ. Sci. Technol. *35*, 3988–3999.

Chen, W.J., and Weisel, C.P. (1998). Halogenated DBP: Concentrations in a distribution system. Journal-American Water Works Association *90*, 151–163.

Chen, J., LeBoeuf, E.J., Dai, S., and Gu, B. (2003). Fluorescence spectroscopic studies of natural organic matter fractions. Chemosphere *50*, 639–647.

Coble, P.G. (1996). Characterization of marine and terrestrial DOM in seawater using excitation-emission matrix spectroscopy. Marine Chemistry *51*, 325–346.

Cooper, W.J., Zika, R.G., and Steinhauer, M.S. (1985). Bromide-oxidant interactions and THM formation: a literature review. Journal (American Water Works Association) 116–121.

Cowman, G.A., and Singer, P.C. (1995). Effect of Bromide Ion on Haloacetic Acid Speciation Resulting from Chlorination and Chloramination of Aquatic Humic Substances. Environ. Sci. Technol. *30*, 16–24.

Croue, J.P., Korshin, G.V., and Benjamin, M.M. (1999). Characterization of natural organic matter in drinking water (Amer Water Works Assn).

Davis, M.K. (2010). Water and wastewater engineering (McGraw-Hill Science/Engineering/Math).

Deborde, M., and von Gunten, U. (2008). Reactions of chlorine with inorganic and organic compounds during water treatment—Kinetics and mechanisms: A critical review. Water Research *42*, 13–51.

Dickenson, E.R.V., Summers, R.S., Croué, J.-P., and Gallard, H. (2008). Haloacetic acid and Trihalomethane Formation from the Chlorination and Bromination of Aliphatic β-Dicarbonyl Acid Model Compounds. Environ. Sci. Technol. *42*, 3226–3233.

Duong, H.A., Berg, M., Hoang, M.H., Pham, H.V., Gallard, H., Giger, W., and Gunten, U. von (2003). Trihalomethane formation by chlorination of ammonium- and bromide-containing groundwater in water supplies of Hanoi, Vietnam. Water Research *37*, 3242–3252.

Fabbricino, M., and Korshin, G. (2004). Probing the mechanisms of NOM chlorination using fluorescence: formation of disinfection by-products in Alento River water. Water Science and Technology: Water Supply *4*, 227–233.

Gallard, H., and von Gunten, U. (2002). Chlorination of Phenols: Kinetics and Formation of Chloroform. Environ. Sci. Technol. *36*, 884–890.

Harrington, G.W., Bruchet, A., Rybacki, D., and Singer, P.C. (1996a). Characterization of natural organic matter and its reactivity with chlorine. In ACS Symposium Series, (ACS Publications), pp. 138–158.

Harrington, G.W., Bruchet, A., Rybacki, D., and Singer, P.C. (1996b). Characterization of natural organic matter and its reactivity with chlorine. In ACS Symposium Series, (ACS Publications), pp. 138–158.

Hautala, K., Peuravuori, J., and Pihlaja, K. (2000). Measurement of aquatic humus content by spectroscopic analyses. Water Research *34*, 246–258.

Hua, G., and Reckhow, D.A. (2007a). Comparison of disinfection byproduct formation from chlorine and alternative disinfectants. Water Research *41*, 1667–1678.

Hua, G., and Reckhow, D.A. (2007b). Characterization of disinfection byproduct precursors based on hydrophobicity and molecular size. Environmental Science & Technology *41*, 3309–3315.

Hua, G., and Reckhow, D.A. (2008). DBP formation during chlorination and chloramination: Effect of reaction time, pH, dosage, and temperature. Journal (American Water Works Association) *100*, 82–95.

Hua, B., Veum, K., Koirala, A., Jones, J., Clevenger, T., and Deng, B. (2007). Fluorescence fingerprints to monitor total trihalomethanes and N-nitrosodimethylamine formation potentials in water. Environmental Chemistry Letters *5*, 73–77.

Hua, G., Reckhow, D.A., and Kim, J. (2006). Effect of bromide and iodide ions on the formation and speciation of disinfection byproducts during chlorination. Environmental Science & Technology *40*, 3050–3056.

Johnson, J.D., and Jensen, J.N. (1986). THM and TOX formation: routes, rates, and precursors. Journal (American Water Works Association) 156–162.
Jones, D.B. (2009). The formation and control of iodinated trihalomethanes in drinking water treatment. Clemson University.

Jones, D.B., Saglam, A., Triger, A., Song, H., and Karanfil, T. (2011). I-THM formation and speciation: preformed monochloramine versus prechlorination followed by ammonia addition. Environmental Science & Technology *45*, 10429–10437.

Jones, D.B., Saglam, A., Song, H., and Karanfil, T. (2012). The impact of bromide/iodide concentration and ratio on iodinated trihalomethane formation and speciation. Water Research *46*, 11–20.

Karanfil, T., Hong, V., Orr, O., and Song, H. (2007). Exploring HAA Formation Pathways During Chloramination (Awwa Research Foundation).

Korshin, G.V., Li, C.W., and Benjamin, M.M. (1996). Use of UV spectroscopy to study chlorination of natural organic matter. (ACS Publications), pp. 182–195.

Korshin, G.V., Li, C.-W., and Benjamin, M.M. (1997a). Monitoring the properties of natural organic matter through UV spectroscopy: A consistent theory. Water Research *31*, 1787–1795.

Korshin, G.V., Li, C.-W., and Benjamin, M.M. (1997b). The decrease of UV absorbance as an indicator of TOX formation. Water Research *31*, 946–949.

Korshin, G.V., Kumke, M.U., Li, C.-W., and Frimmel, F.H. (1999). Influence of chlorination on chromophores and fluorophores in humic substances. Environmental Science & Technology *33*, 1207–1212.

Korshin, G.V., Wu, W.W., Benjamin, M.M., and Hemingway, O. (2002). Correlations between differential absorbance and the formation of individual DBPs. Water Research *36*, 3273–3282.

Korshin, G.V., Benjamin, M.M., Chang, H.-S., and Gallard, H. (2007). Examination of NOM Chlorination Reactions by Conventional and Stop-Flow Differential Absorbance Spectroscopy. Environ. Sci. Technol. *41*, 2776–2781.

Krasner, S.W., Sclimenti, M.J., and Means, E.G. (1994). Quality degradation: implications for DBP formation. Journal of the American Water Works Association;(United States) *86*.

Leenheer, J.A. (2007). Progression from model structures to molecular structures of natural organic matter components. Annals of Environmental Science *1*, 15.

Li, C.-W., Korshin, G.V., and Benjamin, M.M. (1998). Monitoring DBP formation with differential UV spectroscopy. Journal of American Water Works Association *90*, 88–100.

Li, C.-W., Benjamin, M.M., and Korshin, G.V. (2000). Use of UV spectroscopy to characterize the reaction between NOM and free chlorine. Environmental Science & Technology *34*, 2570–2575.

Liang, L., and Singer, P.C. (2003). Factors influencing the formation and relative distribution of haloacetic acids and trihalomethanes in drinking water. Environmental Science & Technology *37*, 2920–2928.

Marhaba, T.F., and Kochar, I.H. (2000). Rapid prediction of disinfection by-product formation potential by fluorescence. Environmental Engineering and Policy *2*, 29–36.

Minear, R.A., and Amy, G. (1996). Water Disinfection And Natural Organic Matter: Characterization And Control (Acs Symposium Series,) Author: Roger A. Mine.

Mopper, K., and Schultz, C.A. (1993). Fluorescence as a possible tool for studying the nature and water column distribution of DOC components. Marine Chemistry *41*, 229–238.

Norwood, D.L., Christman, R.F., and Hatcher, P.G. (1987). Structural characterization of aquatic humic material. 2. Phenolic content and its relationship to chlorination mechanism in an isolated aquatic fulvic acid. Environ. Sci. Technol. *21*, 791–798.

Novak, J.M., Mills, G.L., and Bertsch, P.M. (1992). Estimating the Percent Aromatic Carbon in Soil and Aquatic Humic Substances Using Ultraviolet Absorbance Spectrometry. J. Environ. Qual. *21*, 144–147.

Peuravuori, J., Koivikko, R., and Pihlaja, K. (2002). Characterization, differentiation and classification of aquatic humic matter separated with different sorbents: synchronous scanning fluorescence spectroscopy. Water Research *36*, 4552–4562.

Plewa, M.J., Wagner, E.D., Richardson, S.D., Thruston, A.D., Woo, Y.-T., and McKague, A.B. (2004). Chemical and biological characterization of newly discovered iodoacid drinking water disinfection byproducts. Environmental Science & Technology *38*, 4713–4722.

Pourmoghaddas, H., and Stevens, A.A. (1995). Relationship between trihalomethanes and haloacetic acids with total organic halogen during chlorination. Water Research *29*, 2059–2062.

Puchalski, M.M., Morra, M.J., and Von Wandruszka, R. (1992). Fluorescence quenching of synthetic organic compounds by humic materials. Environ. Sci. Technol. *26*, 1787–1792.

Reckhow, D.A., Singer, P.C., and Malcolm, R.L. (1990). Chlorination of humic materials: byproduct formation and chemical interpretations. Environmental Science & Technology *24*, 1655–1664.

Richardson, S.D. (2003). Disinfection by-products and other emerging contaminants in drinking water. TrAC Trends in Analytical Chemistry *22*, 666–684.

Richardson, S.D., Plewa, M.J., Wagner, E.D., Schoeny, R., and DeMarini, D.M. (2007). Occurrence, genotoxicity, and carcinogenicity of regulated and emerging disinfection by-products in drinking water: a review and roadmap for research. Mutation Research/Reviews in Mutation Research *636*, 178–242.

Richardson, S.D., Fasano, F., Ellington, J.J., Crumley, F.G., Buettner, K.M., Evans, J.J., Blount, B.C., Silva, L.K., Waite, T.J., and Luther, G.W. (2008). Occurrence and mammalian cell toxicity of iodinated disinfection byproducts in drinking water. Environmental Science & Technology *42*, 8330–8338.

Roccaro, P., Vagliasindi, F.G.A., and Korshin, G.V. (2009). Changes in NOM fluorescence caused by chlorination and their associations with disinfection by-products formation. Environmental Science & Technology *43*, 724–729.

Świetlik, J., and Sikorska, E. (2004). Application of fluorescence spectroscopy in the studies of natural organic matter fractions reactivity with chlorine dioxide and ozone. Water Research *38*, 3791–3799.

Traina, S.J., Novak, J., and Smeck, N.E. (1990). An Ultraviolet Absorbance Method of Estimating the Percent Aromatic Carbon Content of Humic Acids. J. Environ. Qual. *19*, 151–153.

Wolfe, R.L., Ward, N.R., and Olson, B.H. (1984). Inorganic chloramines as drinking water disinfectants: a review. J. Am. Water Works Assoc *76*, 74.

Yang, X., and Shang, C. (2004). Chlorination Byproduct Formation in the Presence of Humic Acid, Model Nitrogenous Organic Compounds, Ammonia, and Bromide. Environ. Sci. Technol. *38*, 4995–5001.